Aus dem Institut für Virologie
Direktor: Prof. Dr. Stephan Becker
des Fachbereichs Medizin der Philipps-Universität Marburg

Philipps Universität Marburg

La Crosse virus NSs sequesters Elongin C - a possible mechanism for inducing degradation of the largest subunit Of RNA polymerase II

Inaugural-Dissertation zur Erlangung des Doktorgrades der Naturwissenschaften (Dr. rer. nat.)

dem Fachbereich Medizin der Philipps-Universität Marburg vorgelegt von

Andreas Schön
aus Mönsterås, Schweden

Marburg, 2015

Angenommen vom Fachbereich Medizin der Philipps-Universität Marburg am: 2015.10.16

Gedruckt mit Genehmigung des Fachbereichs.

Dekan: Prof. Dr. Helmut Schäfer

Referent: Prof. Dr. Friedemann Weber

Korreferent: Prof. Dr. Guntram Suske

“Let's keep a little optimism here!”

Han Solo, Star Wars: Episode VI - Return of the Jedi

Content

Abbreviations

BUNV	Bunyamwera virus
CTD	C-terminal domain
CTDpSer 2	CTD phosphorylated on serine 2
CTDpSer 5	CTD phosphorylated on serine 5
E1	Ubiquitin-activating enzyme
E2	Ubiquitin-conjugating enzyme
E3	Ubiquitin ligase
h.p.i.	Hours post infection
IFN	Interferon
II_A	Post-translationally un-modified RPB1
II_O	Post-translationally modified RPB1
ISG	Interferon stimulated genes
L protein	Viral RNA-dependent RNA-polymerase
LACV	La Crosse virus
mRNA	Messenger RNA
N protein	Nucleocapsid protein
NSs	Non-structural protein on the S segment
RIG-I	Retinoic acid-inducible gene I
RNA	Ribonucleic acid
RNAPII	RNA polymerase II
RNP	Ribonucleoprotein
RPB1	The largest subunit of RNAPII
RVFV	Rift Valley fever virus
SBV	Schmallenberg virus
VHL	Von Hippel Lindau
wt	Wild type
ΔNSs	NSs deletion

Abstract

Viruses in the *Bunyaviridae* family cause disease in humans ranging from a mild transient fever to viral haemorrhagic fever. The *orthobunyavirus* genus is the largest within the family and contains the La Crosse virus (LACV). LACV is endemic in the USA, causing 85 % of neuroinvasive viral disease in children under the age of 15. The main pathogenicity factor of LACV is the NSs protein, an inhibitor of the type I interferon (IFN) induction. Previous work in our group identified the mechanism of LACV NSs inhibition. During infection, the NSs protein of LACV induces the proteasomal degradation of the largest subunit, RPB1, in transcription elongating RNA polymerase II. As a possible host cell interactor of LACV NSs that could mediate the degradation of RPB1, was Elongin C identified. Elongin C has been described to have two main functions in the cell: 1) as a subunit of the Elongin complex that increases RNA polymerase II transcription elongation rates, and 2) as a subunit of several cellular and viral ubiquitin E3 ligases.

Here, I demonstrate that LACV NSs specifically sequesters Elongin C from the nucleoli, but does not change the sub-cellular localization of the other two subunits of the Elongin complex, Elongin A and B. The LACV NSs re-localization of Elongin C from the nucleoli had minimal effects on the nucleolar structure or the localization of a major nucleolar protein, Nucleolin. The re-localization of Elongin C by LACV NSs could be prevented by inhibiting the main protein export factor of the nucleus, CRM1, but the same inhibition did not rescue RPB1 from degradation. However, siRNA mediated knockdown of Elongin C partially rescued RPB1 from degradation concomitantly with a partially rescued of type I IFN induction. In attempts to map the functional domains of LACV NSs, I was able to dissect the inhibition of general host cell transcription and type I IFN induction. All LACV NSs mutants, generated at conserved sites in the NSs protein throughout the orthobunyavirus genus, had lost the ability to inhibit type I IFN induction while they all retained the inhibition of general transcription. However, two of the mutants did not show robust phenotypes, requiring further studies to clarify their respective roles. For the rest of the mutants, the inhibition of general transcription correlated with RPB1 degradation, while the loss of type I IFN inhibition correlated partly with loss of Elongin C re-localization and/or inhibition of transcriptionally active RPB1.

Thus, I have established that the re-localization of Elongin C by LACV NSs might play a role in type I IFN inhibition. Furthermore, I was able to dissect the inhibition of general host transcription and type I IFN induction transcription, pointing towards two different mechanisms of inhibition. General transcription is inhibited by RPB1 degradation, while type I IFN inhibition correlates partly with RNA polymerase II elongation inhibition.

Zusammenfassung

Viren der Familie Bunyaviridae verursachen Krankheiten beim Menschen die von einem leichten vorübergehendem Fieber bis hin zu viralem hämorrhagischen Fieber reichen. Die Orthobunyavirus Gattung ist die größte in der Familie und enthält das La Crosse Virus (LACV). LACV ist endemisch in den USA, wo es für 85% der neuroinvasiven Viruserkrankung bei Kindern unter dem Alter von 15 Jahren verantwortlich ist. Der Hauptpathogenitätsfaktor von LACV ist das NSs Protein, das die Typ I Interferon Antwort hemmt. Frühere Arbeiten in unserer Gruppe identifizierten den Mechanismus mit dem das LACV NSs die Hemmung vermittelt. Während der Infektion induziert das NSs Protein von LACV den proteasomalen Abbau der größten Untereinheit, RPB1, in der Transkriptions-elongierenden RNA-Polymerase II. Als möglicher Wirtszell-Interaktor von LACV NSs, das den Abbau von RPB1 vermitteln könnte, wurde Elongin C identifiziert. Für Elongin C wurden zwei Hauptfunktionen in der Zelle beschrieben: 1) als eine Untereinheit des Elongin Komplex, das die Transkriptions-Elongationsrate der RNA-Polymerase II erhöht, und 2) als Untereinheit von mehreren zellulären und viralen Ubiquitin E3-Ligasen.

Hier zeige ich, dass LACV NSs speziell Elongin C aus den Nukleoli sequestriert, aber nicht die subzelluläre Verteilung von den anderen beiden Untereinheiten, Elongin A und B, des Elongin Komplexes beeinflusst. Die LACV NSs-vermittelte Umverteilung von Elongin C aus den Nukleoli hat minimale Auswirkungen auf die Kernstruktur oder die Verteilung eines Haupt-Nukleoli Proteins, Nukleolin. Die Umverteilung von Elongin C durch LACV NSs konnte durch Hemmung des Hauptproteinexportfaktors des Kerns, CRM1, verhindert werden aber nicht den Abbau von RPB1. siRNA-vermittelte Herunterregulation der Elongin C-Genexpression schützt RPB1 teilweise vor dem Abbau, begleitet von einer teilweise geretteten Typ I Interferon Antwort. In Versuchen die funktionellen Domänen von LACV NSs zu identifizieren, waren wir in der Lage die Hemmung der allgemeinen Transkription von der Transkriptionshemmung der Typ I Interferon Antwort zu trennen. Alle LACV NSs Mutanten, die an konservierten Stellen der ganzen Orthobunyavirus Gattung im NSs-Protein erzeugt wurden, haben die Fähigkeit verloren die Typ I Interferon Antwort zu hemmen, während sie die Hemmung der allgemeinen Transkription beibehalten haben. Zwei der Mutanten zeigten keinen robusten Phänotypen und erfordern weitere Studien um ihre jeweiligen Rollen zu klären. Für den Rest der Mutanten korreliert die Hemmung der allgemeinen Transkription mit dem RPB1-Abbau, während der Verlust der Hemmung der Typ I Interferon Antwort teilweise mit dem Verlust der Elongin C Umverteilung und / oder Hemmung der transkriptionell-aktiven RPB1 korreliert.

So haben wir festgestellt, dass die Umverteilung von Elongin C durch LACV NSs eine Rolle bei der Hemmung der Typ I Interferon Antwort spielen könnte. Darüber hinaus konnten wir die Hemmung der allgemeinen Wirtstranskription von der Transkriptionshemmung der Typ I

Interferon Antwort trennen, hinweisend auf zwei verschiedene Mechanismen der Hemmung. Die allgemeine Transkription wird durch den RPB1-Abbau gehemmt, während die Hemmung der Typ I Interferon Antwort teilweise mit der Hemmung der RNA-Polymerase II-Elongation korreliert.

1. Introduction

1.1. La Crosse Virus neuroinvasive disease

The La Crosse virus (LACV) was isolated in May 1964, from autopsy samples taken from a 4-year old girl who died in 1960 of meningoencephalitis in the town of La Crosse, Wisconsin. Based on serology the virus was demonstrated to belong to the California encephalitis group, in the orthobunyaviruses genus of the *Bunyaviridae* family of viruses [154]. LACV is endemic to the eastern USA, with a geographical distribution correlating with the main vector, the eastern tree-hole mosquito (*Ochlerotatus triseriatus*) [163]. However, LACV is currently spreading to un-affected areas of USA [60] possibly due to the introduction of the Asian tiger mosquito (*Stegomyia albopicta*) which can transmit the virus [55]. The eastern tree-hole mosquito has been demonstrated to maintain LACV in nature, via cyclic infection of chipmunks (*Tamias striatus*) or gray squirrels (*Sciurus carolinensis*), in which the virus reaches high enough titer to infect naïve blood sucking mosquitos [21, 53]. The LACV is released subcutaneously, upon infected mosquito feeding, and then replicates primarily in striated muscle cells, resulting in virus release into the blood stream. The mechanism how the virus reaches the brain is not known but two possibilities have been suggested; one study suggested that viral infection of the vascular endothelial cells in the brain releases virus into the central nervous system [21] while the other study suggested that the virus can reach the nasal turbinates and enters the CNS by this route [16].

Due to the vector transmission, LACV infections occur from July to September, with around 70 cases/year of severe neuroinvasive infections in children under the age of 15, which accounts for 85% of viral neuroinvasive disease in this age group. In 0.5 – 2 % of the severe infections, the patient dies. However most LACV infections are either asymptomatic or under-diagnosed, with estimates of up to 300.000 infections/year in endemic areas [2, 52, 60]. Mild LACV infection causes general symptoms such as fever, headache and vomiting while in severe cases, most patients experienced seizures or disorientation. The diagnosis of LACV neuroinvasive infection, which manifests itself as encephalitis, meningitis or meningoencephalitis, is based on the clinical signs and serological tests for LACV specific IgM/IgG antibodies in serum and/or cerebrospinal fluid [95, 98, 154]. Long-lasting effects, in children who recovered from severe infection, have been demonstrated with decreased IQ scores, compared to age-matched groups, and an increased incidence of attention-deficit-hyperactivity disorder [95]. LACV infections have also been studied in relation to socioeconomic costs with estimates, for patients with severe infection, of up to 3.1 million $/patient [155]. There is no approved antiviral therapy against LACV, with severe cases being treated symptomatically. The broad-spectrum antiviral

ribavirin, to which LACV is sensitive in cell culture [35], was tested for treating severe LACV infections. However, no difference in infection resolution time or severity of the disease was observed, compared to placebo treatment, probably due to low concentration in the cerebrospinal fluid. Higher doses had severe side-effects and were therefore discontinued [96].

Several host factors have been implicated in the development of LACV neuroinvasive disease, in especially young individuals. The importance of innate immune activation by LACV infection, both in the periphery [151] and in the CNS [133], to limit the infection have been demonstrated. A reduced amount of myeloid dendritic cells in the periphery [151] and/or low levels of innate immune components in the developing brain of young individuals [133] have both been suggested to contribute in disease development in young individuals. A small study also demonstrated a possible involvement of certain HLA-types in disease incidence and severity [34]. However, the mechanism why young individuals develop severe disease is not clear.

1.2. Bunyaviridae

1.2.1. The *Bunyaviridae* family

The *Bunyaviridae* family of viruses contain around 350 viruses divided in 5 genera: *Orthobunyavirus*, *Nairovirus*, *Phlebovirus*, *Hantavirus* and *Tospovirus* [3, 162]. All viruses are vector borne, e.g. transmitted by mosquitoes or ticks, except the hantaviruses, which are shed into the excrements and saliva of their persistently infected rodent hosts [57]. The prototype virus of the whole family is the Bunyamwera virus (BUNV), which belongs to the *Orthobunyavirus* genus. Examples of other viruses within each genus are: Crimean-Congo Hemorrhagic fever virus (*Nairovirus*), Rift Valley fever virus (RVFV) (*Phlebovirus*), Puumala virus (*Hantavirus*) and Tomato spotted wilt virus (*Tospovirus)* [57, 140]. The viruses in the family cause a wide range of disease in humans and animals (*Orthobunyavirus*, *Nairovirus*, *Phlebovirus*, *Hantavirus)* or plants (*Tospovirus)*. In humans the diseases caused by viral infection range from febrile illness, to severe symptoms with hepatitis, encephalitis or haemorrhagic fever, while diseases in animals range from decrease milk production, to congenital malformation of foetuses and/or abortions [3, 57, 140, 162].

1.2.2. *Bunyaviridae* structure and genomic organization

Bunyaviridae virions are circular pleomorphic in structure with a diameter of 75-115 nm [1]. The virions consist of a membranous bilayer [23] from which the receptor binding glycoproteins protrude [150]. The viral genome consists of 3 segments of negative-sense, single-stranded

RNA, where the name of each segment is based on its nucleotide length; small (S segment), medium (M segment) and large (L segment) [105] (Fig. 1B). For all genera in the family the 3 segments encodes for a total of 4 structural proteins where the S segment encodes for the nucleoprotein (N), the M segment encodes for the two glycoproteins (G_C) and (G_N) and the L segment encoding for the RNA-dependent RNA-polymerase (L) [44, 51, 88, 104]. Viruses in the *Orthobunyavirus*, *Phlebovirus* and *Tospovirus* genera also express two non-structural proteins, the non-structural protein on the M segment (NSm) and the non-structural protein on the S segment (NSs) [51, 88] (Fig. 1B). Each segment has two untranslated regions, on either side of the open reading frame (ORF). The very 3' and 5' of each segment, in the respective untranslated region, are complementary in sequence. This complementarity allows for base pairing between the untranslated regions, forming a short stretch of double-stranded RNA called the "panhandle", making the genomic content appear semi-circular in isolation [105]. The panhandle sequence is shared between viruses in the same genus, but not in-between *Bunyaviridae* genera [107, 120]. The viral RNA segment is coated by N proteins, forming ribonucleoprotein complexes that associates with viral polymerase L [106] (Fig. 1A).

1.2.3. *Bunyaviridae* replication cycle

Upon infection the surface glycoprotein G_C binds to an unknown receptor on permissive cells, inducing a clathrin-dependent endocytosis [70, 112, 129]. Membrane fusion is induced by a decrease in endosomal pH, causing the G_C protein to undergo a conformational change [113] exposing a fusion peptide, mapped to amino acid 1066 to 1087 for LACV G_C [142]. LACV fusion have been determined to occur in the early endosome [70], while the related orthobunyavirus Oropouche virus fuses in the late endosome [129]. Upon fusion the ribonucleoprotein complexes are released into the cytoplasm [3]. *Bunyaviridae* transcription and replication occur in the cytoplasm [127]. The incoming L protein, present on the ribonucleoprotein complexes, performs primary transcription where viral mRNA is synthesised. During both viral transcription and replication, the panhandle is vital as a promoter [12]. *Bunyaviridae* mRNA transcription is dependent on cap-snatching, where the 5' capped first ~15 nucleotides are cleaved of from host cell mRNA and used as primers for viral transcription [108]. The LACV endonuclease domain, responsible for cap-snatching, is located in the N terminus of the L protein, which has high sequence similarity both within the orthobunyavirus genus and between genera [121]. *Bunyaviridae* mRNA lack a poly-A tail, where transcription of the LACV S segment was determined to end at a polyuridine tract, similarly to termination sites for other negative sense viruses [109]. *Bunyaviridae* transcription and replication, in mammalian cells, is dependent on ongoing translation [3, 14, 15, 119].

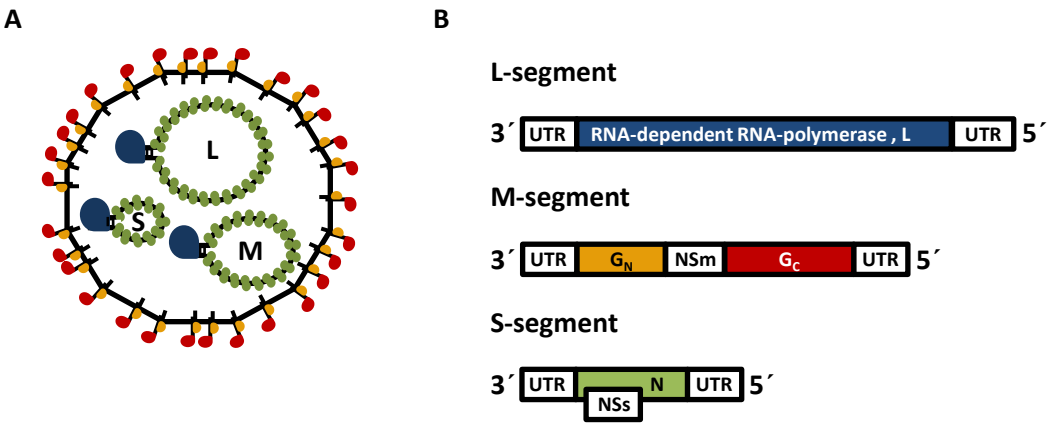

Figure 1. Schematic representation of **A)** a *Bunyaviridae* virus particle and **B)** the coding strategy employed by orthobunyaviruses. The colours of the viral proteins in part A correspond to the colour of the respective ORF of the genome in part B.

As the viral replication proceeds, both the genome and the antigenome, are encapsidated by the N protein. The *Orthobunyavirus* N proteins from LACV, BUNV, Schmallenberg virus (SBV) and Leanyer virus have all been determined to possess a positively charged cleft, accommodating 10-11 nucleotides/N protein, in-between two globular domains. Each globular domain of the N protein have a short arm responsible for multimerization, by extending over to the next N protein on a ribonucleoprotein complex [8, 91, 102, 122].

The M segment mRNA encodes for a polyprotein containing the glycoproteins G_N and G_C, and for some genera a non-structural protein (NSm) separating the two viral surface proteins [88], (Fig 1B). The polyprotein is translated at the ER and then cleaved into the three proteins by an unknown protease. Both glycoproteins are type I integral membrane proteins that heterodimers in the ER and are then transported to the Golgi compartment [134, 135]. The targeting sequence for both G_N and G_C to the Golgi compartment, where viral assembly occur, has been mapped to the trans-membrane domain of the G_N protein [29, 134, 137]. Infection with *Bunyaviridae* viruses causes a large reorganization of the Golgi compartment. Tubular structures, between 0.2-1 µm long with a terminal globular domain, protrude from the Golgi cisternae and contain the N, L and NSm proteins, as well as double stranded RNA, indicating that these structures are the replication site [45, 128]. The NSm protein is an integral membrane protein essential for viral viability, playing a role in virus assembly and in the formation of the tubular structures in Golgi [45, 136]. Assembled virions move through the Golgi compartment, during which a maturation process occurs [103, 128]. The virions are released from infected cells via transport through the exocytic pathway [138] requiring the participation of the actin cytoskeleton [3, 45, 130].

1.3. The *Orthobunyavirus* NSs protein

Most viruses in the orthobunyavirus genus code for a non-structural protein on the S-segment (NSs). The NSs protein is translated from a +1 open reading frame embedded in the nucleoprotein mRNA [51] (Fig. 1B). Depending on its expression level, the BUNV NSs protein was observed to localize to the cytoplasm (low expression) or nucleus (high expression) [152, 164]. Orthobunyavirus NSs proteins are hydrophobic proteins with a transient expression in the beginning of the infection. The degradation of Orthobunyavirus NSs proteins occur via the proteasome, as demonstrated for BUNV NSs [50, 157].

The main function of the NSs protein, during infection of mammalian cells, has thus far primarily been studied for BUNV, LACV and SBV [19, 26, 43, 158]. These studies where aided by the development of reverse genetic systems by which recombinant wild-type (wt) viruses or viruses lacking NSs expression (ΔNSs) were generated. By comparing wt and ΔNSs infected cells, the main function was determined to be the inhibition of the antiviral type I interferon system of mammalian cells [20, 26, 43, 158, 165]. Both wt and ΔNSs viruses induced the activation of the antiviral transcription factor interferon regulatory factor 3 (IRF3), but the NSs expressing wt virus inhibited type I interferon transcription [82, 160]. The lack of type I interferon transcription inhibition by SBV ΔNSs was recently demonstrated to be a good vaccine candidate in cattle. The vaccine virus was safe and induced neutralizing antibodies and protection against challenge SBV wt [84].

1.3.1. Other NSs functions

Besides the main function of orthobunyavirus NSs proteins in inhibiting type I IFN induction during infection of mammalian cells, several other functions have been demonstrated. The NSs proteins of LACV [19], BUNV [26, 89] and SBV [13, 43] have been reported to decrease host cellular translation, inducing a so-called host cell shutoff. The exact mechanism of NSs induced host cell shutoff is not known but is thought to be in large parts due to the transcription inhibition and to a lesser extent on an as yet un-known second mechanism [64].

The NSs protein of BUNV was demonstrated to inhibit the induction of apoptosis [64, 82] while the LACV and SBV NSs proteins where demonstrated to induce apoptosis [13, 19, 114]. Furthermore, the NSs proteins of the California serogroup viruses, to which LACV belongs, were demonstrated to possess sequence-similarities with the C-terminal 2/3 of the Drosophila Reaper protein. In agreement with this, both LACV NSs and the Reaper protein induced apoptosis in an *in vitro* system [37].

The NSs proteins of BUNV [164] and LACV [18] have both been demonstrated to decrease viral RNA synthesis in mammalian cells via an unknown mechanism. However, BUNV NSs was demonstrated to have no effect on viral RNA synthesis in insect cells [83].

Orthobunyaviruses infect both mammalian and insect cells, but the function of the NSs during infection of insect cells is not well known. The NSs proteins of both LACV and BUNV did not have any effect on host cell transcription in insect cells [152, 160]. However, both LACV and BUNV NSs have been described to play a role in subverting the insect cell antiviral RNAi system [20, 141, 147].

1.4. Innate immunity

The initiation of the innate immune response is dependent on the recognition by cellular pattern recognition receptors (PRRs) of so-called pathogen-associated molecular patterns (PAMPs), which for viruses are primarily nucleic acids [74]. Currently three families of PRRs have been described that recognize RNA viruses: toll-like receptors, nucleotide-binding oligomerization domain-containing (NOD)-like receptors and retinoic acid-inducible gene I (RIG-I)-like receptors (RLRs) [74, 167]. The ribonucleoprotein complexes of both LACV and the phlebovirus RVFV have been demonstrated to be recognized by a member of the RLR family [166], why a more detailed description of this pathway of innate immune induction will be given.

1.4.1. The RLR pathway

The RLR family consist of three proteins: melanoma differentiation associated factor 5 (MDA5), laboratory of genetics and physiology 2 (LGP2) and retinoic acid-inducible gene I (RIG-I). MDA5 and LPG2 both recognize long double-stranded RNA [74], while RIG-I recognizes 5’ triphosphorylated double-stranded RNA [167]. The panhandle structures on LACV and RVFV ribonucleoprotein complexes contains both double-stranded RNA and a 5’ triphosphate, which was determined to be recognized by RIG-I [166]. Upon PAMP recognition by RIG-I a conformational switch occurs, exposing two caspase-recruiting domains (CARDs) that is responsible for downstream signalling, via CARD-CARD interaction, with the mitochondrial antiviral signalling protein (MAVS), located in the outer mitochondrial membrane [74, 167]. MAVS is a platform to which other downstream factors are recruited, among others TNF receptor-associated factor 3/6 (TRAF3/6) [74]. TRAF3/6 interacts with the complex of TANK-binding kinase 1 and inhibitor of kappa light polypeptide gene enhancer in B-cells kinase epsilon that then phosphorylates the antiviral transcription factor IRF3. The now activated IRF3 homodimerizes and translocates to the nucleus where it binds to eg. the *IFN-β*

promoter [61, 90]. The IRF3 dimer bound to the promoter can then recruit RNA polymerase II (RNAPII) for transcription [48]. The MAVS/TRAF3 complex also activates the nuclear factor kappa-light-chain-enhancer of activated B cells (NF-κB) pathway, allowing NF-κB to translocate into the nucleus where it promotes the transcription of pro-inflammatory genes [68, 69]. Furthermore, NF-κB is also required, in addition to IRF3 and a third transcription factor AP-1, for transcription of IFN-β mRNA [40, 48, 90].

1.4.2. Interferons and their signalling

Three classes of interferons (IFN); type I, type II and type III, have been described [131]. Type II IFN consists of the single IFN-γ, that is primarily expressed by, and act on, immune cells [131]. Type III IFN consists of the four IFN-λ1-4 while type I interferon consists of a single IFN-β and 14 IFN-α isoforms [90, 131]. Both type I and III interferon induces the expression of interferon stimulated genes (ISG) by binding to their respective receptors, which is the case of type I IFN is the IFN-α receptor expressed on almost every cell [61, 131]. Binding of type I IFN to its receptor induces a Janus kinase (JAK)/Signal Transducers and Activators of Transcription (STAT) signalling pathway [61, 131]. Type I IFN binding to its IFN-α receptor activates STAT1/2 proteins, which are phosphorylated and heterodimerizes [11, 170]. The STAT1/2 heterodimer associates with IRF9, after which the complex translocate to the nucleus where it binds to promoters of ISGs containing IFN-stimulated response elements [11, 170].

1.4.3. Interferon stimulated genes

Type I interferon signalling induces the expression of around 300 interferon stimulated genes (ISGs). The ISGs have different functions e.g. direct antiviral effects, cell-to-cell communication or regulation of the response to the infection [41, 62, 72]. Most of the proteins involved in recognition and downstream signalling, described above, are all ISGs. Some examples and functions of ISGs restricting orthobunyavirus infection will be given [31, 117]. RIG-I is expressed at a constitutive low level, but is up-regulated by IFN stimulation, to detect and initiate signalling upon recognition of 5’ triphosphorylated double-stranded RNA in the cytoplasm [166, 167]. RIG-I induced singling leads to the induction of IRF7 expression. IRF7 is highly homologous to IRF3, but has broader activation ability by inducing transcription of both IFN-β and IFN-α genes that potentiating the antiviral response [71, 97, 126]. The human homolog of murine Myxovirus resistance 1 protein, the MxA protein, has a potent antiviral effect against both orthobunyaviruses and phleboviruses [63]. Both *in vitro* and *in vivo* overexpressed MxA severely reduces viral titers, by inhibiting viral replication [49], and increases survival of infected mice [66]. The inhibition of viral replication is partially due to sequestration of the N protein into the COP-I compartment, between the smooth ER and Golgi

[81, 123]. Orthobunyaviruses infections activate the antiviral protein kinase R (PKR) [146]. PKR recognizes and is activated by double stranded RNA. Activated PKR-homodimers phosphorylate the eukaryotic translation initiation factor 2 α, thereby inhibiting cellular translation [101].

1.5. Cellular Transcription

Expression of any protein, be it ISGs or constitutively expressed proteins, initiates with the transcription of the gene. Three mammalian RNA polymerase types (RNAP types): I, II and III have been described that transcribes different RNAs [169]. RNAP type I synthesises ribosomal RNA, RNAP type II synthesises mRNAs and non-coding RNAs and the RNAP type III synthesises tRNAs. All three polymerases are multisubunit complexes; RNAPI (14 subunits), RNAPII (12 subunits), RNAPIII (17 subunits), where five of the subunits are shared between the three polymerases [171]. Most studies on structure, assembly and function have been performed on RNAPII [169, 171]. The 12 subunits of RNAPII are called RPB 1 to 12, where the number indicates the size in a falling scale 1 being the largest subunit. The assembly of the RNAPII complex occurs in the cytoplasm, aided by several proteins, and have been demonstrated to be crucial for its function [22, 169, 171]. None of the RNAPII subunits have a nuclear localization signal (NLS) which is instead provided by interacting proteins [32, 46, 171].

1.5.1. Transcription preinitiation complex assembly

The induction of transcription by RNA polymerase II starts with assembly of the transcription preinitiation complex (PIC) composed of RNAPII and general transcription factors [153]. The nomenclature of the general transcription factors are: transcription factor (TF) followed by the Roman numeral II (for RNAPII) and finally a letter A – H [153]. The initiation of PIC assembly is largely driven by cell and tissue specific transcription factors. These transcription factors bind to their sequence in the gene promoter, followed by recruitment of the general transcription factors and RNAPII [6]. However, several of these specific transcription factors do not directly interact with the PIC components. Instead the interaction is mediated by the Mediator complex composed of 26 MED subunits of highly dynamic composition. The Mediator complex assists both during PIC assembly and throughout the RNAPII transcription cycle [6, 39]. The assembly of the PIC starts with the recruitment/recognition of the TATA-box in the core promoter by the TATA binding protein, a subunit of TFIID [153]. A sequential recruitment and assembly of the PIC then follows with the order of recruitment being: TFIIA-TFIIB-RNAPII-TFIIF-TFIIE-

TFIIH. Extensive co-operation between the general transcription factors assures that RNAPII is correctly positioned, the transcription bubble formed and transcription initiated [153].

1.5.2. The RPB1 CTD

The largest subunit of RNAPII, RPB1, contains the catalytically active centre, and possesses a C-terminal domain (CTD) that is essential for cell viability, but not for the direct catalytic function of RNAPII [42]. The CTD is composed for heptad repeats with the consensus sequence tyrosine-serine-proline-threonine-serine-proline-serine ($Y_1S_2P_3T_4S_5P_6S_7$) conserved from yeast to mammals. However the amount of repeats varies between organisms: while mammals have 52 repeats, the yeast *S. cerevisiae* have 26 [42]. The CTD serves as a platform to which different factors bind successively throughout the RNAPII transcription cycle. The recruitment if these factors are regulated by post-translational modifications of the CTD: Y_1, T_4 and $S_{2/5/7}$ can be reversibly phosphorylated, T_4 and $S_{5/7}$ can be dynamically O-glycosylated and $P_{3/6}$ can isomerize to the *cis*- or *trans*-conformation [42, 67, 177]. In total 10368 possibilities of CTD modifications exist, however some modifications exclude others so the possible combinations *in vivo* are not known. Modelling and experimental data suggest that phosphorylation of the CTD makes the structure more extended, allowing interactions with transcription factors and mRNA modifying proteins [42, 67, 177]. Two main forms of RPB1 can be detected by Western blot: the faster migrating RPB1 II_A (II_A) form and the slower migrating RPB1 II_O (II_O) form. The difference in the mobility of the two forms is due to post-translational modifications of the CTD [42]. In the RNAPII that is recruited to the PIC, RPB1 is in the II_A form, which is then post translationally modified into the transcriptionally active II_O form. The post-translational modifications of RPB1 CTD is highly dynamic and reversible where the most studied modifications are the phosphorylation and de-phosphorylation of S_2 and S_5 [42, 67, 177]. CTD serine 5 is phosphorylated by the TFIIH subunits cyclin-dependent kinase 7 (CDK7) and de-phosphorylated by the phosphatase Ssu72. CTD serine 2 is phosphorylated by the positive transcription elongation factor b (P-TEFb) subunit CDK9 while it is de-phosphorylated by the phosphatase Fcp1 [42]. Phosphorylated CTD serine 5 (CTDpSer 5) and CTD serine 2 (CTDpSer 2) are both II_O forms of RPB1. CTDpSer 5 is a marker for transcriptionally initiated RNAPII, while CTDpSer 2 is a marker for transcriptionally elongating RNAPII [42, 67, 177].

1.6. Orthobunyavirus NSs inhibit transcription elongation

Incoming ribonucleoprotein complexes of LACV were demonstrated to activate RIG-I [166] and both LACV and BUNV infection lead to activation of the antiviral transcription factor IRF3 [82, 160]. However, the type I IFN induction was inhibited in wt Orthobunyavirus infected cells at the later stage of RNAPII transcription elongation [152].

The BUNV NSs inhibits the phosphorylation of RPB1 CTD serine 2 [152], which have been proposed to be mediated by NSs interaction with the MED8 subunit of the Mediator complex [89]. The interaction domain on the NSs was mapped to the very C terminus of the protein. Indeed, a rescued BUNV expressing the first 83 amino acid residues of the NSs was unable to inhibit both general and IFN-β transcription [89]. However, a BUNV mutant with a truncated NSs lacking the first 22 N-terminal amino acids was also deficient in IFN-β inhibition and CTD serine 2 blockade. This indicated that the BUNV NSs-inhibition of serine 2 phosphorylation and innate immune activation, is dependent not only on the C-terminal MED8 interaction domain, but also other parts of the NSs protein [156].

Another mechanism of inhibiting RNAPII transcription elongation was demonstrated for the LACV NSs protein. LACV NSs induces the proteasomal degradation RPB1 CTDpSer 2 [160]. Similarities between LACV wt infection and the DNA damage response (DDR) were noted, where both NSs and DDR induced degradation of RPB1 in transcription-elongating RNAPII. In addition to the RPB1 degradation also other markers of the DDR were seen in LACV wt infected cells such as pak6 transcription and serine 139 phosphorylation of histone H2AX [160]. A similar, but slightly delayed, proteasomal degradation of RPB1 was recently reported in SBV wt-infected cells [13]. The SBV NSs function, in inducing the proteasomal degradation of RPB1, was mapped to the C terminal part of the protein, by ectopic expression of 6 NSs mutants at conserved positions [13].

To further the understanding of LACV NSs induced degradation of RPB1 CTDpSer 2, attempts were made in the group of Prof. Friedemann Weber to find host cell interactors of the NSs protein. In *in vitro* pull down experiments, with components of E3 ligases due to the proteasomal-dependent degradation, the Elongin C protein was identified as a possible interaction candidate of LAVC NSs (unpublished, see [159]).

1.7. The Elongin C protein

1.7.1. The Elongin complex

Several factors have been shown to either promote or inhibit RNAPII transcription elongation [38]. One of the factors promoting RNAPII transcription elongation is the Elongin complex, composed of the three subunits Elongin A (110 kDa), Elongin B (18 kDa) and Elongin C (14 kDa) [9]. *In vitro* the heterotrimeric Elongin complex was demonstrated to increase the RNAPII transcription elongation rate by 5-fold, compared to reactions without the Elongin complex [9, 24, 25]. However, the Elongin complex had no effect on RNAPII initiation or synthesis of the first 9 mRNA nucleotides [25, 100]. The Elongin A subunit alone stimulated transcription elongation *in vitro*, while neither Elongin B nor C alone had any effect on RNAPII transcription. The combination of Elongin A and C increased transcription elongation, compared to Elongin A alone, while Elongin B had no effect. Elongin A was therefore concluded to be the transcriptionally active subunit while Elongin C potentiates the effect. Elongin B had no effect on the function of Elongin A but was seen to stabilizing the Elongin complex [9].

The interactions between the three subunits of the Elongin complex are dependent on the Elongin C subunit. Elongin B and C form a stable complex, Elongin B/C, that can activate Elongin A, however Elongin B does not interact with Elongin A [9]. Elongin C interacts with Elongin B via the N terminal amino acid residues 19 to 30, while the extreme C terminal part of Elongin C is needed for full Elongin complex formation (Elongin A/B/C interaction) and both the Elongin B/C and C terminal regions are needed to increase Elongin A activity on RNAPII [149]. Elongin A interacts with Elongin C via its so-called BC box motif, (STP)Lxxx(CSA)xxxϕ [93], which is shared between different Elongin B/C interactors e.g. the Von Hippel Lindau (VHL) [10], Cullin 2 and Cullin 5 protein [78].

Functional studies on the Elongin complex have focused on the Elongin A proteins since this is the transcription-active subunit. Elongin A was demonstrated to be important in the transcription of stress response genes in both mammalian [79] and *Drosophila* cells [54]. Mammalian and *Drosophila* Elongin A interacted with RPB1, with a preferred interaction of mammalian Elongin A with RPB1 CTDpSer 5. However, only partial co-localization was noted, indicating that Elongin is not a general transcription elongation factor but is needed for specific sets of genes [54, 79]. Knockout of Elongin A in mice demonstrated the vital role of the Elongin complex during development, since knockout embryos died 10-13 days post-gestation. In these embryos a poor development of the CNS was seen and induction of apoptosis was noted [99]. A partial explanation for the embryonic lethality in Elongin A knockout mice was the lack of stem cell differentiation into neurons, normally induced by retinoic acid. Indeed, by microarray on Elongin A knockout stem cells, genes involved in neuronal development were significantly

down-regulated. The down regulation correlated with a lack of transcriptionally elongating RNAPII on retinoic acid inducible genes, which was rescued by supplementing the cells with Elongin A [175].

1.7.2. Ubiquitin E3 ligases

One of the major pathways of protein degradation in the cell is the ubiquitin/proteasome system [116]. The protein substrate to be degraded is ubiquitinated in a multistep process involving at least 3 enzymes: the ubiquitin-activating enzyme (E1), the ubiquitin-conjugating enzyme (E2) and the ubiquitin ligase (E3) [116]. The E1 activate the ubiquitin protein in an ATP-dependent reaction, after which the activated ubiquitin is transferred to the E2. The E3 ligase interacts with both the substrate to be ubiquitinated and the E2, orienting and bringing the substrate into close proximity of the E2 [116, 173]. The first step is the monoubiquitination of the substrate, where the activated C terminus of the ubiquitin protein is covalently attachment to a lysine residue on the substrate protein. This initial monoubiquitination is the first step in polyubiquitination, where the C terminus of a new ubiquitin protein is covalent attached to one of the seven lysine residues or the N terminus of the initial ubiquitin [173]. Polyubiquination chains containing lysine 48-linked ubiquitin's, marks the substrate for proteasomal degradation. One of the main E3 ligase families contains a Cullin protein [5, 116, 173], for which Cullin 2 or 5 both have been demonstrated to form E3-ligases containing Elongin B/C [93].

Cullin 2 forms an E3 ligase containing the tumour suppressor protein VHL, Elongin B/C and Rbx1 [78, 93, 111]. *In vitro* studies on this complex had ubiquitin E3 ligase activity [73], where the substrate, by VHL interaction, was determined to be the hypoxia stabilized transcription factor HIF-1 [94]. Cullin 2 has also been determined to interact with the MED8 subunit, of the Mediator complex, forming an E3 ligase containing Elongin B/C, and Rbx2. This E3 ligase was able to perform polyubiquitination, however no specific substrate was identified [27]. Cullin 5 interacts with suppressor of cytokine signalling (SOCS) proteins, forming an E3 ligase containing Elongin B/C and Rbx2. However, substrates for these E3 ligases have not been identified [77, 78, 93].

1.7.3. Transcription–coupled nucleotide excision repair

If transcriptionally active RNAPII encounters a damage/block in the DNA the polymerase stalls at this position. To resolve the DNA damage/block the process of transcription–coupled nucleotide excision repair (TC-NER) is initiated. During TC-NER, stalled RNAPII is recognized by Cockayne Syndrome B protein which signals for induction of the repair pathway. To make room for the repair complex formed on the damage DNA, RNAPII can either

backtrack on the DNA, to be able to resume transcription after the damage has been repaired, or the RNAPII complex is disassemble via ubiquitin mediated proteasomal degradation of the largest subunit RPB1 [86, 161]. The DNA damage induced ubiquitinylation of RPB1 is a highly organized process in which two E3 ligases have been confirmed to be involved.

The yeast E3 ligase Rsp5 and its mammalian homolog NEDD4 have been demonstrated to support ubiquitinylation of RPB1. *In vitro*, Rsp5 was demonstrated to preferentially ubiquitinylate RPB1 in transcriptionally elongating RNAPII stalled at damaged DNA in comparison to free RPB1 or RPB1 in transcriptionally elongating RNAPII on undamaged DNA. Rsp5 was further demonstrated to interact with phosphorylated CTD [143, 144]. Also human NEDD4 was confirmed to be the primary E3 ligase targeting RPB1 in RNAPII stalled by UV damage [7].

The second E3 ligase, determined to be needed for polyubiquitination and subsequent degradation of RPB1, contains the yeast homologs of Elongin C, Elongin A, Cullin 5, and probably Rbx1 [124, 125]. In mammals, an ubiquitin E3 ligase consisting of Elongin A/B/C-Cullin 5-Rbx2 or Rbx1 was detected, which *in vitro* polyubiquitinylated RPB1 [174]. Cullin 5 and Elongin A were both present in the nucleus, and after UV-treatment a strong co-localization between the two protein was seen [174] at sites of DNA damage [168]. Elongin A mainly interacted with, and induced degradation of, the CTDpSer 5 form of RPB1, upon DNA damage [79, 168, 174].

2. Aim of the thesis

Infection of orthobunyavirus causes a rapid induction of the antiviral type I IFN system [20, 26, 43], due to RIG-I recognition of incoming RNPs [166] leading to IRF3 dependent transcription of type I IFN [20, 152]. To counteract the innate immune induction, orthobunyaviruses express the NSs protein which rapidly inhibits host cell transcription, of both antiviral and constitutively expressed genes [152, 160]. LACV NSs was demonstrated to inhibit host cell transcription by inducing the proteasomal degradation of the largest subunit, RPB1, in transcriptionally elongating RNA polymerase II. In attempts to find host cell interaction candidates of LACV NSs, the Elongin C protein was identified previously. Elongin C was a promising candidate since it has been demonstrated to be a subunit of both, the Elongin complex which increases RNA polymerase II transcription elongation rates, and several cellular and viral ubiquitin E3 ligases.

The objective of my thesis was to characterise the LACV NSs interaction with Elongin C, and the role this interaction might have on the function of the NSs protein. Furthermore, loss-of-function mutants of LACV NSs where used to map functional domains of the protein.

3. Material

3.1. Cell lines

Table 1. Cell lines used for experiments.

Name[a]	Organism	Tissue type
HuH-7 (JCRB: 0403)	*Homo sapiens*, Human	Hepatocellular carcinoma
A549 (ATCC: CCL-185)	*Homo sapiens*, Human	Lung Carcinoma
HEK-293 (ATCC: CRL-1573)	*Homo sapiens*, Human	Embryonic kidney
BHK-21 (ATCC: CCL-10)	*Mesocricetus auratus*, Syrian/Golden hamster	Kidney fibroblast
Vero76 (ATCC: CRL-1587)	*Cercopithecus aethiops*, Givet or African green monkey	Kidney epithelium
CV-1 (ATCC: CCL-70)	*Cercopithecus aethiops*, Givet or African green monkey	Kidney fibroblast

[a] the ATCC or JCRB catalogue nr. is given as reference. The cells were kept in culture for several passages and might therefore not perform as cells directly received from ATCC or JCRB.

3.2. Viruses

Table 2. Viruses available at the beginning of the work.

Virus	Name	Description
La Crosse virus [a]	LACV wt	Recombinant LACV wt rescued via reverse genetics [19].
La Crosse virus ΔNSs [a]	LACV ΔNSs	Recombinant LACV not expressing the NSs protein. Rescued via reverse genetics where the initial two start codons in the NSs ORF were exchanged to two threonine codons and the third codon to a stop codon. These exchanges did not cause any change in the N ORF [19].
Vesicular Stomatitis Virus [a]	VSV	Vesicular Stomatitis Virus, strain: Indiana
Rift Valley fever virus-CF-NSs [b]	ZH-CF-NSs	Recombinant wt RVFV rescued via reverse genetics. The NSs protein has been tagged with a C-terminal 3×Flag for detection [58] [c].
Rift Valley fevr virus-3×NF-ΔMx [b]	ZH-3×NF-ΔMx	Recombinant RVFV where the NSs has been replaced by the first 105 amino acids of the MxA protein tagged with an N-terminal 3×Flag for detection [58] [c].
Rift Valley fever virus-3×NF-NSsLAC [b]	ZH-3×NF-NSsLAC	Recombinant RVFV where the NSs has been replaced by the LACV NSs protein tagged with an N-terminal 3×Flag for detection [58] [c].

[a] experiments with these viruses were performed under BSL-2 conditions. [b] experiments with these viruses were performed under BSL-3 conditions. [c] the referenced publication do not illustrate the rescue of these particular viruses but gives the explanation of the cloning and rescue procedure of them.

Table 3. Rift Valley fever virus (RVFV) expressing La Crosse virus (LACV) NSs mutants, generated during the work for this thesis.

Name[a]	Virus	Description
rRVFV LAC L11A	RVFV	Recombinant RVFV where the RVFV NSs has been replaced by the LACV NSs L11A mutant tagged with an N-terminal 3×Flag.
rRVFV LAC 18to22A	RVFV	Recombinant RVFV where the RVFV NSs has been replaced by the LACV NSs 18to22A mutant tagged with an N-terminal 3×Flag.
rRVFV LAC 33to38A	RVFV	Recombinant RVFV where the RVFV NSs has been replaced by the LACV NSs 33to38A mutant tagged with an N-terminal 3×Flag.
rRVFV LAC 41to48A	RVFV	Recombinant RVFV where the RVFV NSs has been replaced by the LACV NSs 41to48A mutant tagged with an N-terminal 3×Flag.
rRVFV LAC 57to59A	RVFV	Recombinant RVFV where the RVFV NSs has been replaced by the LACV NSs 57to59A mutant tagged with an N-terminal 3×Flag.
rRVFV LAC 67to71A	RVFV	Recombinant RVFV where the RVFV NSs has been replaced by the LACV NSs 67to71A mutant tagged with an N-terminal 3×Flag.
rRVFV LAC 78to87A	RVFV	Recombinant RVFV where the RVFV NSs has been replaced by the LACV NSs 78to87A mutant tagged with an N-terminal 3×Flag.

[a] all experiments with these viruses were performed under BSL-3 conditions

3.3. Primers

Table 4. Cloning and sequencing primers.

Lab. Collection Nr.	Primer Name	Sequence	Description
#45	pI.18_for2	TCCATGGGTCTTTTCTGCAG	Forward primer for sequencing of insert in pI.18 plasmid (see Table 5. Plasmids used in transfection or rescue experiments.Table 5)
#46	pI.18_rev2	GTGACACGTTTATTGAGTAGG	Reverse primer for sequencing of insert in pI.18 plasmid (see Table 5)
RVFV #44	3'XhoI-ZH548_N	GACACTCGAGTTAGGCTGCTGTCTTGTAAGCCTGA	Reverse primer for amplifying the ORF of RVFV N.
RVFV #78	HHcS_ZHPro4rev	TCTGTCGCCGGCCACACAAAGACCCCCTAGTGCT	Forward primer for sequencing of RVFV NSs ORF.
RVFV #97	5'Esp3I-ZH548_N	GACAGACGTCTCACATGGACAACTATCAAGAGCTTGCGAT	Forward primer for amplifying the ORF of RVFV N.
RVFV #117	3xFlag_5'NcoI	GACAGACGTCTCACATGGACTACAAAGACCATGACGG	Forward primer annealing to Flag sequence. Contains a 5' Esp3I site that upon digestion generates a NcoI site.
RVFV #118	LACV_NSs 3'XhoI	GACAGACCGTCTCTTCGACTAAATACCCAGATAATCTGTGG	Reverse primer anneling to the 3'end of LACV NSs. Contains a 3' Esp3I site that upon digestion generates a XhoI site
RVFV #183	NSs diagnostic RVFV	GGTGGGGCAGCCTTAACC	Reverse primer for NSs expression- and sequence-analysis

3.4. Plasmids

Table 5. Plasmids used in transfection or rescue experiments.

Lab. Collection Nr.	Plasmid Name	Antibiotic resistance	Description
#25	pI.18-HA-PKR-DN	Ampicillin	Contains a dominant negative region of PKR (nucleotide +4 to +524 of the PKR ORF, NM_002759.3). Tagged with a 5'HA.
#26	pI.18_RVFV_L	Ampicillin	Expression plasmid containing the ORF of RVFV L protein (nucleotides +16 to +6302 of the RVFV L segment, strain ZH-548, DQ375403.1).
#28	pI.18_RVFV_N	Ampicillin	Expression plasmid containing the ORF of RVFV N protein (nucleotide +36 to +1062 of the RVFV S segment, strain ZH-548, DQ380151.1).
#36	pHH21_RVFV_vL	Ampicillin	Rescue plasmid containing the full-length RVFV L segment in viral sense orientation (RVFV, strain ZH-548, DQ375403.1)
#37	pHH21_RVFV_vM	Ampicillin	Rescue plasmid containing the full-length RVFV M segment in viral sense orientation (RVFV, strain ZH-548, DQ380206.1).
#40	pHH21_RVFV_vN_MCS	Ampicillin	Rescue plasmid containing the full-length RVFV S segment in viral sense orientation, NSs ORF replaced by a tandem cloning site (RVFV S segment, strain ZH-548, DQ380151.1).
#48	pRL-SV40	Ampicillin	Contains the ORF of Renilla luciferase under the control of the SV40 enhancer/promoter (Promega, #E2231)
#77	ISG54-Luc	Ampicillin	Contains the ORF of Firefly luciferase under the control of the ISG54 promoter [110].
#217	pI.18 3xFLAG-LACV_NSs	Ampicillin	Contains the ORF of LACV wt NSs (strain LACV/human/1978, EF485033.1) tagged with a 5' 3×Flag.
#219	pI.18 3xFLAG-ΔMx	Ampicillin	Contains nucleotide +4 to +318 of the Mx1 ORF (XM_005260978.2) tagged with a 5' 3×Flag.
#220	pI.18 3xFlag LAC-NSs-L11A	Ampicillin	Contains the ORF of LACV wt NSs where amino acid position 11 has been changed from a leucine to an alanine via site-directed mutagenesis. Tagged with a 5' 3×Flag.
#221	pI.18 3xFlag LAC-NSs-18to22A	Ampicillin	Contains the ORF of LACV wt NSs where amino acid position 18 to 22 has been changed to alanines via site-directed mutagenesis. Tagged with a 5' 3×Flag.

#222	pI.18 3xFlag LAC-NSs-33to38A	Ampicillin	Contains the ORF of LACV wt NSs where amino acid position 33 to 38 has been changed to alanines via site-directed mutagenesis. Tagged with a 5' 3×Flag.
#223	pI.18 3xFlag LAC-NSs-41to48A	Ampicillin	Contains the ORF of LACV wt NSs where amino acid position 41 to 48 has been changed to alanines via site-directed mutagenesis. Tagged with a 5' 3×Flag.
#224	pI.18 3xFlag LAC-NSs-57to59A	Ampicillin	Contains the ORF of LACV wt NSs where amino acid position 57 to59 has been changed to alanines via site-directed mutagenesis. Tagged with a 5' 3×Flag.
#225	pI.18 3xFlag LAC-NSs-67to71A	Ampicillin	Contains the ORF of LACV wt NSs where amino acid position 67 to 71 has been changed to alanines via site-directed mutagenesis. Tagged with a 5' 3×Flag.
#226	pI.18 3xFlag LAC-NSs-78to87A	Ampicillin	Contains the ORF of LACV wt NSs where amino acid position 78 to 87 has been changed to alanines via site-directed mutagenesis. Tagged with a 5' 3×Flag.

Table 6. Plasmids generated for rescuing RVFV expressing the indicated LACV NSs mutants.

Lab. Collection Nr.	Plasmid Name	Antibiotic resistance	Description
#597	pHH21-RVFV-vN-LAC-FLAG-NSs L11A	Ampicillin	Rescue plasmid containing the full-length RVFV S segment in which the RVFV NSs was replaced by 3×Flag LACV NSs L11A. The insert was amplified from plasmid #220[a].
#598	pHH21-RVFV-vN-LAC-FLAG-NSs 18to22A	Ampicillin	Rescue plasmid containing the full-length RVFV S segment in which the RVFV NSs was replaced by 3×Flag LACV NSs 18to22A. The insert was amplified from plasmid #221[a].
#599	pHH21-RVFV-vN-LAC-FLAG-NSs 33to38A	Ampicillin	Rescue plasmid containing the full-length RVFV S segment in which the RVFV NSs was replaced by 3×Flag LACV NSs 33to38A. The insert was amplified from plasmid #222 [a].
#600	pHH21-RVFV-vN-LAC-FLAG-NSs 41to48A	Ampicillin	Rescue plasmid containing the full-length RVFV S segment in which the RVFV NSs was replaced by 3×Flag LACV NSs 41to48A. The insert was amplified from plasmid #223[a].
#601	pHH21-RVFV-vN-LAC-FLAG-NSs57to59A	Ampicillin	Rescue plasmid containing the full-length RVFV S segment in which the RVFV NSs was replaced by 3×Flag LACV NSs 57to59A. The insert was amplified from plasmid #224 [a].

#602	pHH21-RVFV-vN-LAC-FLAG-NSs 67to71A	Ampicillin	Rescue plasmid containing the full-length RVFV S segment in which the RVFV NSs was replaced by 3×Flag LACV NSs 67to71A. The insert was amplified from plasmid #225 a.
#603	pHH21-RVFV-vN-LAC-FLAG-NSs 78to87A	Ampicillin	Rescue plasmid containing the full-length RVFV S segment in which the RVFV NSs was replaced by 3×Flag LACV NSs 78to87A. The insert was amplified from plasmid #226 a.

[a] The indicated ORF was amplified via PCR using primers RVFV #117/#118. The insert was cloned into plasmid #40 via conventional cloning of Aar1 digested vector and Esp3I digested insert.

3.5. Small interfering RNAs (siRNAs)

Table 7. siRNAs used for knockdown of the indicated targets.

Target name	siRNA name	Supplier	Order Nr.	GeneSolution	Transcript target
Control	All Star Neg. CTRL	Qiagen	SI03650318		
Elongin C	Hs_TCEB1_1 Hs_TCEB1_2 Hs_TCEB1_4 Hs_TCEB1_5	Qiagen	S100741251 S100741258 S100741272 S103056711	GS6921	NM_001204857 NM_001204858 NM_001204859 NM_001204860 NM_001204861 NM_001204862 NM_001204863 NM_001204864 NM_005648
Elongin B	Hs_TCEB2_1 Hs_TCEB2_3 Hs_TCEB2_5 Hs_TCEB2_6	Qiagen	SI00094591 SI00094605 SI03086671 SI03117016	GS6923	NM_007108 NM_207013
Elongin A	Hs_TCEB3_5 Hs_TCEB3_6 Hs_TCEB3_7 Hs_TCEB3_8	Qiagen	SI04152316 SI04226887 SI04258422 SI04309396	GS6924	NM_003198

3.6. Real time PCR primers

Table 8. Commercially available primer sets for SYBR Green-based real time PCR.

Target	QuantiTect Primer Name	Supplier	Order Nr.	Detected transcripts
IFN ß	Hs_IFNB1_1_SG	Qiagen	QT00203763	NM_002176
IFIT1 (ISG56)	Hs_IFIT1_1_SG	Qiagen	QT00201012	NM_001001887.1 NM_001548.4 NM_001270927.1 NM_001270928.1 NM_001270929.1 NM_001270930.1
Ribosomal 18s RNA	Hs_RR18s	Qiagen	QT00199367	X03205.1

Table 9. Primers for real time PCR with SYBR Green-based detection.

Primer Name	Description	Sequence	Reference
LACV N forward	Detects LACV N RNA	GGGTATATGGACTTCTGTG	[160]
LACV N reverse	Detects LACV N RNA	GCCTTCCTCTCTGGCTTA	[160]
Gamma actin forward	Forward primer detecting intron 3 in human γ-actin.	GCTGTTCCAGGCTCTGTTCC	[36]
Gamma actin reverse	Reverse primer detecting intron 3 in human γ-actin	ATGCTCACACGCCACAACATGC	[36]

Table 10. Primers for real time PCR with TaqMan-based detection.

Primer Name	Description	Sequence	Reference
RVFL-2912fwdGG	Forward primer for detection of RVFV L RNA	TGAAAATTCCTGAGACACATGG	[17]
RVFL-2981revAC	Reverse primer for detection of RVFV L RNA	ACTTCCTTGCATCATCTGATG	[17]
RVFL-probe-2950	Probe for detection of RVFV L RNA	6FAM-CAATGTAAGGGGCCTGTG TGGACTTGTG-BHQ1	[17]

3.7. Antibodies

Table 11. Primary and secondary antibodies used in Western blot.

Name	Species	Clonality	Supplier	Catalogue	Dilution
Anti-acetyl-Histone 3	Rabbit	Polyclonal	Merck Millipore	06-599	1:500
Anti-β-Tubulin	Rabbit	Polyclonal	Abcam	ab6046	1:500
Anti-Flag	Rabbit	Polyclonal	Sigma-Aldrich	F7425	1:3200
Anti-RVFV (MP-12)	Rabbit	Serum	Dr. A. Brun, Instituto Nacional de Investigación Agraria y Alimentaria, Madrid, Spain		1:2000
Anti-SIII p15 (Elongin C)	Mouse	Monoclonal	BD Biosciences	610761	1:250
Anti-TCEB3 (Elongin A)	Rabbit	Polyclonal	Sigma Aldrich	HPA005910	1:1000
CTD-pSer2	Rat	Serum	Prof. Dr. D. Eick, Helmholtz Zentrum, München		1:500
CTD-pSer5	Rat	Serum	Prof. Dr. D. Eick, Helmholtz Zentrum, München		1:500
Elongin B (FL-118)	Rabbit	Polyclonal	Santa Cruz	Sc-11447	1:250
LACV N	Rabbit	Polyclonal	Prof. Dr. G. Kochs, Institute of Virology, Universitäts Klinikum Freiburg		1:15000
Pol II (N-20) (RPB1)	Rabbit	Polyclonal	Santa Cruz	sc-899	1:500
Peroxidase-conjugated anti-Mouse IgG	Goat	Polyclonal	Thermo Fisher	0031430 1901971	1:20000
Peroxidase-conjugated anti-Rabbit IgG	Goat	Polyclonal	Thermo Fisher	0031460 1901972	1:20000
Peroxidase-conjugated anti-Rat IgG	Donkey	Polyclonal	Jackson ImmunoResearch	712-036-150	1:20000

Table 12. Primary and secondary antibodies used in immunofluorescence.

Name	Species	Clonality	Supplier	Catalogue Nr.	Dilution
Anti-Flag	Rabbit	Polyclonal	Sigma-Aldrich	F7425	1:500
Anti-Nucleolin	Rabbit	Polyclonal	Abcam	ab22758	1:1000
Anti-SIII p15 (Elongin C)	Mouse	Monoclonal	BD Biosciences	610761	1:250
Anti-TCEB3 (Elongin A)	Rabbit	Polyclonal	Sigma Aldrich	HPA005910	1:500
Elongin B (FL-118)	Rabbit	Polyclonal	Santa Cruz	Sc-11447	1:100
LACV G_C	Mouse	Monoclonal	Prof. Dr. F.G. Scarano, Departments of Neurology and Microbiology, University of Pennsylvania School of Medicine, Philadelphia		1:400
LACV N	Rabbit	Polyclonal	Prof. Dr. G. Kochs, Institute of Virology, Universitäts Klinikum Freiburg		1: 500
Alexa Fluor 488 anti-Mouse IgG	Donkey	Polyclonal	Life Technologies	A21202	1:200
Alexa Fluor 555 anti-rabbit IgG	Donkey	Polyclonal	Life Technologies	A31572	1:200
Alexa Fluor 555 anti-mouse IgG	Donkey	Polyclonal	Life Technologies	A31570	1:200
Alexa Fluor 488 anti-rabbit IgG	Donkey	Polyclonal	Life Technologies	A21206	1:200

3.8. Cell culture

Table 13. Cell culture and transfection reagents

Name	Supplier	Catalogue Nr.
Avicel	FMC BioPolymer	
DMEM, powder, high glucose	Gibco – Life Technologies	52100-021
Dulbecco's Modified Eagle Medium (DMEM)	Gibco – Life Technologies	21969-035
Fetal Bovine Serum (FBS)	Gibco – Life Technologies	10270-106
L-Glutamine (200 mM)	Gibco – Life Technologies	25030-024
Opti-MEM I Reduced Serum Medium	Gibco – Life Technologies	31985-047
Penicillin-Streptomycin (5,000 U/mL)	Gibco – Life Technologies	15070-063
Sodium bicarbonate	Thermo Fisher	25080-094
Sodium pyruvate	Sigma	S8636-100ML
Trypsin-EDTA (0.05%)	Gibco – Life Technologies	25300-054
Lipofectamine RNAiMAX	Life Technologies	13778-150
Nanofectin	PAA	Q051-005
TransIT-LT1	Mirus	MIR 2306

3.9. Isolation, cloning and detection of nucleic acids

Table 14. Cloning reagent, nucleic acid isolation kits and restriction enzymes

Name	Supplier	Catalogue Nr.
E.Z.N.A. Gel Extraction Kit	Omega Bio-Tek	D2500-02
QIAquick Gel Extraction Kit (250)	Qiagen	28706
QIAquick PCR Purification Kit (250)	Qiagen	28106
Shrimp Alkaline Phosphatase (SAP)	Fermentas	EF0511
T4 DNA Ligase	Thermo Scientific	EL0014
E.Z.N.A. Plasmid Midi Kit	Omega Bio-Tek	D6904-04
NucleoBond PC100	Macherey-Nagel	740573.100
E.Z.N.A. Plasmid Mini Kit I	Omega Bio-Tek	D6943-02
peqGOLD Plasmid Miniprep Kit	peqlab	12-6942-02
QIAamp Viral RNA Mini Kit (250)	Qiagen	52906
RNeasy Mini Kit (50)	Qiagen	74104
*Aar*I	Fermentas	ER1581
*Esp3*I	New England Biolabs	R0580S

Table 15. Nucleic acid amplification and detection kits

Name	Supplier	Catalogue Nr.
JumpStart Taq DNA Polymerase	Sigma	D9307-250UN
KOD Hot Start DNA Polymerase	Calbiochem	D2500-02
QIAGEN OneStep RT-PCR Kit	Qiagen	210212
QuantiTect Reverse Transcription Kit	Qiagen	205313
QuantiTect SYBR Green PCR Kit	Qiagen	204143
SensiMix II Probe Kit	Bioline	BIO-91002

3.10. Additional chemicals and kits

Table 16. Additional Chemicals and Kits

Name	Supplier	Catalogue Nr.
2-Mercaptoethanol	Sigma-Aldrich	M3148
2-propanol	Sigma-Aldrich	33539
Actinomycin D	Sigma-Aldrich	A1410
α-amanitin	AppliChem	A1485,0001
Ammonium persulfate	Sigma-Aldrich	A3678
Ampicillin-ratiopharm 1,0 g	Ratiopharm	L61978
Bacto agar	BD	214010
Bovine Serum Albumin	Sigma-Aldrich	A7906
Bromophenol blue	Sigma-Aldrich	B7021
Chloroform	Merck	102445
Chromatography paper	Kobe	4006052
Color Protein Standard (Broad Range)	New England Biolabs	P7712S
Crystal Violet	Sigma-Aldrich	C3886
DAPI (4′,6-Diamidino-2-phenylindole dihydrochloride)	Sigma-Aldrich	D9542
DNaseI (RNase free)	Thermo Scientific	EN0521
Dual-Luciferase Reporter Assay System	Promega	E1960
Ethanol	Sigma-Aldrich	32205
Ethidium bromide	Roth	2218.1
Ethylenediaminetetraacetic acid (EDTA)	Roth	8043.2
FluorSave Reagent	Calbiochem	345789
Formaldehyde	Acros Organics	119690025
Glacial acetic acid	Merck	100063
Glycerol	Roth	3783.2
Glycin	Acros Organics	220910010
Glycogen	Roche	10901393001
Hydrochloric acid	Sigma-Aldrich	30720
Immobilon-P membrane, PVDF	Millipore	IPVH00010

Leptomycin B	USBiological	L1671-38B
Methanol	Sigma-Aldrich	32213
Non-fat dry milk-powder	Saliter	
O'GeneRuler 1 kb Plus DNA Ladder	Thermo Scientific	SM1343
Orange DNA Loading Dye (6X)	Thermo Scientific	R0631
Parafomaldehyde	Roth	0335.3
Peptone from casein	Merck	107213
peqGOLD TriFAST	Peqlab	30-2020
Phosphatase Inhibitor Cocktail Set II	Calbiochem	524625
Polyetylenglycol 8000	Sigma-Aldrich	P2139
Potassium chloride (KCl)	Sigma-Aldrich	31248
Protease inhibitor cocktail (COMPLETE)	Roche	04 693 116 001
Protein Assay Dye Reagent Concentrate	Biorad	500-0006
RiboLock RNase Inhibitor	Thermo Scientific	EO0381
Rotiphorese Gel 30 Acrylamid-Bisacrylamid (37,5:1)	Roth	3029.1
SDS (Dodecyl sulfate sodium salt)	Roth	4360.2
Sodium Chloride (NaCl)	Sigma-Aldrich	31434
SuperSignal West Chemiluminescent Substrate	Thermo Scientific	34096
TEMED (N,N,N′,N′-Tetramethylethylenediamine)	Sigma-Aldrich	T9281
T-PER Tissue Protein Extraction Reagent	Thermo Scientific	78510
Trichloroacetic acid	Sigma-Aldrich	T4885
Tris(hydroxymethyl)aminomethane	Acros Organics	140500010
Triton X-100	Sigma-Aldrich	T9284
Tween 20	Sigma-Aldrich	P7949
Yeast extract	Roth	2363.3

4. Methods

4.1. Cell-based methods

4.1.1. Cell culture

All cell lines were cultivated in the cell culture medium Dulbecco's Modified Eagle Medium (DMEM) supplemented with Foetal Bovine Serum (FBS) to a final concentration of 10 %, 2 mM L-glutamine, 50 units/ml penicillin and 50 µg/ml streptomycin. The cells were propagated at 37 °C and 5 % CO_2. For sub-culturing, the cell monolayer was washed once in phosphate buffered saline (PBS) and detached from the culture flask by trypsin-EDTA treatment. The detached cells were resuspended in cell culture medium and used further for seeding in new flasks/wells.

4.1.2. Plasmid transfections

Transfection of plasmids into attached cells was performed using Nanofectin (PAA) or TransIT-LT1 (Mirus) according to manufacturer's instructions. Shortly, the volume of plasmid(s) needed for the experiment was added to OptiMEM, followed by the transfection reagent. After careful mixing the solution was incubated at room temperature for 15 min. The transfection solution was then added drop-wise into the serum-containing cell culture medium in each well, evenly distributed in the medium by mild shaking using a HS 250 B shaker (IKA Labortechnik) for 5 min at room temperature. After 4 h of incubation at 37 °C (5 % CO_2) the cell culture medium was exchanged by fresh medium and the cells further incubated.

4.1.3. siRNA transfection

For siRNA knockdowns, the transfection reagent Lipofectamine RNAiMAX (Life Technologies) was used according to the manufacturer's instructions. The knockdowns were based on a pre-mixed siRNA solution (GeneSolution) containing four siRNAs directed against four different sequences in the target transcript. The siRNA solution was diluted in OptiMEM, to get a 50 nM final concentration of in the well. The solution was mixed thoroughly, followed by the addition of the appropriate volume of transfection reagent. The solution was thoroughly mixed again and then incubated for 15 min at room temperature. The so-called "reverse transfection" method was then performed. The siRNA solution was added to the empty well followed by seeding of the cells, suspended in an adjusted volume of cell culture medium to get a final concentration of 50 nM siRNA. Following a 4 h incubation at 37 °C (5% CO_2), to allow

for cell-attachment, the cell culture medium was exchanged by fresh medium and the cells further incubated for 72 h. The knockdown procedure described above was then performed an additional time, the day before infection, where the desired amounts of cells for the experiment were seeded.

4.2. Virus-based methods

4.2.1. Virus propagation and sampling

All infections were performed in the Institute for Virology, Philipps University Marburg, under BSL-2 conditions (for LACV) or BSL-3 conditions (for RVFV). The cells were first washed once with PBS and the virus inoculum, diluted in OptiMEM to reach the desired multiplicity of infection (MOI), was then added to the cells. Infections were performed by incubating the flask/plate at 37 °C (5 % CO_2) for 1 h with careful shaking backwards and forwards and from side to side every 10 min. The inoculum was removed and fresh cell culture medium added. As controls, in parallel to the infections, the cellular transcription was inhibited using either the specific RNAPII inhibitor α-amanitin or the general transcription inhibitor Actinomycin D. α-amanitin binds close to the active centre of RPB1 and locks the trigger loop needed for correct addition of nucleotides in an open inactive conformation, thereby inhibiting RNA polymerase II transcription [28, 30]. Actinomycin D is a general RNA synthesis inhibitor through its ability of intercalating the DNA [115, 139]. The control cells where treated as mock cells during virus infection, but post adsorption of the viruses cell culture medium containing the different inhibitors were added to the cells. In experiments where the nuclear export via CRM1 was inhibited, Leptomycin B (LMB) was used. LMB specifically inhibits CRM1 by covalently binding to its Cys-529 residue [85]. The cells were pre-treated for 1 h with LMB and then infected. After infection, LMB containing cell culture medium was added. All cells were incubated at 37 °C (5 % CO_2) for the indicated time of the experiment.

4.2.2. Growing virus stocks

The same procedure for growing virus stocks was used under BSL-2 and BSL-3 conditions. Sub-confluent Vero 76 cells (25 – 30%) seeded in a T175 flask were washed and infected with 5000 plaque forming units (pfu) of the virus, diluted in OptiMEM. Following infection, and removal of the inoculum, fresh cell culture medium was added and the cells maintained at 37 °C (5 % CO_2) for 72 h. The virus-containing supernatant was clarified by centrifugation at 1500 rpm for 5 min at room temperature using a Multifuge 4KR centrifuge (Heraeus). The virus stock was then aliquoted and stored at -80 °C.

4.2.3. Virus titration

Plaque assay with Avicel overlay was used to titrate the virus stocks, under both BSL-2 and BSL-3 conditions. One aliquot of the virus stock was thawed and a dilution series in duplicates, from 10^{-1} – 10^{-8}, was performed in OptiMEM. Confluent CV-1 cells were washed and dilutions 10^{-3} – 10^{-8} were added to successive wells and the cells were infected for 1 h. The inoculum was removed and DMEM supplemented with 1 mM sodium pyruvate, 3.7 g/l sodium bicarbonate, 10 % FBS, 2 mM L-glutamine, 50 units/ml penicillin, 50 µg/ml streptomycin and 1.5 % Avicel was added as an overlay. The cells were then incubated for 72 h at 37 °C (5 % CO_2). To assure that the cell layer did not detach during staining, a 20 % (w/v) trichloroacetic acid (Sigma-Aldrich) dissolved in ddH2O was drop-wise added to the overlay before washing the cells. After thorough, but careful washing, the cells were incubated in staining solution (0.75 % crystal violet, 3.75 % formaldehyde, 20 % ethanol, 1 % methanol) for 10 min. The staining solution was discarded, the cell layer washed twice with PBS and the plaques were counted. For calculation of the stock titer the dilution factor and the volume of the inoculum were accounted for.

4.2.4. Preparation of BSL-3 samples

The procedure for bringing out samples from the BSL-3 security laboratory is described in "SOP Inaktivirung von umhüllten Viren (University of Marburg, UMR104)".

For protein samples, the cell monolayer were washed once with PBS and then lysed in lysis buffer containing one part T-PER (Thermo Scientific) and one part Sample buffer (35.75 mM Tris-HCl (pH 6.8), 7.15 % Glycerol, 1.425 % SDS, 1.075 mM Bromphenol Blue) and supplemented with Complete Protease inhibitor (Roche) and Phosphatase Inhibitor Cocktail Set II (Calbiochem). The cell lysate was then boiled, 100 °C for 10 min, followed by transfer to a new Eppendrof tube. The protein sample was brought out of the BSL-3 laboratory via a 5% Microchem Plus bath. Outside the sample was boiled once more, at 100 °C for 10 min, and then stored at -20 °C until analysis.

RNA samples, either viral RNA from cell culture medium or total cellular RNA, were brought out of the BSL-3 laboratory using QIAamp Viral RNA Mini Kit (Qiagen) or RNeasy Mini Kit (Qiagen), respectively. Viral RNA, from cell culture medium, was isolated in AVL buffer while total cellular RNA was isolated in RLT buffer. Both buffers contain 4 M guanidinium thiocyanate and were incubated with the respective samples for 10 min at room temperature, after which an equal volume of 100 % or 70 % ethanol, for viral RNA or total cellular RNA isolation, respectively, was added. The solution was briefly vortexed and pelleted, after which it was transferred to a new Eppendorf tube and removed from the BSL-3 laboratory through a 5 %

Microchem Plus bath. The RNA was then immediately isolated according to manufacturer's protocol and stored at -20 °C until analysis.

4.3. Rescuing recombinant RVFV expressing LACV NSs mutants

Seven domains in orthobunyavirus NSs proteins were identified to be conserved throughout the genus. We constructed alanine mutants for these conserved domains, in LACV NSs, to determine their importance for the different functions of the NSs protein. To be able to performed experiments and detect the LACV NSs under viral infection we used a reverse genetics system for RVFV developed in our group. Due to the expression of the NSs protein from a +1 ORF in the same mRNA as the N protein during authentic LACV infection (see Fig. 1B), no Flag-tag could be added to the NSs sequence without disturbing the N sequence. RVFV expresses the N and NSs from two separate mRNAs, due to ambisense coding of the S segment. The NSs protein of RVFV was therefore replaced by the LACV NSs mutants, by conventional cloning into a plasmid containing the full-length RVFV S segment. Plasmids containing the full-length RVFV segments, transcribed by a RNA polymerase I driven promoter, where then transfected into cells to rescue RVFV expressing the different LACV NSs mutants. Plasmids encoding for RVFV N and L proteins, under the control of a RNAPII promoters, were co-transfected to initiate viral transcription and replication.

4.3.1. Conventional cloning of LACV NSs mutants into RVFV S-segment

In order to construct RVFV expressing LACV NSs, the cloning strategy published in [58] was performed where RVFV NSs was replaced by LACV NSs mutants. We used plasmid RVFV #40, containing the full-length RVFV S-segment in viral sense, with the NSs ORF replaced by a tandem cloning site containing two mirrored *Aar*I sites. Upon digestion with *Aar*I, non-compatible sticky ends were formed, which were compatible with *Nco*I and *Xho*I recognition sequences. The 5' overhangs of the vector were de-phosphorylated with shrimp alkaline phosphatase (Fermentas). We amplified the LACV mutants using the KOD Hot Start DNA Polymerase (Calbiochem) according to the manufacturer's instructions with primers RVFV #117 and RVFV #118 and plasmids #220 – 226 as templates. The two primers contained a 5' *Esp3*I site, which upon digestion of the PCR product generated a 5' *Nco*I and a 3' *Xho*I recognition sequence. The vector and PCR products were separated on a 1 % agarose gel in TAE buffer at 100 V for 1 h, the bands were stained with 0.5 µg/ml ethidium bromide in ddH2O for 20 min and then excised from the gel. The PCR-insert and vector were then gel-purified using E.Z.N.A. Gel Extraction Kit (Omega) according to manufacturer's protocol. A 3:1 ratio, of insert to vector, was used to ligate the PCR products into the RVFV S-segment plasmid using

T4 DNA ligase (Fermentas) according to the manufacturer's instructions. The ligated plasmids were transformed into competent DH10B bacteria, plated on 100 µg/ml ampicillin LB-agar plats (10 g/L peptone, 5 g/L yeast extract, 10 g/L NaCl, 15 g/L agar) and incubated overnight at 37 °C. The same vector preparation, as used for ligation of the LACV NSs mutants, was re-ligated and used as negative control in the transformation of the DH10B cells. One colony from each plate was picked and used as both template in a colony PCR and as inoculum for an over-night culture in 100 µg/ml ampicillin LB medium (10 g/L peptone, 5 g/L yeast extract, 10 g/L NaCl). To assure correct insertion a colony PCR was performed with Taq polymerase (Sigma) according to the manufacturer's instructions with primers RVFV #78 and RVFV #118. As template for the PCR the colony on a pipette-tip was dipped into the PCR reaction and then transferred to the LB medium, the template amount in the protocol was replaced by ddH2O to achieve the correct volume. The PCR reaction was run according to the manufacturer's instruction. The PCR products were separated on a 1 % agarose gel in TAE buffer at 100 V for 1 h, and the bands stained in 0.5 µg/ml ethidium bromide in ddH2O for 20 min, after which the PCR product was visualized using a Gel Doc 2000 (BioRad). The over-night cultures, from the same colony that was used in the colony PCR, were isolated using the E.Z.N.A. Plasmid Mini Kit I (Omega Bio-Tek) according to the manufacturer's instructions. To assure that the correct mutant had been ligated in the corresponding plasmid the inserts were sequenced by Seqlab Sequence Laboratories/Microsynth AG (Göttingen, Germany) in both forward and reverse direction using primers RVFV #78 and RVFV #183.

4.3.2. Rescue of recombinant RVFV expressing LACV NSs mutants

For rescue of RVFV expressing the LACV NSs mutants, a RNA polymerase I/II driven plasmid system was used, described in [58]. A 2:1 co-culture of HEK-293 and BHK-21 cells, in 6-well plates, were transfected, in duplicates, with a solution containing, in a ratio 1:2, helper plasmids #25 (PKR-DN), #28 (RVFV N), #26 (RVFV L) and the full-length plasmids #37 (RVFV vM), #36 (RVFV vL) and the respective RVFV S segment containing LACV NSs mutants, #597 – 603. The transfection was performed under BSL-3 conditions using TransIT-LT1 (Mirus) as transfection reagent. After 4 h of incubation at 37 °C (5 % CO_2) the cell culture medium was exchanged and the cells further incubated for 96 h. The virus-containing supernatants were clarified by centrifugation at 1500 rpm for 5 min at room temperature using a Multifuge 4KR centrifuge (Heraeus). The cleared supernatants were then used as inoculum to amplify the rescued viruses, by two successive propagations on BHK-21 cells, where 72 h, at 37 °C (5 % CO_2), incubations were used for each propagation. The second passage of the rescued viruses was used to grow virus stocks, on Vero 76 cells, as described above in section 7.2.2. The virus stocks were titrated by plaque assay as described in section 7.2.3.

4.3.3. Validation of the correct LACV NSs mutant inserted in the RVFV backbone

Viral RNA was isolated from virus stocks as described above in section 7.2.4. The isolated viral RNA was DNase I-treated, to assure that no rescue plasmid contamination would interfere with the interpretation of the result. OneStep RT-PCR (Qiagen) reactions according to the manufacturer's protocol was performed on the viral RNA, amplifying the ORF of RVFV N using primers RVFV #97/RVFV #44 or the ORF of NSs using primers RVFV #78/RVFV #183. The RT-PCR products were separated on a 1 % agarose gel in TAE (40 mM Tris, 20 mM acetic acid, 1 mM EDTA) at 100 V for 1 h followed by staining of the DNA bands with 0.5 µg/ml ethidium bromide in ddH2O for 20 min. The PCR products were visualized with a Gel Doc 2000 (BioRad). To assure that the correct LACV NSs mutant was rescued in the corresponding virus the NSs RT-PCR products were sequenced at Seqlab Sequence Laboratories/Microsynth AG (Göttingen, Germany) in both the forward and reverse direction using primers RVFV #78 and RVFV #118.

4.4. Interferon induction assay

4.4.1. VSV RNA isolation

As an inducer of the type I IFN system, we used vesicular stomatitis virus (VSV) RNA isolated from virus particles. BHK-21 cells (90 % confluent), were infected at a MOI 0.001 of VSV by adding an appropriate volume of stock virus directly to the cell culture medium on the cells. The cells were then incubated for 72 h at 37 °C (5 % CO2). The cell supernatant, containing released viruses, was cleared from cell debris by centrifugation at 1500 rpm for 7 min at 4 °C using a Multifuge 1 S-R centrifuge (Heraeus). To precipitate viral particles, the cleared supernatant was then mixed with 30% PEG8000 in NTE (10 mM Tris (pH 6.5), 1 mM EDTA, 255 mM NaCl) in an Erlenmeyer flask and incubated at 4 °C for 30 min with mild shake. The mixture was transferred to a Falcon tube and the viruses pelleted by centrifugation at 6000 rpm for 1 h at 4 °C in an Avanti J-26 XP (Beckman Coulter). The pellet was then re-suspended in 1.5 mL TriFAST (Peqlab) by incubating for 5 min with vortexing every second min. To isolate RNA, the solution was transferred to a 15 mL Falcon tube and 300 µl Chloroform added. The tube was shaken vigorously, incubated at room temperature for 10 min, and centrifuged at 4600 rpm for 11 min at 4 °C using a Multifuge 1 S-R centrifuge (Heraeus). This allowed the separation of the solution in three phases. The upper phase was transferred to a new 15 ml Falcon tube, 750 µl isopropanol and 30 µg glycogen were added and the solution was then incubated at -20 °C for 16 h. The RNA was then precipitated by centrifugation at 4600 rpm for 33 min at 4 °C using a Multifuge 1 S-R centrifuge (Heraeus). The supernatant was discarded and the RNA pellet

washed twice with 70 % ethanol. After drying, the pellet of RNA was resuspended in TE buffer (10 mM Tris-HCl (pH 8.0), 1 mM EDTA) to a concentration of 250 ng/µl. The VSV RNA preparation was aliquoted and stored at -80 °C.

4.4.2. Luciferase reporter gene assay

To test the LACV NSs mutant's ability to inhibit induction of innate immunity we used an interferon induction assay. A master mix containing the inducible firefly luciferase (under the ISG54-promoter, plasmid #77) and the constitutively expressed renilla luciferase (under the SV40-promoter, plasmid #48) was prepared in OptiMEM. The master mix was divided and one of the LACV NSs mutants (plasmids #220 – 226), LACV NSs wt (plasmid #217) or a control plasmid (#219) was added in the presence or not of VSV RNA at a final concentration of 250 ng/well. The Nanofectin (PAA) transfection reagent was used according to the manufacturer's instructions, and the transfection mixes were incubated at room temperature for 20 min. The transfection solutions were then added drop-wise to monolayers of HEK-293 cells (50 % confluent) in 12-well plates. The transfection complexes were evenly distributed in the cell culture medium by mild shaking on a HS 250 B (IKA Laborteknik) for 5 min at room temperature. The cells were then incubated for 4 h at 37 °C (5 % CO_2), after which the cell culture medium was exchanged and the cells further incubated for 20 h. Firefly and renilla luciferase activity was measured with the Dual-Luciferase Reporter Assay System (Promega). The cell culture medium was removed and the cells immediately lysed in passive lysis buffer, provided in the kit, by direct addition to the well followed by incubation for 20 min with vigorous shaking at room temperature. 1/10 of the lysis buffer volume was used for luciferase activity measurement in a black 96-well microplate (Greiner Bio-One). The luciferase activity was measured in a Centro LB 960 (Berthold Technologies) using the program MiroWin 2000 (Mikrotek Laborsystem GmbH). For calculations of the respective luciferase activity induction, all samples were compared to the control plasmid transfected sample without co-transfection of VSV RNA.

4.5. Molecular biology methods

4.5.1. Western blot for protein detection

The isolation of protein samples brought out of the BSL-3 has already been described in section 6.2.3. The same protocol was followed for preparing samples under BSL-2 conditions, however only one boiling step of the sample for 10 min at 100 °C was performed. The protein samples were loaded onto SDS-PAGE gels, containing a upper stacking gel (4 % acrylamide/bisacrylamid (37.5:1 ratio), 125 mM Tris-HCl (pH 6.8), 0.1 % SDS, 0.05 % APS

and 1 % TEMED and a lower separation gel containing either 5 % or 15 % acrylamide/bisacrylamid (37,5:1 ratio), 375 mM Tris-HCl (pH 8.8), 0,1 % SDS, 0,05 % APS and 0,05 % TEMED. The SDS-PAGE gels were run in Mini-Protean Tetra System chambers (Biorad) using running buffer (25 mM Tris (pH 8.3), 192 mM glycine, 0.1 % SDS) at a constant current of 200 V, allowing the separation of the proteins according to their molecular weight. The transfer of proteins to methanol-preactivated Immobilon-P membrane (PVDF, Millipore) was performed by wet-blot (5% gels) or semi-dry blotting (15% gels). For wet blot the Criterion blotter (Biorad) was used with Towbin buffer (25 mM Tris, 192 mM Glycin, 20 % methanol) and was run at 250 mA for 1.5 h. The semidry blotting was performed in Trans-blot SD cell (Biorad) using semidry blotting buffer (48 mM Tris, 39 mM Glycine, 0.0375 % SDS, 20 % methanol) and was run at 75 mA/gel for 1 h. After blotting, the membranes was washed once in TBS buffer (20 mM Tris-HCl (pH 7.6), 137 mM NaCl) followed by blocking in 5 % (w/v) non-fat milk powder dissolved in TBST (TBS buffer, 0.1 % Tween-20) for 1 h at room temperature with mild shaking. Phosphospecific antibodies were diluted in 5 % BSA (w/v) in TBST, while all other antibodies were diluted in 1 % (w/v) non-fat milk powder dissolved in TBST. The membranes were incubated over-night at 4 °C in the primary antibody solutions. The next day the membranes were washed three times in TBST followed by incubation in 5 % (w/v) non-fat milk powder dissolved in TBST containing the appropriate peroxidase conjugated secondary antibody. Before detection the membranes were washed three times in TBST followed by three times in TBS. The proteins bands were visualized in a ChemiDoc XRS+ (Biorad) using SuperSignal West Chemiluminescent Substrate (Thermo Scientific).

4.5.2. Immunofluorescence

To detect the cellular localization of our target proteins indirect immunofluorescence was performed. The cell monolayer, grown on coverslips, were infected or transfected and at the end of the experimental incubation the cells were washed once in PBS and fixed in 3 % (w/v) paraformaldehyde in PBS for 20 min at room temperature. The cells were then washed three times with PBS. Permeabilization of the cells was performed by incubating the cells in a solution of PBS containing 0.5 % Triton-X 100 for 15 min at room temperature. The cells were then washed three times with PBS. To block unspecific primary antibody binding, the cell layer was incubated in 1 % FBS in PBS for 20 min at room temperature. The cells were then incubated for 1 h with the primary antibodies diluted in 1 % FBS in PBS. The cells where again washed three times in PBS, followed by incubation in secondary antibodies, and DAPI, diluted in 1% FBS in PBS, for 45 min under dark conditions. Following the staining with secondary antibodies the cells were washed three times in PBS and two times with ddH2O before the coverslips were mounted on object glasses (Thermo Scientific) using FluorSave (Calbiochem). The FluorSave was allowed to polymerize and the mounted coverslips were stored at 4 °C until

analysis. The stained proteins were visualized, and images taken, with an AxioVert 200 M microscope coupled to an AxioCam MRm camera (Zeiss).

4.5.3. Real time RT-PCR

For the detection of cellular mRNA and viral RNA levels, isolated using the RNeasy Kit (Qiagen), real time reverse transcription PCR was used. The RNA concentration of each sample was measured on a Nanodrop spectrophotometer (Thermo Scientific) and removal of possible DNA contamination in the RNA preparation was performed with the gDNA wipeout buffer, provided in the QuantiTect Reverse Transcription Kit (Qiagen). Equal amounts of RNA were then reverse transcribed using the supplied primer mix, which consists of an oligo-dT and random primers. The synthetized cDNA was then used as template for the real time PCR reactions with the QuantiTect SYBR Green PCR Kit (Qiagen), or for RVFV L RNA detection with the SensiMix II Probe Kit (Bioline). The internal control 18S ribosomal RNA and the mRNAs for IFN-β, ISG56 were detected with QuantiTect Primers (Qiagen) while γ-actin-intron assay [36], LACV N [160] and RVFV L [17] were detected with indicated published primers. Due to the high amount of 18S ribosomal RNA the cDNA was diluted 1:100 for this specific gene analysis. The real time PCR reaction and measurement was performed on a StepOne System (Applied Biosystems). For relative RNA calculations the ΔΔCt method [92] was used with 18S ribosomal RNA as internal control. Two controls for each primer-pair were used; 1) ddH2O was used as template in one reaction and 2) a non-reverse transcribed Mock sample RNA. A melt curve analysis, at the end of the real time PCR program, was performed to assure that the SYBR green signal detected came from one amplicon with the same T_m.

4.6. Statistical analysis

When statistical analysis was performed, comparing two groups of samples, a two-tailed, unpaired t-test was performed using Microsoft Excel. P-values ≤ 0.05 were considered as significant, indicated with (*) in figures where statistical analysis were performed.

5. Results[1]

The major function of the NSs protein of the *Bunyaviridae* is the inhibition of innate immune induction of mammalian hosts [132]. However, the mechanism varies between the genera and from virus to virus. As for other members of the *Bunyaviridae* genus orthobunyaviruses, LACV NSs acts on the transcriptional level. Indeed, our group had demonstrated that LACV NSs induces the proteasomal-degradation of the largest subunit, RPB1, in transcriptionally elongating RNA polymerase II [160].

5.1. Time course for induction of RPB1 disappearance under infection

5.1.1. Time course of wt LACV induced RPB1 disappearance

To confirm previous result of LACV NSs induced RPB1 disappearance, and to determine the kinetics of RPB1 disappearance in LACV wt-infected cells, time course experiments were performed with samples taken 1, 2, 3 and 4 hours post infection (h.p.i.). We also compared with the kinetics of RPB1 disappearance in cells treated with either the general transcription inhibitor Actinomycin D or the RNAPII specific inhibitor α-amanitin.

The Western blot result of a representative time course is depicted in Fig. 2. Total RPB1, with the II_A (transcriptionally inactive) and the II_O (transcriptionally elongating) forms, and the specific markers for transcription initiated (CTDpSer 5) or elongating (CTDpSer 2) RPB1 is presented. As no antibody against LACV NSs is available, we monitored the infection by detection of the N protein, which is expressed from the same mRNA as the NSs protein (Fig. 1B). The two viruses displayed different growth kinetics. LACV wt grew faster, with weak N protein detection already 1 h.p.i., while LACV ΔNSs grew slightly slower with N protein detection 3 h.p.i. (Fig. 2). The growth kinetics for LACV wt correlated with the disappearance kinetics for RPB1, with a lack of total RPB1 seen already 1 h.p.i. However, unlike the disappearance of RPB1 observed previously for LACV wt, where first the II_O form disappears and an increased signal of the area in-between the II_O and II_A form was noted [160], a synchronized disappearance of both RPB1 forms was observed (Fig. 2).

[1] The results presented in this thesis have not been published so far in any peer-reviewed scientific journal. However a manuscript is under preparation. Not all data produced during the work will be presented.

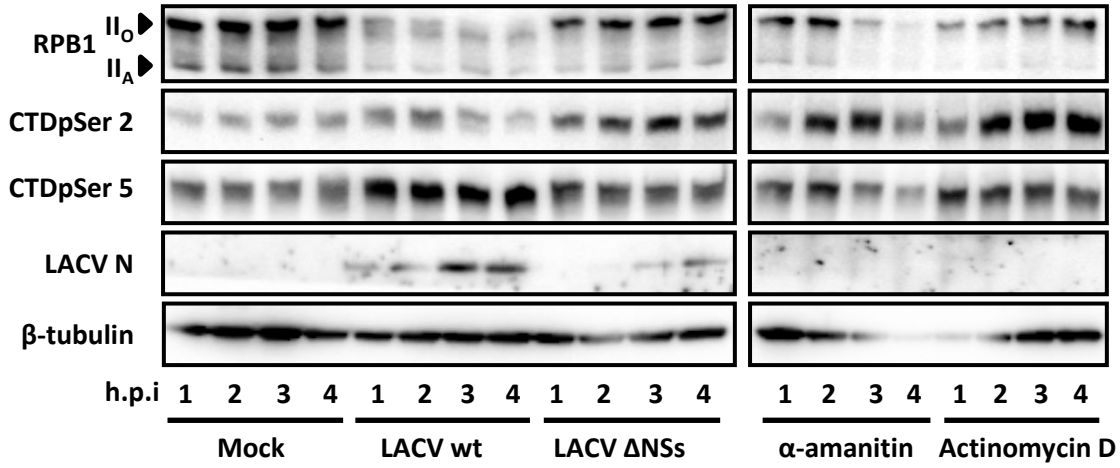

Figure 2. LACV NSs induces RPB1 degradation faster than transcription inhibitors. HuH-7 cells were Mock -treated, infected with LACV wt or LACV ΔNSs (MOI 10), or treated with α-amanitin (10 µg/ml) or Actinomycin D (10 µg/ml). The infection/treatment was allowed to progress for the indicated time until samples were taken and analysed by SDS-PAGE and Western blot. The figure is representative of at least three independent experiments.

The slight difference in the disappearance pattern for RPB1, between these and previously published results [160], might be the difference in cell line (Vero cells in [160] versus Huh7 cells here) used for the experiments. However, when comparing the disappearance of total RPB1 in LACV wt infected cells with total RPB1 in LACV ΔNSs infected cells, the II_O form of RPB1 is most affected of the two forms in agreement with published observations [160]. No degradation of RPB1 was detected in LACV ΔNSs infected cells. The transcriptionally elongating form of RPB1, CTDpSer 2, started to diminish at 3 h.p.i. in wt LACV infected cells (Fig. 2). A possible explanation for the slight delay in induction of disappearance between total RPB1 and the transcriptionally elongating form in LACV wt infected cells, might be the different antibodies used where the phosphor-specific one is more sensitive. The antibody used to detect total RPB1 recognizes one epitope on RPB1 while the phosphor-specific antibody has up to 52 epitopes it could recognize. The initial disappearance of CTDpSer 2 is in agreement with published results, demonstrating that LACV NSs targets the transcriptionally elongating form of RPB1. However, unlike the disappearance of total RPB1 and CTDpSer 2, the transcriptionally initiated form of RPB1, CTDpSer 5, was observed to increase in LACV wt infected cells (Fig. 2). This increased signal for CTDpSer 5 might be an attempt by the cells to promote transcription in response to the NSs induced disappearance of the elongating CTDpSer 2 form of RPB1. A similar, but not as pronounced, increase in transcriptionally initiated RPB1 was seen for Actinomycin D. The treatment of cells with α-amanitin induced the disappearance of total RPB1 3 h after the start of inhibitor treatment, slight delay compared to LACV wt infection. Both treatment with α-amanitin and Actinomycin D caused the II_A form of RPB1 to disappear initially, followed by the II_O form in α-amanitin treated cells. Actinomycin D treatment of cells did not have any effect on the II_O form but slightly increased the CTDpSer 2

signal. Finally, α-amanitin treatment induced a slight decrease in the CTDpSer 5 form 3 h.p.i., but no striking effect was seen on the CTDpSer 2 form (Fig. 2).

5.1.2. Time course of RPB1 disappearance in cells infected with a heterologous virus expressing LACV NSs

To be able to detect LACV NSs expression under viral infection, we took advantage of a recombinant Rift Valley Fever virus (RVFV, phlebovirus) expressing the LACV NSs with an N terminal 3×Flag-tag [58]. The 3×Flag tag could not be added directly to the NSs in the authentic LACV background since the NSs is expressed from a +1 shifted ORF embedded in the N protein mRNA (Fig. 1B). The N protein is essential for viral replication and therefore no change in the sequence of NSs could be made without disturbing the N sequence. To compare the kinetics of RPB1 degradation, and the possible correlation with NSs expression, HuH-7 cells were infected with RVFV expressing either 3×Flag-tagged LACV NSs or RVFV NSs.

Under infection with RVFV expressing LACV NSs, the induction of total RPB1 disappearance was detected 3 h.p.i., as a lack of the II_O form of RPB1 (Fig. 3). This is slightly later then for LACV wt seen in Fig. 2. However, the expression of the LACV NSs protein correlated with the induction of RPB1 disappearance. The RVFV NSs does not induce any disappearance of RPB1. However, would we have allowed the infection to progress, the RVFV NSs inhibition of THIIH [75, 76, 87] would most likely have caused a RPB1 disappearance as a secondary effect due to transcription inhibition, as seen for α-amanitin.

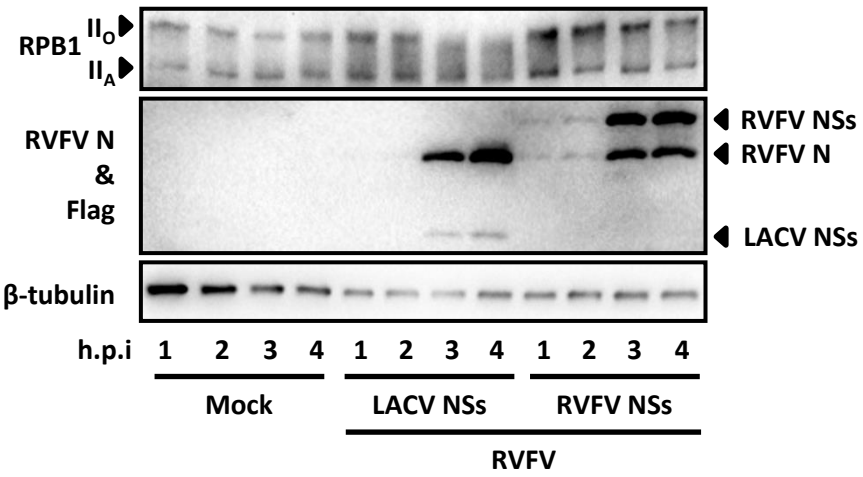

Figure 3. LACV NSs expressed by RVFV induces degradation of RPB1 with similar kinetics as the LACV wt. HuH-7 cells were either Mock-treated or infected with RVFV expressing either LACV NSs or RVFV NSs (MOI 10) for the indicated times. Samples were taken and analysed by SDS-PAGE and Western blot. The image is representative of three independent experiments.

Interestingly, even though the expression of the two NSs proteins are regulated by the same promoter in the RVFV, levels of LACV NSs are much weaker than of RVFV NSs (Fig. 3), most likely indicating a lower stability of LACV NSs. A lower stability of LACV NSs compared to the NSs protein of another orthobunyavirus Snowshoe hare virus have also been reported [50]. The RVFV N protein, used as a control for the infection, displayed similar kinetics and expression for the two viruses.

In summary, LACV NSs induces the disappearance of RPB1 faster than the specific RNAPII inhibitor α-amanitin. Furthermore, the induction of RPB1 disappearance correlates with the expression of LACV NSs, and LACV NSs is sufficient to degrade RPB1 independently of the viral background.

5.2. LACV NSs Pull down assays of Elongin C

After having identified the mechanism of LACV NSs inhibition of the antiviral type I IFN induction, by degradation of RPB1 in transcriptionally elongating RNAPII [160], it was of interest to identify host-cell interactors of the LACV NSs protein. Attempts in our group to identify NSs interactors had been performed via pull down assays on E3 ligase subunits. The reason for these directed attempts was both the requirement of the proteasomal pathway for RPB1 degradation during LACV wt infection and the demonstration of an interaction between MED8 and Bunyamwera virus NSs [89]. MED8 is part of the Mediator complex, but has also been demonstrated to form an ubiquitin E3 ligase [27].

The *in vitro* pull down assays performed in our group to find LACV NSs interactors were based on bacterially expressed GST-tagged LACV NSs or a control protein. Our control protein is the first 106 amino acids of the MxA protein, which retains no MxA functions, and has approximately the same molecular size as the LACV NSs protein. The pull downs attempts were carried out by mixing the GST-tagged proteins, immobilized on glutathione-agarose beads, with radiolabelled *in vitro* transcribed/translated interaction candidates. The only reproducibly pulled down interactor of LACV NSs was Elongin C (unpublished, see [159]). No interaction was seen between LACV NSs and Elongin A or Elongin B. Elongin C was a promising interaction candidate since it has been demonstrated to be a subunit in both the Elongin complex, that increases RNAPII transcription elongation rates, and as a subunit of several cellular and viral ubiquitin E3-ligases, see chapter 4.7. in the introduction.

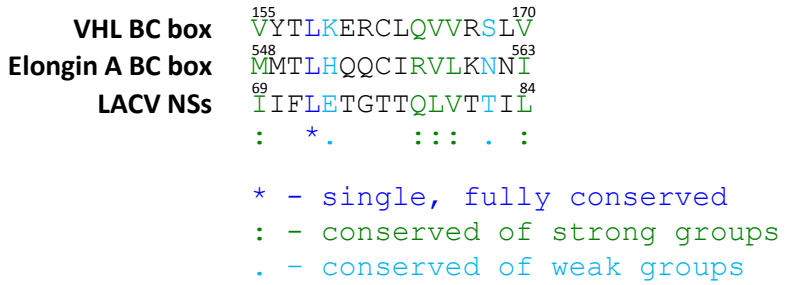

Figure 4. LACV NSs contains a partial BC box motif. Clustal W alignment of LACV NSs and the BC boxes from VHL and Elongin A. Only the respective BC boxes and the aligned sequence of LACV NSs are shown for clarity, with amino acid residue numbers of the first and last residue depicted on-top of the respective sequence.

All known Elongin BC interactor contain a so called BC box motif [(STP)Lxxx(CSA)xxxϕ] [93], which is required for interaction with Elongin C. Interestingly, using the Clustal W program to align the protein sequence of LACV NSs with the BC boxes from the VHL and Elongin A proteins, a partial BC box motif in LACV NSs was identified (Fig. 4). Importantly, the crucial leucine residue at position 4, was also present at the correct position in the potential LACV NSs BC box (Fig. 4).

I performed different pull down assays to reproduce the *in vitro* interaction seen between LACV NSs and Elongin C. Flag-tagged LACV NSs and control protein, same as above, were expressed by *in vitro* transcription/translation, plasmid transfection into cells or by the RVFV described in section 8.1.2. For the expression of Elongin C or control proteins, different expression systems where used. Plasmids encoding Elongin C and the control protein, coupled to Renilla luciferase, were used in an *in vitro* transcription/translation expression system. Another approach was to use plasmids encoding Elongin C, control protein or Elongin B, tagged with a HA-tag, to either transiently express the different proteins or create stable cell-lines. Different combinations of proteins, isolated by the respective expression systems, were combined in pull down experiments. However, despite some initially encouraging results, no robust and reproducible interaction was detected between LACV NSs and Elongin C.

5.3. Subcellular localization of endogenous proteins during infection

5.3.1. Subcellular localization of Elongin C under LACV wt infection

The interaction between LACV NSs and Elongin C might be too weak or transient for reproducible detection with pull-down assays. As an alternative, we investigated the subcellular localization of Elongin C, and the possible effect LACV NSs might have on it. For this purpose HuH-7 cells were mock treated, infected with LACV wt or LACV ΔNSs or treated with the

specific RNAPII inhibitor α-amanitin. After completion of the infection, the cells were stained against endogenous Elongin C and the LACV N protein.

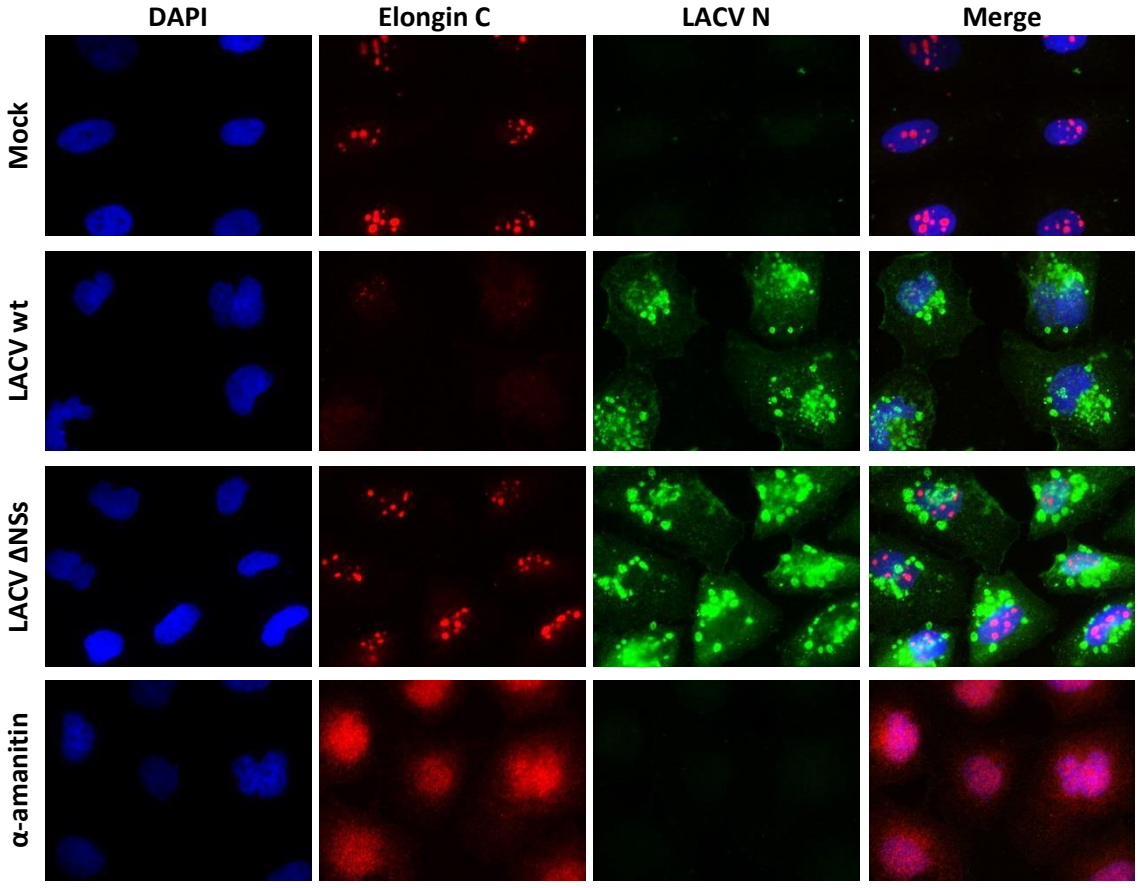

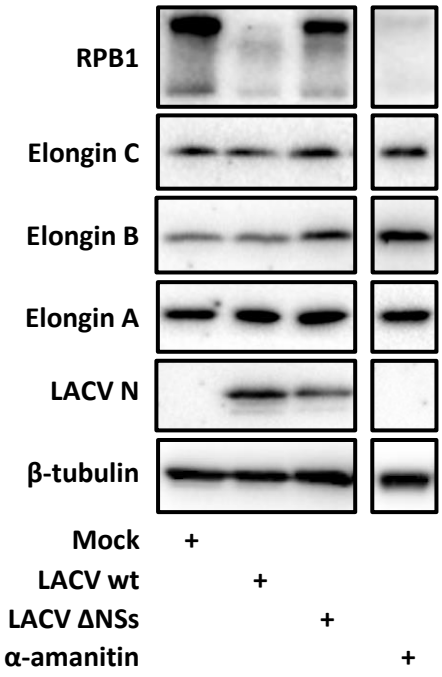

Figure 5. Elongin C is re-localized by LACV NSs from the nucleoli. HuH-7 cells were grown on coverslips and either Mock-treated, infected with LACV wt or LACV ΔNSs (MOI 1) or treated with α-amanitin (10 µg/ml) for 16 h. The cells were fixed, permeabilized and stained against endogenous Elongin C and LACV N protein, the nucleus was counterstained with DAPI. Images were taken with a Apotome (Zeiss) at a magnification of ×630. Protein samples for SDS-PAGE and Western blot were prepared in parallel to the immunofluorescence samples and separated on 5 or 15 % SDS-PAGE gel. The indicated proteins were stained for and detected via chemiluminescence in a Chemidoc XRS+ (BioRad). Images and blots are representative of at least three independent experiments.

As can be seen for mock treated cells in (Fig. 5), Elongin C primarily localized to patches in the nucleus, which most likely corresponds to the nucleoli, with weaker staining of the whole nucleus. The microscope setting for taking images was adjusted so as not to overexpose the Elongin C in the nucleoli. However, a diffuse and weak staining of Elongin C in the cytoplasm was also seen in the microscope (data not shown). To our knowledge this is the first time Elongin C has been demonstrated to primarily localize to the nucleoli. This localization was unexpected since the nucleolus is the primary site of ribosomal RNA synthesis by RNAPI [56], whose transcription Elongin C has not been implicated in. Infection of the cells with LACV wt caused a loss of the Elongin C signal, from the nucleoli specifically but also from the complete nucleus (Fig. 5, LACV wt). The loss of signal was induced by the NSs protein since infection with LACV ΔNSs did not have any effect on Elongin C compared to mock (Fig. 5). To assure that the lack of a signal in LACV wt infected cells was not due to a degradation of the protein, samples for SDS-PAGE and Western blot was prepared in parallel. We stained against all three subunits of the Elongin complex, Elongin A/B/C, but did not detect any change for anyone of the subunits (lower part of Fig. 5). Since no degradation of Elongin C was detected, the loss of signal in the immunofluorescence was most probably due to a re-localization of Elongin C by LACV NSs. To assure that the LACV NSs induced RPB1 disappearance, total RPB1 was stained for. This late in infection (16 h.p.i.) barely detectable levels of RPB1 was observed in LACV wt infected cells. For cells treated with the specific inhibitor of RNAPII, α-amanitin, we also saw a redistribution of Elongin C (Fig. 5). However, unlike cells infected with LACV wt, a primarily still nuclear staining for Elongin C was seen. A strong signal for the LACV N was seen for both LACV wt and LACV ΔNSs, with a dot-like appearance that are probably viral factories for replication and transcription [45].

Similar to experiments shown in Fig. 2, time-course experiments for re-localizations of Elongin C were performed. However, a firm correlation between onset of RPB1 disappearance and a re-localization of Elongin C could not be established.

5.3.2. Subcellular localization of Elongin A and B under LACV infection

In Fig. 5, Elongin C was demonstrated to be re-localized by LACV NSs. We then wondered if LACV NSs had any effect on the subcellular localization of the two other subunits of the Elongin complex, Elongin A and B. To answer this question, similar immunofluorescence experiments were performed and HuH-7 cells were stained against Elongin A or Elongin B. In Fig. 5 LACV N was used to stain for infection, however due to the same species origin of the LACV N and Elongin A/B antibodies, the LACV glycoprotein G_C was stained for instead as control for infection. As we already demonstrated in Fig. 5 (lower part), none of the Elongin subunits were degraded during infection with LACV wt. However, unlike Elongin C, neither Elongin A nor Elongin B changed their subcellular localization upon infection with LACV wt (Fig. 6). Both Elongin A and B displayed a primarily nuclear staining with a weak cytoplasmic signal (Fig. 6). As can be seen in the upper panel, the signal for Elongin A had a dot-like appearance in the nucleus. A slightly stronger signal was observed in cells displaying the G_C signal, compare (LACV wt or LACV ΔNSs infected with Mock, Fig. 6). Upon treatment with α-amanitin, the signal for Elongin A concentrated in the dot-like structures and less overall staining was observed. Elongin B displays a homogenous staining of the nucleus (lower panel, Fig. 6), without any changes upon infection or RNAPII inhibitor treatment. A perinuclear staining was observed for the G_C protein, probably ER/Golgi where viral glycoprotein translation and viral budding occur, respectively (Fig. 6).

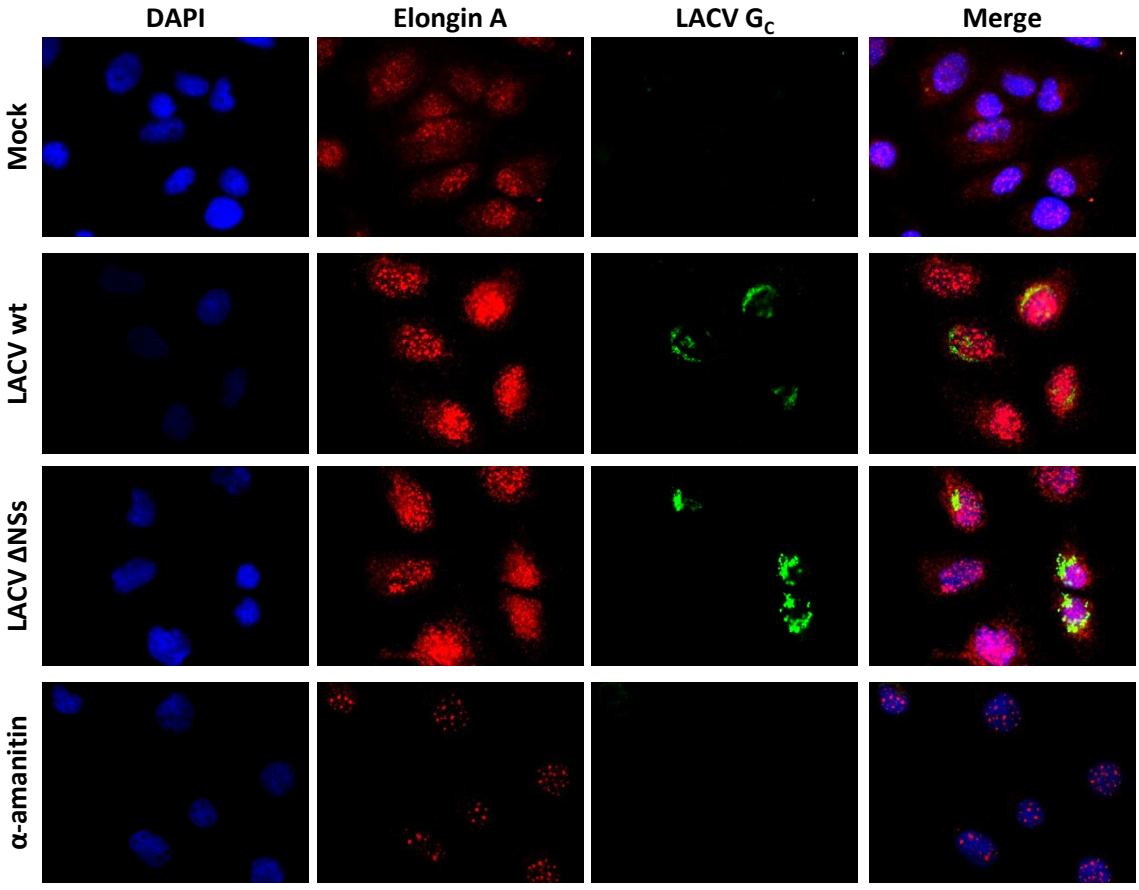

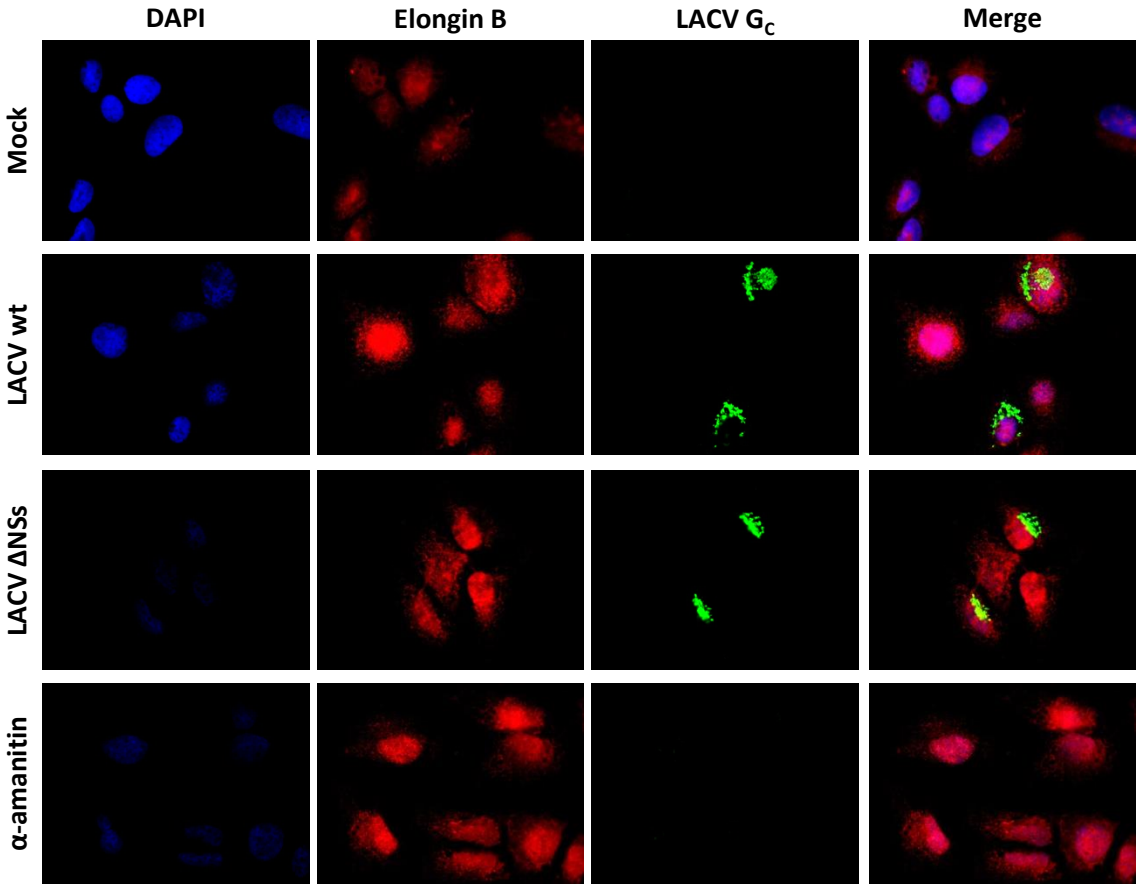

Figure 6. LACV NSs does not affect the subcellular localization of Elongin A or B. HuH-7 cells were grown on coverslips and either Mock-treated, infected with LACV wt or LACV ΔNSs (MOI 1) or treated with α-amanitin (10 µg/ml) for 16 h. The cells were fixed, permeabilized and then stained against endogenous Elongin A (upper panel) or Elongin B (lower panel) and LACV G_C protein, the nucleus was counterstained with DAPI. Images were taken with a Apotome (Zeiss) at a magnification of ×630. Images are representative of at least three independent experiments.

Thus, LACV NSs specifically re-localizes Elongin C from the nucleoli but has no effect on the subcellular localization of Elongin A or B. Differences to α-amanitin indicate that re-localization is not an unspecific consequence of transcription inhibition by LACV NSs.

5.3.3. LACV wt infection and the nucleolus

The experiments shown in Fig. 5 and Fig. 6 demonstrated that LACV wt infection caused a re-localization of Elongin C from the nucleoli, but had no effect on the two other Elongin subunits. It was of interest to determine if Elongin C actually localized to the nucleoli and if the re-localization was specific for Elongin C or a general effect on nucleolar proteins. To study the effect on the nucleoli, HuH-7 cells were mock-treated, infected with LACV wt or LACV ΔNSs or treated with α-amanitin. Upon completion of the infection the cells were stained for endogenous Elongin C and Nucleolin, one of the most abundant nucleolar proteins [148].

As can be seen for the mock sample in Fig. 7, the signals for Elongin C and Nucleolin co-localized in the nucleoli, further establishing Elongin C as a primarily nucleolar protein. Upon infection with LACV wt the signal for Elongin C disappeared, as seen previously, while Nucleolin remained in the nucleoli (Fig. 7). The Nucleolin staining got slightly more diffuse in appearance and the overall size of the nucleoli decreased in LACV wt infected cells, compared to mock. The change in localization of Elongin C and the slight difference in Nucleolin staining were induced by the expression of the NSs protein, since the LACV ΔNSs infection displayed a staining comparable to the mock sample (Fig. 7). For samples treated with the RNAPII inhibitor α-amanitin, the staining for both Elongin C and Nucleolin were disturbed with a diffuse pattern of the whole nucleus, and no nucleoli could be seen any more in the nucleus (Fig. 7).

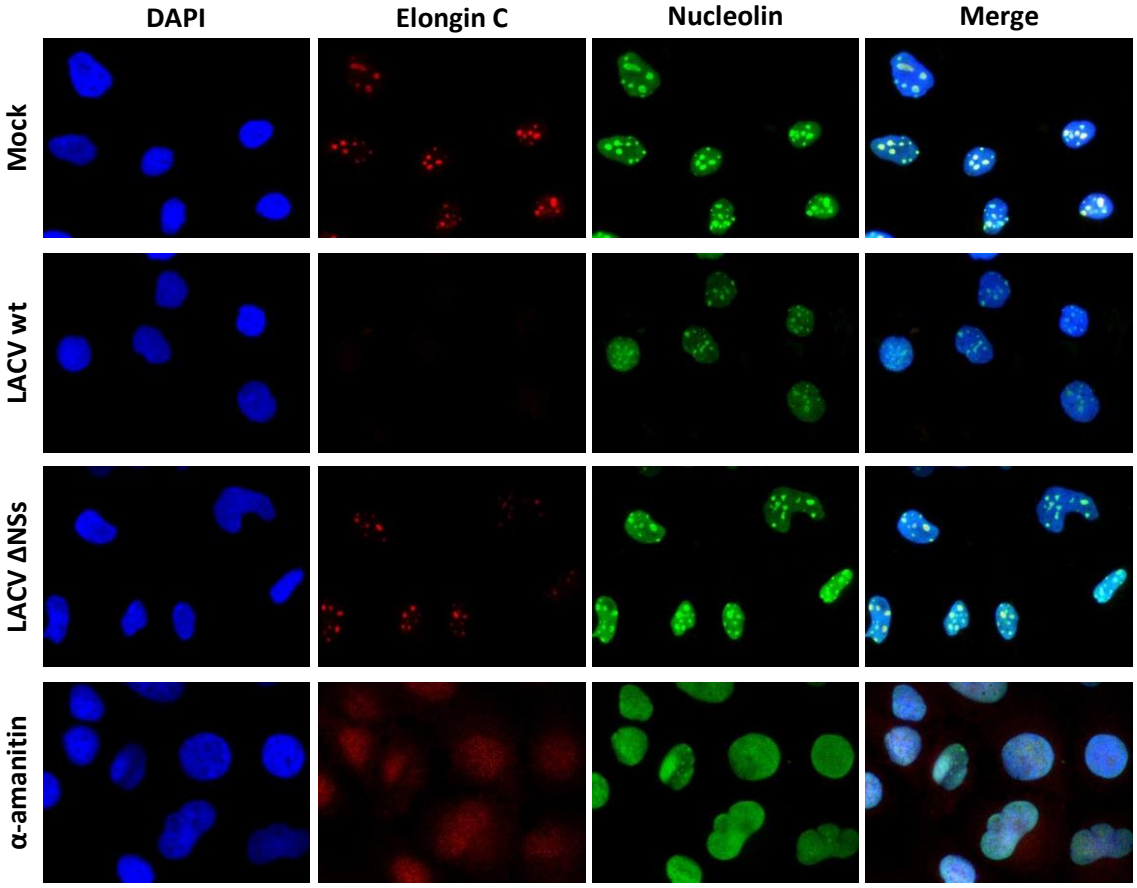

Figure 7. Infection with LACV wt has minimal effects on nucleolar proteins. HuH-7 cells were grown on coverslips and either Mock-treated, infected with LACV wt or LACV ΔNSs (MOI 1) or treated with α-amanitin (10 µg/ml) for 16 h. The cells were fixed, permeabilized and then stained against endogenous Elongin C and Nucleolin, the nucleus was counterstained with DAPI. Images were taken with a Apotome (Zeiss) at a magnification of ×630. Images are representative of at least three independent experiments.

Thus, LACV NSs has minimal effects on Nucleolin and the nucleoli but specifically re-localizes Elongin C from this compartment in the nucleus of infected cells.

5.4. Inhibition of nuclear export

5.4.1. Effect of nuclear export inhibition on Elongin C re-localization during LACV wt infection

The re-localization of Elongin C from the nucleus of infected cells was further studied by inhibiting the nuclear export factor CRM1/exportin 1, the major nuclear export factor for proteins, with Leptomycin B (LMB). HuH-7 cell were pre-treated for 1 h with LMB, followed by either mock treatment, infection with LACV wt or LACV ΔNSs or α-amanitin treatment.

In Fig. 8A mock and LACV wt infected samples, untreated or LMB-treated, are shown. LMB had no effect on the localization of Elongin C in mock (Fig 8A) or LACV ΔNSs/α-amanitin treated cells (data not shown). However, CRM1 inhibition in LACV wt infected cells partially rescues the Elongin C localization to the nucleoli (Fig. 8A). The rescue of Elongin C in the nucleoli was not complete (compare LMB treated mock and LACV wt in Fig. 8A), but was reproducibly observed. A slightly weaker signal for LACV N in LMB treated cells was observed for both LACV wt and LACV ΔNSs infected cells. However, viral growth for both LACV wt and LACV ΔNSs, on cells treated with LMB, were only minimally affected with less than 0.5 log difference compared to untreated cells (Fig. 8B). Therefore the difference observed between untreated and LMB treated cells, for the Elongin C localization in LACV wt infected cells, is due to the export block and not due to an inhibited viral growth.

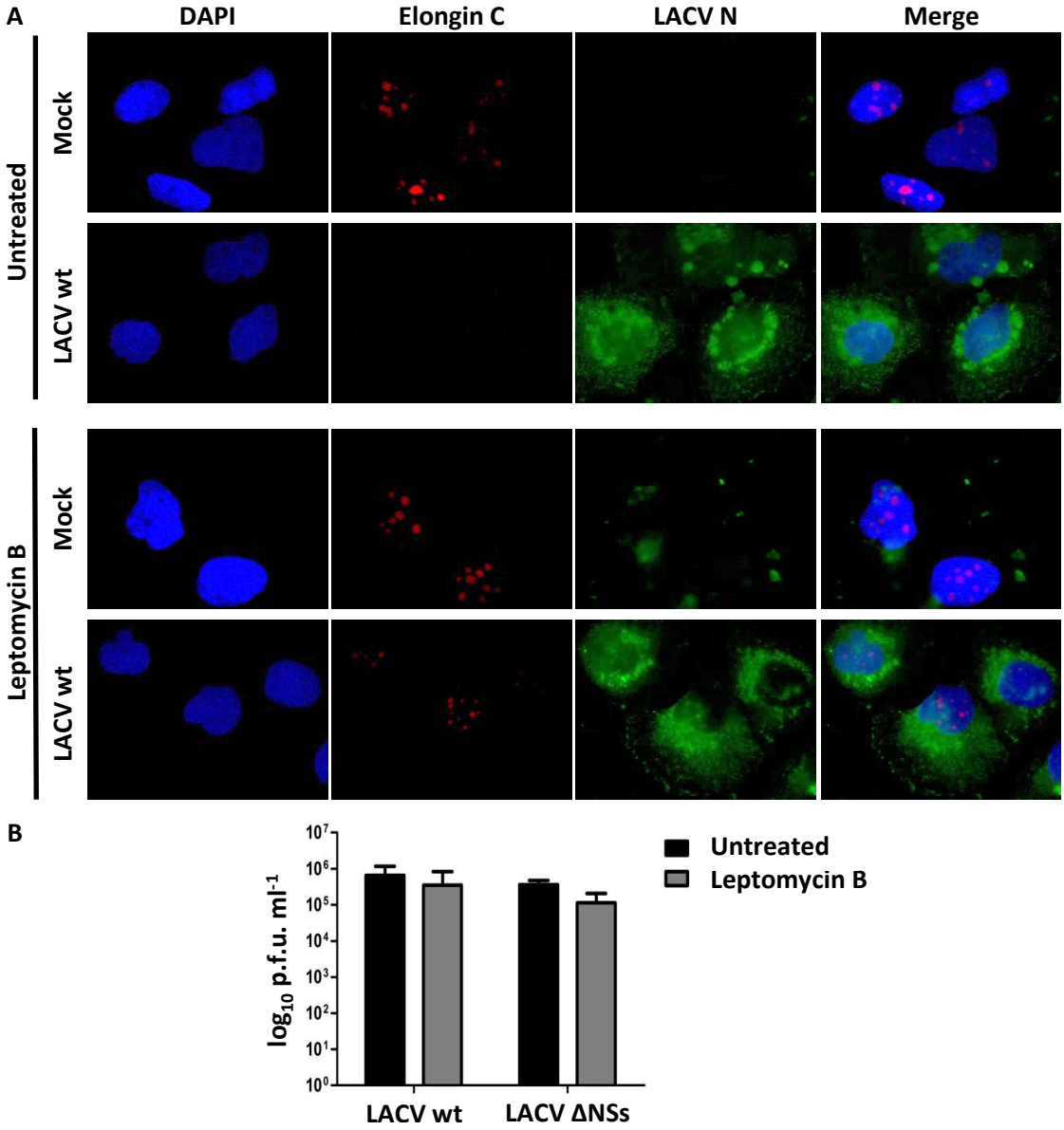

Figure 8. Inhibition of nuclear export via CRM1 partially rescues Elongin C nucleolar localization during LACV wt infection. A) HuH-7 cells, grown on coverslips, were either untreated or Leptomycin B (16 nM) pre-treated. The cells were then Mock-treated or infected with LACV wt (MOI 1) and incubated for 16 h. After fixation and permeabilization the cells were stained against Elongin C and LACV N, the nucleus was counterstained with DAPI. Images were taken with a Apotome (Zeiss) at a magnification of ×630. **B)** CV-1 cells, untreated or Leptomycin B (16 nM) treated were infected with LACV wt or LACV ΔNSs (MOI 0,01). 24 h.p.i. samples were taken and titrated by plaque assay. The graph depicts the mean value, with standard deviation, for three independent experiments while the images are representatives for three independent experiments.

5.4.2. Effect of nuclear export inhibition on RPB1 stability during LACV wt infection

In the previous experiment we demonstrate that inhibition of nuclear export via CRM1 prevented the re-localization of Elongin C from the nucleus in LACV wt infected cell. We therefore wanted to see what effect the inhibition of nuclear export might have, under infection with LACV wt, on RPB1. For this purpose HuH-7 cells were pre-treated with control or LMB-containing medium followed by mock, LACV wt or LACV ΔNSs infection, or α-amanitin treatment. After removal of the inoculum, medium was added to the cells containing either MG132 (proteasomal inhibitor) or LMB alone or the combination of the two, and the cells were then incubated for 8 h. Upon completion of the infection, samples were prepared and separated on 5 or 15 % SDS-PAGE gels followed by Western blot and staining for the indicated proteins.

In Fig. 9 the effect of LMB and/or MG132 treatment on RPB1, under infection or α-amanitin treatment, is depicted. The proteasomal inhibitor MG132 almost completely rescued RPB1 from degradation in LACV wt infected cells, in agreement with previously published results [160]. However, in LACV wt infected cells, treatment with LMB did not rescue RPB1 from degradation (Fig. 9). In LACV wt infected cells, treated with both MG132 and LMB demonstrated a rescue of both total RPB1 and the transcription elongating form (CTDpSer 2), slightly better than for the MG132 alone (Fig. 9).

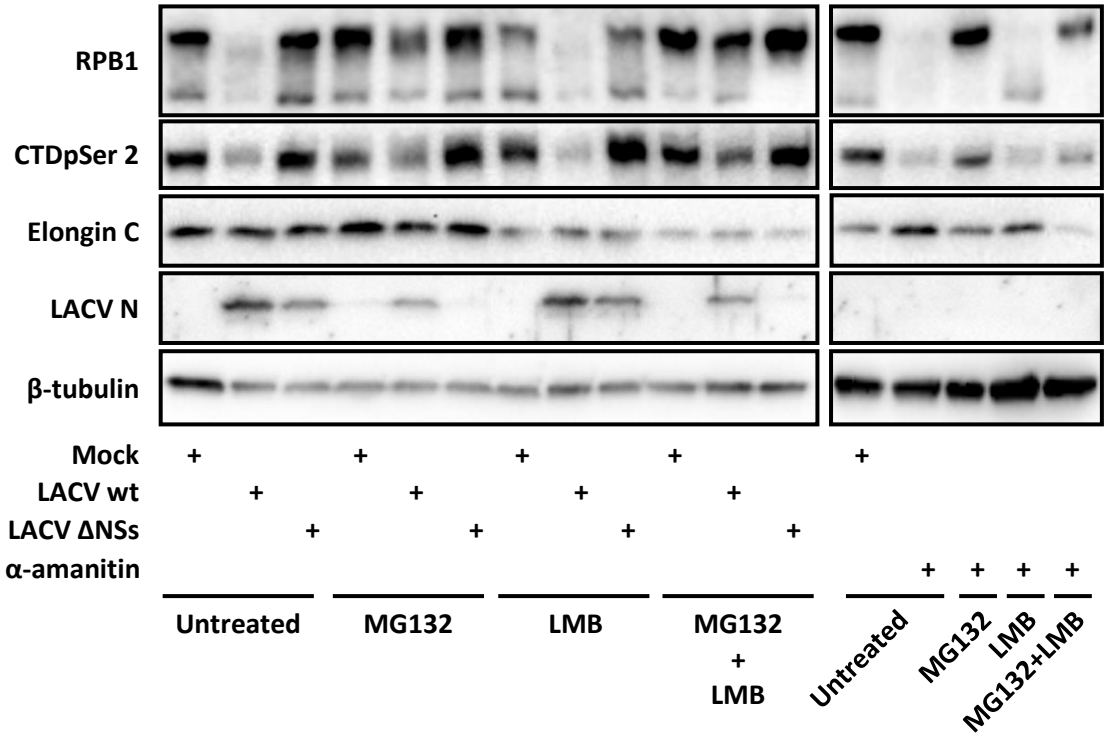

Figure 9. Inhibition of nuclear export does not rescue RPB1 from degradation under LACV wt infection. HuH-7 cells were pre-treated with control or LMB (16 nM) containing medium for 1 h and then Mock-treated, LACV wt or LACV ΔNSs infected (MOI 10) or treated with α-amanitin. Upon completion of the infection, medium was added containing either MG132 (10 μM) or LMB (16 nM) or the combination of the two. 8 h.p.i. samples were prepared and separated on 5 or 15 % SDS-PAGE gels followed by Western blot. The indicated analytes were stained for and detected by chemiluminescence in a Chemidoc XRS+ (BioRad). The figure is representative of at least three independent experiments.

The same effect on RPB1 was also seen for the α-amanitin treated cells: MG132 treatment rescued total RPB1 and the transcriptionally elongating form, while LMB treatment did not inhibit degradation. Also here, the combination of MG132 and LMB demonstrated the dominance of the proteasomal inhibitor (Fig. 9). A curious effect of LMB treatment was the observed slight decrease in the Elongin C signal (Fig. 9). The treatment of the infected cells with MG132 had detrimental effect on the viruses, as can be seen for the LACV N staining (Fig. 9). Especially LACV ΔNSs was affected with no detection of the N protein in MG132 treated cells, but also LACV wt was slightly affected compared to untreated cells.

Thus, LACV NSs re-localizes Elongin C from the nucleoli to the cytoplasm via CRM1, where inhibition of CRM1 dependent export from the nucleus partially rescues the Elongin C signal in the nucleoli. However, inhibition of CRM1 has no effect on RPB1 degradation by LACV NSs, indicating that the degradation of RPB1 occurs directly in the nucleus.

5.5. Mutants of LACV NSs conserved domains

5.5.1. Alignment of orthobunyavirus NSs proteins

In an attempt to map the domain(s) responsible for LACV NSs inhibition of type I IFN induction and Elongin C re-localization, our alanine mutants of the LACV NSs were used. These mutants, at positions in the NSs protein that is conserved within the orthobunyavirus genus, had already been created in the lab (V, Wagner and F, Weber, unpublished), but for clarity a brief description of them will be given here.

The NSs protein sequences from viruses in the orthobunyavirus genus were downloaded from the NCBI protein database. A total of 69 NSs sequences were found, of which 3 sequences were partial and therefore not used for the alignment. In Fig. 10 the alignment of 22 NSs protein sequences, of representative orthobunyaviruses, are shown (an alignment of all 66 NSs sequences can be seen in Appendix 1). The alignments were performed with the ClustalW program and conserved residues were shaded with the BioEdit program using the BLOSUM62 matrix. Only residues that are conserved at the respective position, bases on a consensus calculation performed by the program, are coloured.

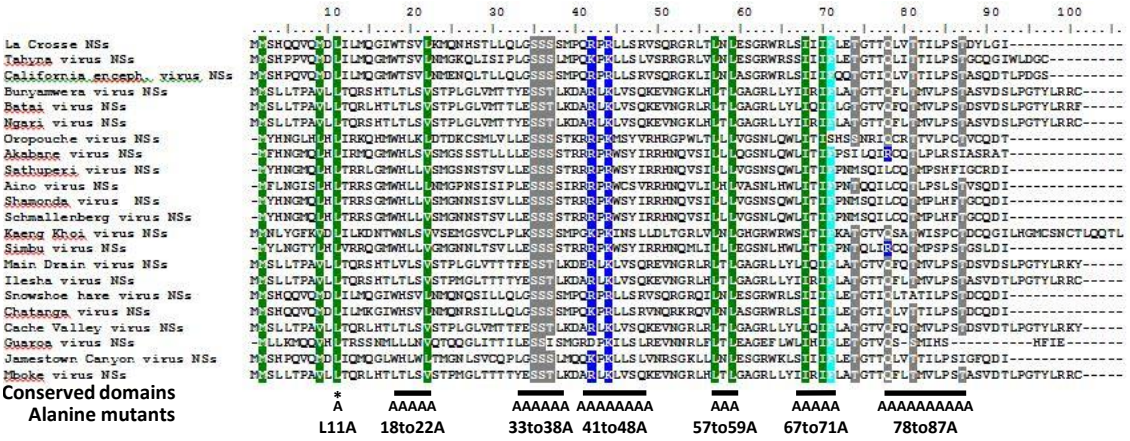

Figure 10. Seven conserved domains identified in protein sequence alignment of Orthobunyavirus NSs proteins. The 22 NSs protein sequences, from representative orthobunyaviruses, were aligned using ClustalW. The resulting alignment was then shaded with BioEdit using the BLOSUM62 matrix set to 80 % identity. Depicted is the resulting alignment where coloured residues either are completely conserved or share biochemical properties.

As can be appreciated in the alignment in Fig. 10 (and Appendix 1) the NSs proteins are fairly similar in sequence for all orthobunyaviruses. Only with the relatively high 80 % similarity level could conserved regions be identified. A total of 7 conserved domains were identified. The conserved residues at theses domains were mutated to alanine, via site-directed mutagenesis, creating 7 LACV NSs mutants termed: L11A, 18to22A, 33to38A, 41to48A, 57to59A, 67to71A and 78to87A. As mentioned we lack antibodies to detect the NSs protein, and therefore all mutants were N terminally Flag-tagged for detection.

5.5.2. Re-localization of Elongin C by the LACV NSs mutants

To characterise the LACV NSs mutants' ability to re-localize Elongin C from the nucleus, immunofluorescence experiments, with transfected HuH-7 cells, were performed on samples taken 16 h post transfection.

Transfection of the plasmid expressing our control protein, the N terminal 106 amino acids of the MxA protein, resulted in a flag staining of the whole cell (Fig. 11). No change in Elongin C localization was seen with the major staining, as before, detected in the nucleoli. The staining for Flag-tagged NSs wt resulted in a very weak and barely detectable staining of the nucleus (Fig. 11). The reasons for this weak staining might be due to 1) the low stability of the LACV NSs protein that has been observed previously (see Fig. 3 and [50]) and/or 2) the use of a RNAPII dependent plasmid, which would inhibit the expression due to the NSs protein inhibition.

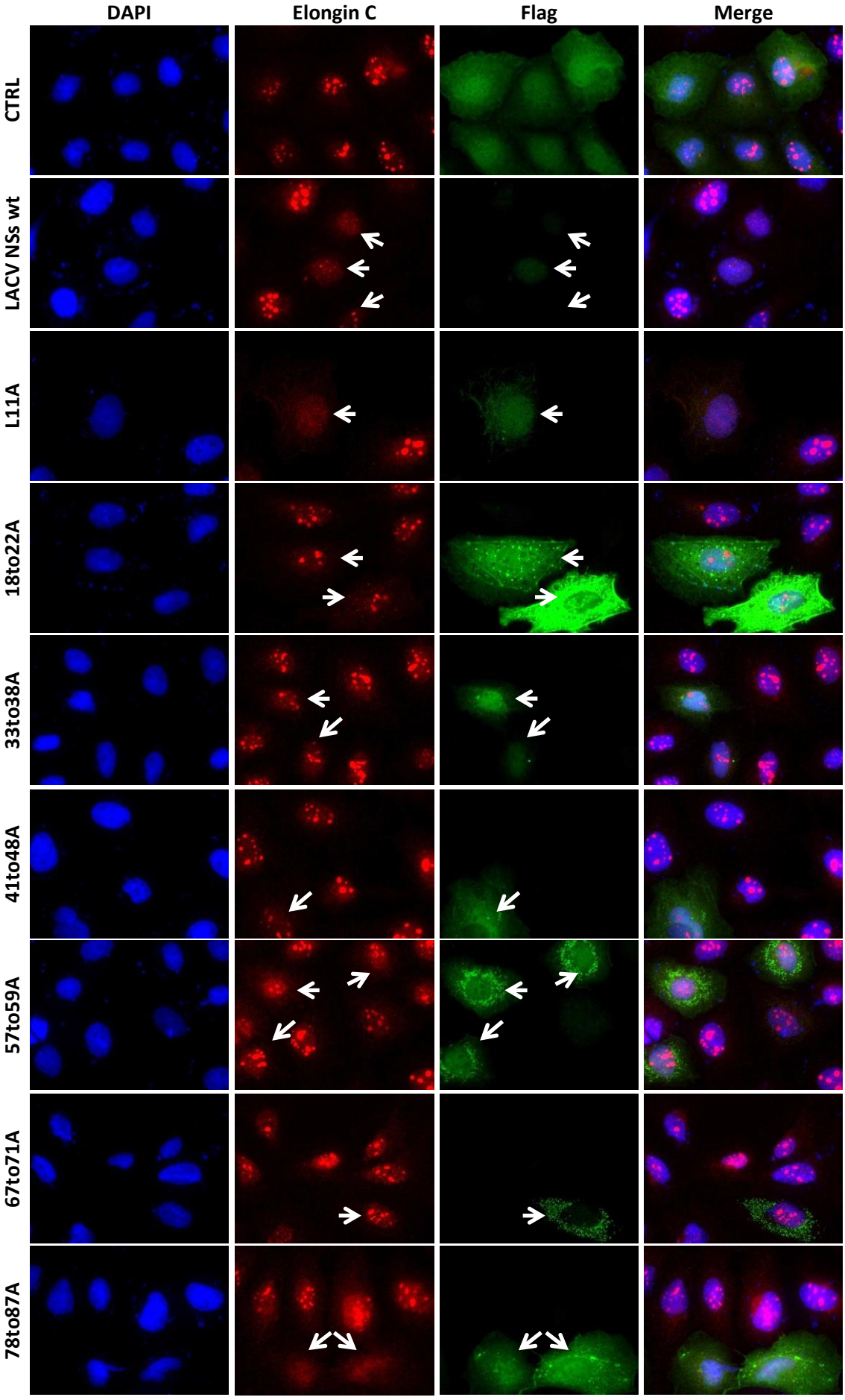
DAPI
Elongin C
Flag
Merge
CTRL
LACV NSs wt
L11A
18to22A
33to38A
41to48A
57to59A
67to71A
78to87A

Figure 11. All LACV NSs mutants, except L11A, have lost the ability to re-localize Elongin C. HuH-7 cells grown on coverslips were transfected with plasmids expressing either a flag-tagged control protein, LACV NSs wt or the LACV NSs mutants and samples were taken 16 h post transfection. After fixation and permeabilization the cells where stained against Elongin C, flag and the nucleus was counterstained with DAPI. Images were taken with a Apotome (Zeiss) at a magnification of ×630. White arrows indicate cells expressing NSs wt or the respective mutant. Images are representative of at least three independent experiments.

However, even though the NSs wt protein was barely detectable, the re-localization of Elongin C was readily observed. The LACV NSs mutants displayed marked difference in the Flag-staining (Fig. 11). The L11A mutant displayed a weak Flag staining of primarily the nucleus, similar to that seen for NSs wt. The expression of the remaining mutants was always stronger, compared to the NSs wt, and the subcellular localization of them varied from mutant to mutant. The 18to22A NSs was seen in the whole cell, 33to38A NSs was primarily nuclear, while the 41to48A mutant NSs was primarily cytoplasmic (Fig. 11). Mutants 57to59A and 67to71A displayed a perinuclear staining that was very prominent in the latter mutant. The most C terminal mutant, 78to87A, was seen throughout the cell with no primary localization (Fig. 11).

The ability of the NSs mutants to re-localize Elongin C also varied, like their respective expressions. The L11A was the only mutant that reproducibly re-localized Elongin C from the nucleoli (Fig. 11). Mutants 18to22A, 33to38A and 41to48A had entirely lost the ability to re-localize Elongin C, which was reproducibly observed in the experiments (Fig. 11). The remaining three mutants, 57to59A, 67to71A and 78to87A displayed varying effects on Elongin C: on the same coverslip either the mutants had an effect, or they did not re-localize Elongin C.

From these results I conclude that most domains of the LACV NSs protein, except the conserved leucine at position 11, are needed for the re-localization of Elongin C.

5.5.3. Inhibition of type I interferon induction by the LACV NSs mutants

To study the effect of the LACV NSs mutants on the type I IFN induction I employed a transfection-based system. Plasmids expressing the Firefly luciferase, under the control of the ISG54-promoter (a type I IFN induction gene [110]), and the constitutively expressed Renilla luciferase, under the control of the SV40-promoter, was transfected into HEK-293 cells together with Flag-tagged control, LACV NSs wt or LACV NSs mutants. Two wells per plasmid expressing a Flag-tagged protein were transfected, where one well was co-transfected with a inducer RNA (VSV-RNA) to initiate a type I IFN induction. Following 24 h incubation, the luciferase activities were measured and compared to control plasmid transfected sample.

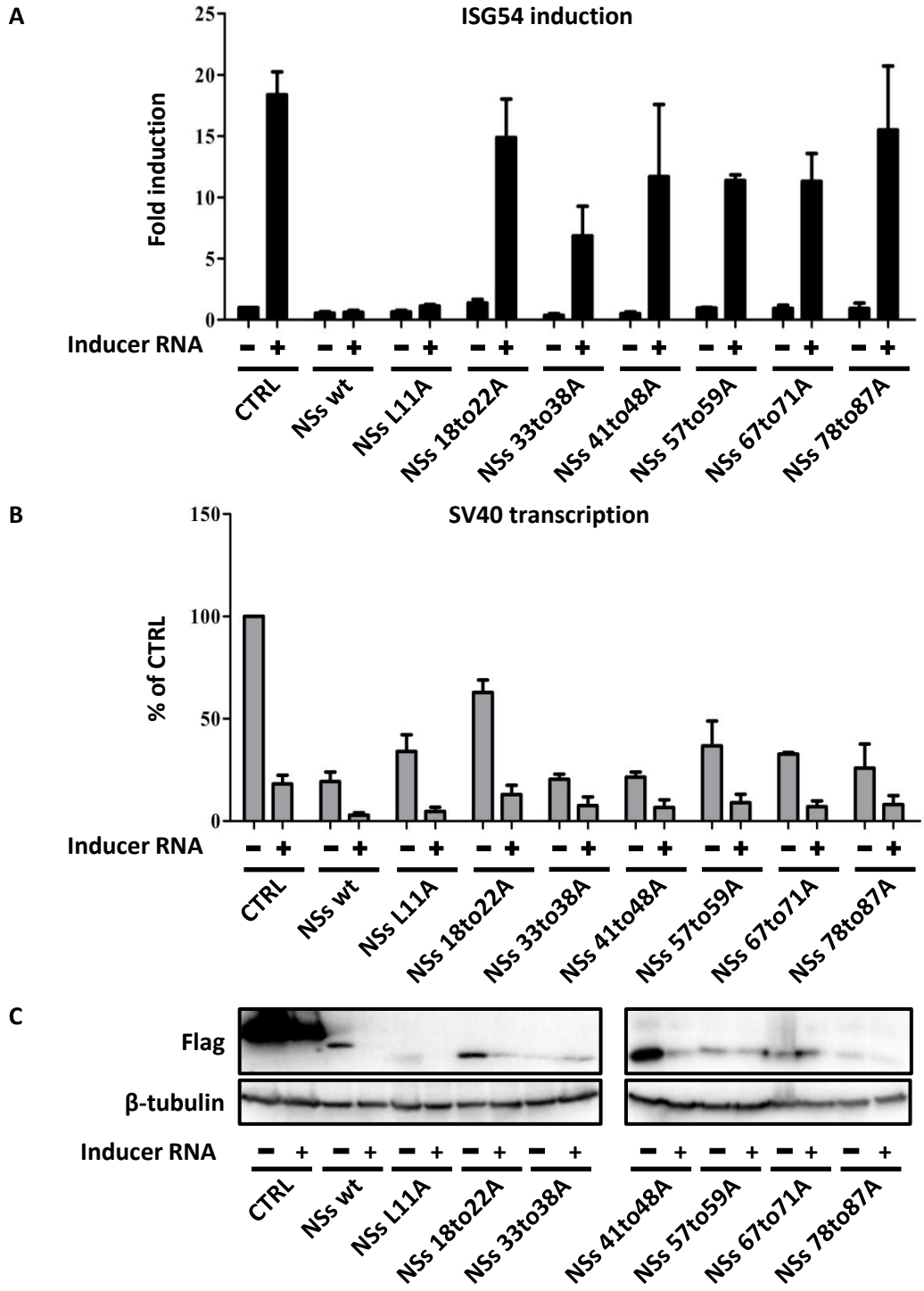

Figure 12. All LACV NSs mutants, except L11A, have lost the ability to inhibit type I IFN induction. HEK-293 cells were transfected with plasmids expressing Firefly luciferase, under control of the ISG54-promoter, and Renilla luciferase, under control of the SV40-promoter, and the indicated Flag-tagged proteins. To half of the samples was an inducer RNA co-transfected to initiate a type I IFN induction. 24 h post transfection the cells were lysed and the luciferase activities measured. A) The fold Firefly luciferase activity compared to the non-induced CTRL sample. B) The percentage of Renilla luciferase activity compared to non-induced CTRL sample. C) Western blots for Flag-tagged constructs and loading control. The graphs depict the mean fold induction (A) or mean percentage (B), with standard deviation, of 3 independent experiments while the pictures in (C) are representative of at least three independent experiments.

The results for the firefly luciferase activity, expressed under the control of the ISG54-promoter, are depicted in Fig. 12A. The transfection of the plasmids had minimal, if any, effect on the induction of the ISG54-promoter in the absence of inducer RNA. Co-transfection of the inducer RNA together with the control plasmid, displayed a ~18-fold induction of the ISG54-promoter activity. The same co-transfection of inducer RNA and LACV NSs wt displayed no induction of the ISG54-promoter activity, reflecting the ability of LACV NSs to inhibit the type I IFN induction. As can be seen in the Fig. 12A, all NSs mutants, except L11A and partially the 33to38A, had lost the ability to inhibit ISG54-promoter activity. While the L11A mutant inhibited to the same extent as LACV NSs wt, the 33to38A mutant displayed a partial inhibition. The remaining 5 mutants did not display any inhibition of the ISG54 promoter (Fig. 12A).

The use of the constitutively active Renilla luciferase expressing plasmid, under the control of the SV40-promoter, is generally used as a transfection control. However, for these experiments the constitutively-expressed Renilla luciferase activity was used as a read-out of the inhibition of general RNAPII transcription, by the LACV NSs mutants. In Fig 12B the percentage of Renilla luciferase activity for all samples, compared to the activity measured for the CTRL plasmid transfected and non-induced sample set to 100 %, are presented. The co-transfection of inducer RNA, to any sample, reduced the Renilla activity, most probably indicating type I IFN induction seen in Fig. 12A. The expression of the NSs wt protein reduced the Renilla activity by 80 %, compared to control protein transfection. The NSs mutants all retained the ability to inhibit general transcription, though with different strengths of inhibition (Fig. 12B). Attempts were also made to detect RPB1 degradation by Western blot, by ectopic expression of LACV NSs wt or the mutants. However, no degradation was detected (data not shown), even for LACV NSs wt, indicating that transient transfection of plasmids encoding for LACV NSs wt or mutants was not efficient enough to induce degradation.

In Fig. 12C, a representative Western blot result for the expression control of the Flag-tagged constructs are shown. In un-induced cells the control protein, ~15 kDa, was highly expressed while the NSs wt, ~10 kDa, had a much lower expression. All the NSs mutants were detected in samples where no inducer RNA had been included, with L11A/33to38A/78to87A having a weaker expression, 18to22A/57to59A/67to71A being expressed to the same extent as NSs wt and the 41to48A mutant being highly expressed (Fig. 12C). When inducer RNA was co-transfected the signal for the flag proteins decreased, for NSs wt and the L11A mutant the signals were hardly detectable (Fig. 12C).

Thus, these results point towards two different mechanisms of transcription inhibition by LACV NSs. One being an inhibition of general transcription, retained by all LACV NSs mutants, and a second inhibition of ISG54-promoter activity where only the L11A mutant, and partially the

33to38A mutant, are still functional. The inhibition of type I IFN induction partially correlates with the re-localized Elongin C. However, the inhibition of the SV40-promoter activity by ectopic expression of LACV NSs wt and the L11A mutant, points to a possible yet un-known inhibition mechanism, most probably coupled to the RNAPII degradation observed in infected cells.

5.6. Recombinant RVFV expressing LACV NSs mutants

5.6.1. Rescuing RVFV expressing the LACV NSs mutants

The above described results for the LACV NSs mutants were all performed by ectopic expression of the different LACV NSs mutants. This does not reflect a viral infection, where the expression of the NSs is governed by the virus.

As already mentioned, we had constructed a recombinant RVFV where the NSs ORF had been replaced by the LACV NSs wt ORF (Fig. 13). We therefore employed the reverse genetics system established in our group [58] for rescuing RVFV expressing the LACV NSs mutants. Briefly, the LACV NSs mutants were amplified via PCR, using plasmids 220 – 226 as template, and inserted into the full-length RVFV S-segment, via a tandem cloning site at the position of the NSs ORF, by conventional cloning. The plasmids were transformed into bacteria and colonize were used for colony PCR and to grow stocks of the plasmids. The colony PCR demonstrated that the right sized and orientation of the inserts were present in all the rescued plasmids (data not shown). After isolation of the respective plasmid, the inserts were sequenced and found to be in the correct plasmid and no extra mutations were detected (data not shown).

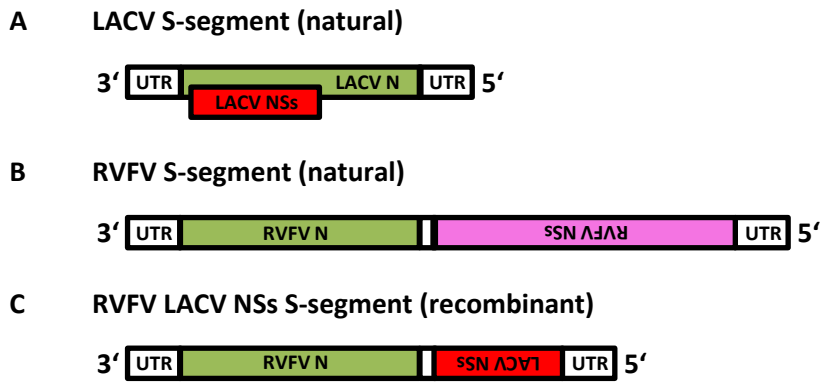

Figure 13. The S segment coding strategy for orthobunyaviruses and phleboviruses. Depicted in the figure is the difference in coding strategies between the two *Bunyaviridae* genera orthobunyavirus (LACV) and phlebovirus (RVFV). In **A)** the LACV S segment with the +1 ORF of NSs compared to the N ORF is shown while **B)** depicts the ambisense coding strategy for the S segment of RVFV. In **C**) the S segment for recombinant RVFV, were the LACV NSs ORF has replaced the RVFV NSs ORF, is depicted.

To rescue the different viruses, plasmids containing full-length RVFV L, M and S (with the different LACV NSs mutants) segments and helper plasmids were transfected into HEK-293/BHK cells, in co-culture. The cells were incubated for 5 days, followed by two virus amplification passaging's on BHK cells, 3 day incubation/passage. The final passage was used to grow stocks of the viruses. All viruses were successfully rescued but the stock titers varied. Table 17 gives an overview of the cloning and rescue of the RVFV expressing the LACV NSs mutants. Despite 3 attempts to grow virus stocks, the RFVF LACV NSs 67to71A virus did not grow to titers that were high enough, and was therefore excluded from further experiments.

Table 17. Overview of the rescue of RVFV expressing the LACV NSs mutants.

Mutant	Cloned & Sequenced	Rescued	Titer (PFU/ml)
RVFV LACV NSs L11A	✓	✓	5.9×10^{6}
RVFV LACV NSs 18to22A	✓	✓	6.5×10^{7}
RVFV LACV NSs 33to38A	✓	✓	7.2×10^{7}
RVFV LACV NSs 41to48A	✓	✓	3.8×10^{6}
RVFV LACV NSs 57to59A	✓	✓	4.0×10^{6}
RVFV LACV NSs 67to71A	✓	✓	2.9×10^{5}
RVFV LACV NSs 78to87A	✓	✓	2.8×10^{7}

5.6.2. Effect of the RVFV LACV NSs mutants on RPB1 stability

To characterize the effect of the virally expressed LACV NSs mutants, I tested their ability to induce degradation of RPB1. For these experiments we used the two cell lines Huh7 cells, used in previous experiments, and A549 cells since they have a strong type I IFN induction and have been used previously to study recombinant RVFV [58]. The cells were either mock-treated or infected with RVFV expressing our control protein instead of the NSs, RVFV wt, RVFV LACV NSs wt or the mutants. At 6 h.p.i. protein samples were collected and separated on 5 or 15% SDS-PAGE gels followed by Western blotting.

In Fig. 14A, the Western blot results for the two cell lines infected with the different viruses are presented. As expected and depicted earlier (Fig. 3), the RVFV expressing LACV NSs wt induced a degradation of RPB1, seen for total RPB1 and for both transcriptionally initiated (CTDpSer 5) and elongating (CTDpSer 2) forms in both cell lines (Fig. 14A). The ability of the LACV NSs mutants to induce the degradation of total RPB1 were partially retained by all mutants, see total RPB1 in Fig. 14A. The strength of the degradation of total RPB1, by the LACV NSs mutants, varied between the mutants and also for the same mutant in the two cell lines e.g. compare LACV NSs 41to48A in A549 and Huh7 cells (Fig. 14A). Due to this

variance in degradation induction the Image lab software was used to quantify the II_O and II_A bands and the area in-between, the CTDpSer 2 and the CTDpSer 5 bands. The quantification values were normalized to β-tubulin and compared to Mock-treated cells. The LACV NSs mutants all retained the ability to degrade RPB1, but to different degrees (Fig. 14B top).

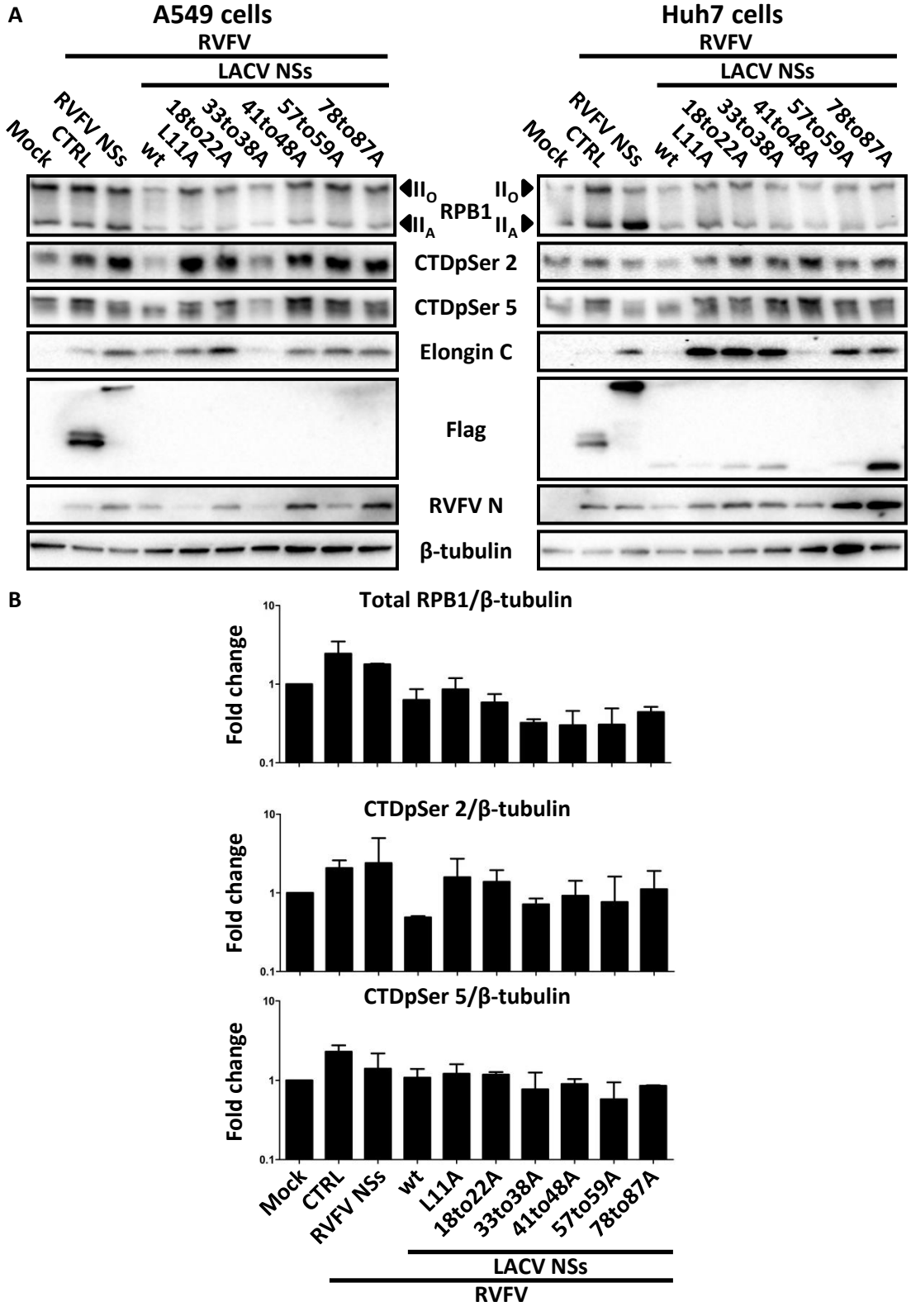

Figure 14. Most of the virally expressed LACV NSs mutants induce the degradation of RPB1. A549 or Huh7 cells were mock-treated or infected with the indicated viruses. At 6 h.p.i. protein samples were taken and used for SDS-PAGE and Western blot. **A)** Representative result for Western blot for the two different cell lines. **B)** Graphs depicting fold change of total RPB1 staining (top), CTDpSer 2 staining (middle) and CTDpSer 5 staining (bottom) for pooled quantification values from A549 and Huh7 cells. The graphs show the relative amount of staining for each sample, normalized to β-tubulin and compared to mock treated sample. The infection with the RVFV expressing LACV NSs mutants were performed once for each indicated cell line.

However, the results have to be taken cautiously since the degradation induced by LACV NSs wt is not that striking in either of the two experiments (Fig. 14A) which is also observable in the quantification (Fig. 14B, top). Unlike the retained ability for all mutants, except L11A, to induce degradation of RPB1, neither of the mutants induced the disappearance of transcriptionally initiated or elongating RPB1 (Fig. 14A and B, middle and bottom). The Flag staining for the expression of the tagged proteins displays a strong signal for the control protein and RVFV NSs wt in both cell lines. The LACV NSs wt and mutants were so weakly expressed that no signals were seen in A549 cells while a weak staining was observed in Huh7 cells, except for the 78to87A mutant that was strongly expressed (Fig. 14A). The RVFV N protein staining of samples from A549 cells showed infection for all viruses, but with different strengths. The N staining were comparable for the majority of the viruses, but RVFV LACV NSs mutants 41to48A and 78to87A showed stronger staining while L11A and 33to38A had weaker staining. In Huh7 cells the RVFV N staining were more comparable between the different viruses with only weak staining in LACV NSs wt infected samples and strong staining in 57to59A and 78to87A infected samples (Fig. 14A). The Elongin C staining were comparable between the samples from A549 cells, except for mock and the 33to38A mutant infected samples with markedly less Elongin C staining. Samples from Huh7 cells showed either a strong signal for all samples or no Elongin C at all (Fig. 14A). However, no pattern in the difference could be determined.

5.6.3. Effect of the RVFV LACV NSs mutants on host cell transcription

Due to the retained ability of most LACV NSs mutants, expressed by RVFV, to induce the degradation of RPB1 the effect on host cell transcription under infection was studied. Similar infections of A549 cells, as performed for experiments depicted in Fig. 14, were done and 6 h.p.i. total cellular RNA was isolated and used as template for RT real-time PCR.

Unlike the retained ability of most LACV NSs mutants in inducing degradation of total RPB1, all RVFV expressed LACV NSs mutants had lost the ability to inhibit innate immune induction, seen both as the induction of IFN-β and ISG56 mRNAs (Fig. 15A and B). However, all LACV

NSs mutants, except the 78to87A mutant, retained some ability to inhibit general transcription, seen by the γ-actin intron assay (Fig. 15C), which measures ongoing transcription [160]. All the RVFV LACV NSs mutant viruses presented with a lower amount of RVFV L RNA, compared to the LACV NSs wt (Fig. 15D), which probably is due to the increased type I IFN induction.

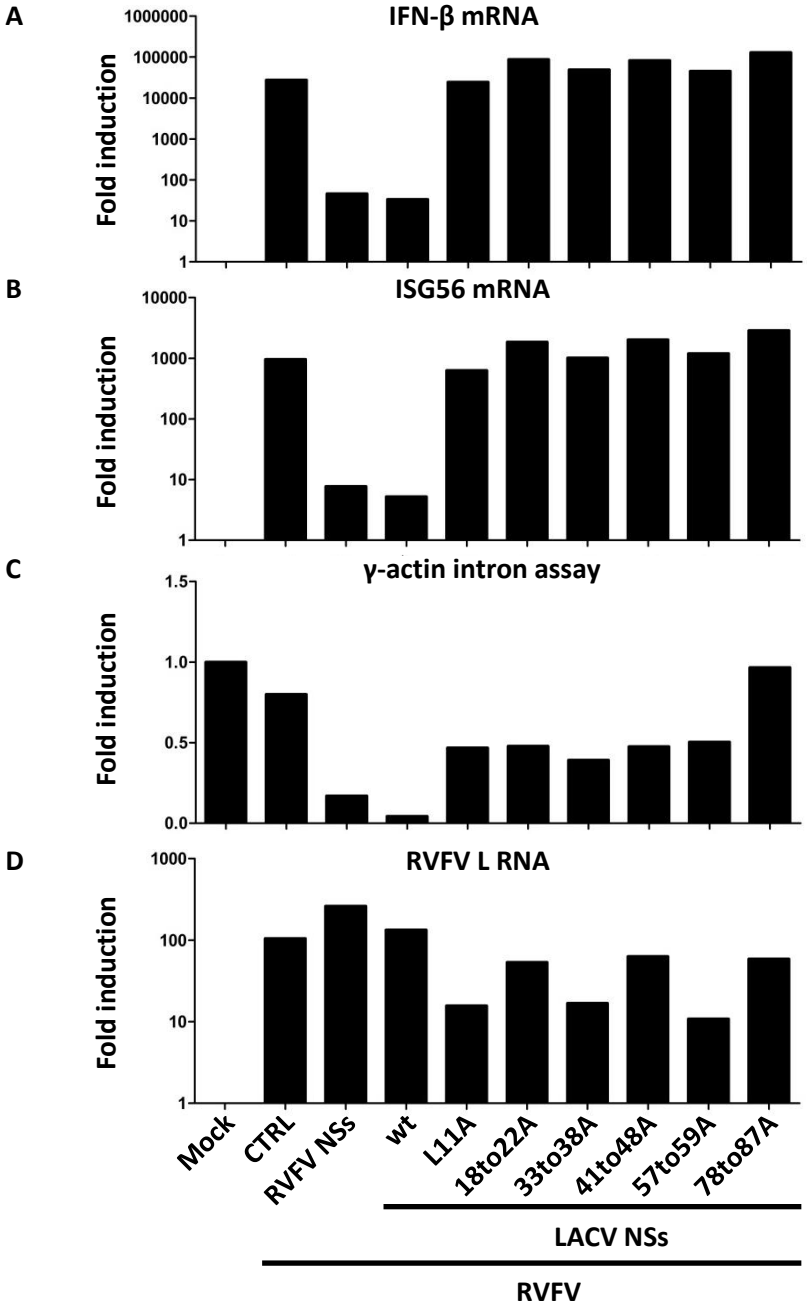

Figure 15. All virally expressed LACV NSs mutants have lost the ability to inhibit type I IFN induction, but partially retain general transcription inhibition. A549 cells were treated as in Fig. 14. At 6 h.p.i. total cellular RNA was isolated and used as template for cDNA synthesis and real time PCR. The graphs depict the fold induction compared to mock-treated cells of **A)** IFN-β mRNA, **B)** ISG56 mRNA, **C)** γ-actin intron assay and **D)** RVFV L RNA levels. IFN-β mRNA, ISG56 mRNA and γ-actin intron assay were detected by SYBR Green while RVFV L RNA was detected via TaqMan. The graphs show the result from one experiment.

To sum up the results for the LACV NSs mutants, all mutants induce the degradation of RPB1, with different efficiencies, compared to mock-treated cells (Fig. 14A), which correlates with the partial inhibition of general host cell transcription (Fig 15C), except for mutant 78to87A. The inhibition of general host cell transcription was also seen for all ectopically expressed LACV NSs mutants (Fig. 12B). The loss of type I IFN induction inhibition for all LACV NSs mutants was observed irrespective of expression system, except for ectopically expressed L11A (Fig. 12A and Fig. 15A & B). A weak pattern could be distinguished where loss of inhibition of the type I IFN induction seems to correlate with the inability to suppress transcriptionally active RPB1. The degradation of RPB1 on the other hand, correlated with inhibition of general transcription. However, these experiments need to be repeated and the difference for the two LACV NSs mutants, L11A in type I IFN induction inhibition and 78to87A in general transcription inhibition, requires further clarification.

5.7. siRNA mediated knockdown of the Elongin complex subunits

5.7.1. RPB1 stability in Elongin subunit knockdown cells

In Fig. 5 we showed that LACV NSs re-localizes Elongin C from the nucleus, specifically from the nucleoli (Fig. 7), but had no effect on the two other subunits of the Elongin complex, Elongin A and B (Fig. 6). To further study the connection between LACV NSs and Elongin C, we performed individual knockdowns of the Elongin complex subunits using siRNAs. A549 cells were again chosen for these experiments due to their robust type I IFN induction upon infection. The knockdowns were performed twice with 72h and 24h incubations in-between each siRNA transfection. The cells were mock-treated or infected with LACV wt or LACV ΔNSs (MOI 10) and then incubated for 16 h. Protein samples for SDS-PAGE and Western blot were prepared and run on 5 or 15 % gels.

All knockdowns of the Elongin subunits were successful: no bands for Elongin B or C were seen, while the Elongin A knockdown at least diminished the amount of the protein (Fig. 16A). Of note, the knockdown of Elongin C resulted in the disappearance of Elongin B, and vice versa, which was reproducibly observed. Since Elongin B and Elongin C forms a complex (Elongin B/C), the lack of stability if one of the components is missing is not unexpected.

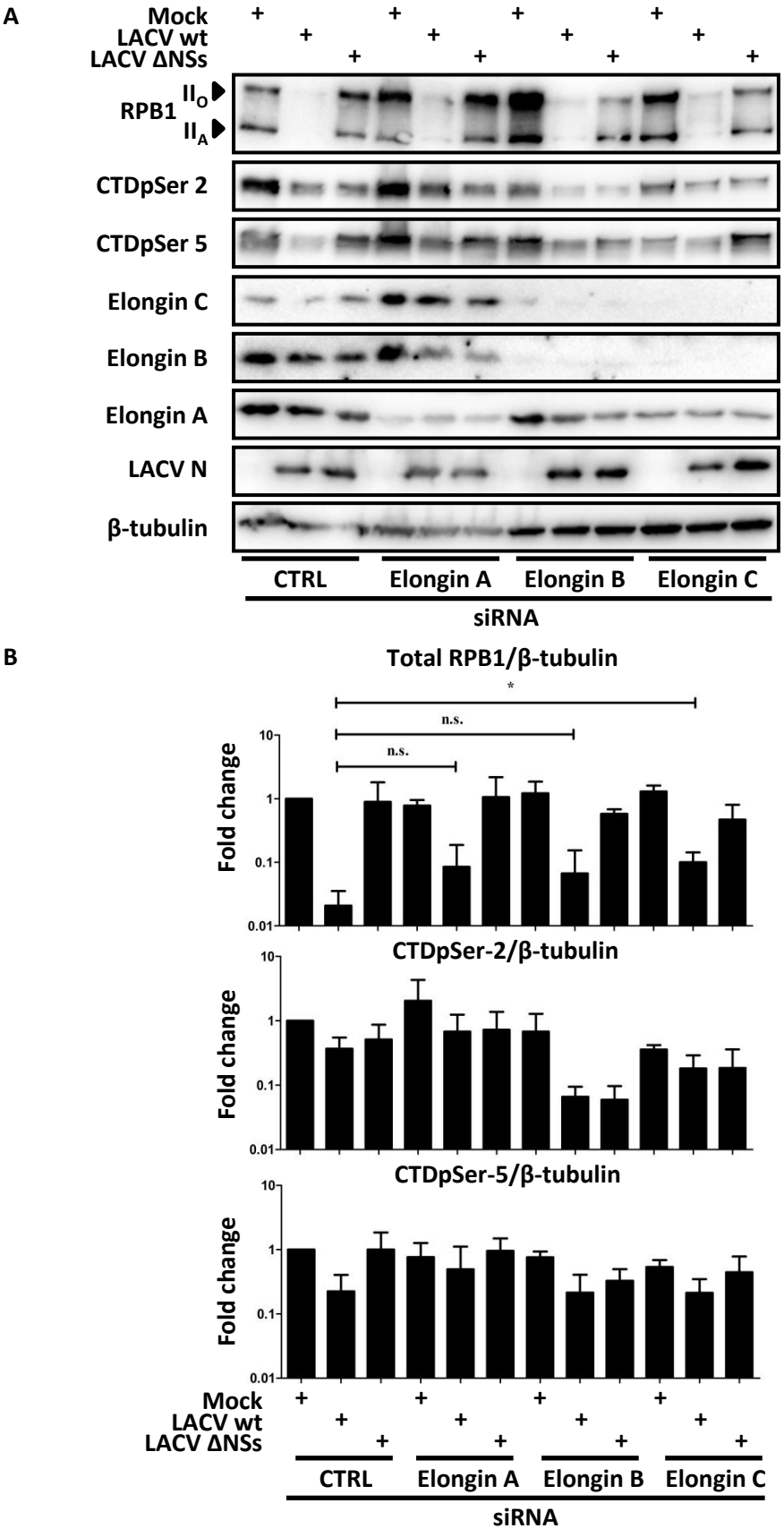
A
Mock
LACV wt
LACV ΔNSs
RPB1 IIO
RPB1 IIA
CTDpSer 2
CTDpSer 5
Elongin C
Elongin B
Elongin A
LACV N
β-tubulin
CTRL
Elongin A
Elongin B
Elongin C
siRNA
B
Total RPB1/β-tubulin
n.s.
n.s.
*
Fold change
CTDpSer-2/β-tubulin
CTDpSer-5/β-tubulin
Mock
LACV wt
LACV ΔNSs
CTRL
Elongin A
Elongin B
Elongin C
siRNA

Figure 16. Knockdown of Elongin C partially rescues RPB1 from degradation in LACV wt-infected cells. A549 cells were either treated with control or siRNAs against the indicated subunits of the Elongin complex. The knockdown was performed twice over a 96 h time period after which the cells were either mock, LACV wt or LACV ΔNSs (MOI 10) infected and incubated for 16 h. The protein samples were run on either 5 or 15 % SDS-PAGE gel followed by Western blot and staining against the indicated analytes. **A)** representative result for protein staining's. **B)** quantification of the total RPB1 staining (top), CTDpSer 2 staining (middle) and CTDpSer 5 staining (bottom). The graphs shows the relative amount of staining for each sample, normalized to β-tubulin and compared to mock control siRNA treated sample. The graphs depict the mean values, with standard deviations, for at least three independent experiments, (*) $P \leq 0.05$. Images are representative for at least three independent experiments.

The knockdown of any Elongin subunit had little effect on the RPB1 stability in mock-treated cells (see total RPB1, Fig. 16A). The slightly stronger signal for total RPB1 in Elongin B knockdown cells were not reproducibly observed. However, infection with LACV wt demonstrated a weak, but reproducible rescue of total RPB1 when any of the Elongin subunits was knocked down (Fig. 16A). As seen previously, LACV ΔNSs infection did not induce degradation of RBP1. To better discern an effect by the Elongin knockdowns we quantified total RPB1, the II_A and II_O forms and the area in-between, the CTDpSer 2 and CTDpSer 5 bands and the loading control β-tubulin, using the Image Lab software (BioRad). The relative values for the different staining's were then normalized to the loading control value, and compared to the control siRNA-treated and mock-infected sample (Fig. 16B). A Students t-test demonstrated that, only in Elongin C knockdown cells was the rescue of total RPB1 statistically significant ($P \leq 0.05$). As can be seen in both the staining for total RPB1 (Fig. 16A) and in the quantification graph for total RPB1 (Fig. 16B upper), a partial rescue was also seen for the knockdowns of Elongin A and B. In contrast to total RPB1, the transcriptionally active RPB1, CTDpSer 2 and 5, were not rescued in any of the knock down cells infected with LACV wt (Fig. 16A). The knockdown of Elongin B or C slightly weakened the signal for transcriptionally elongating RPB1 (CTDpSer 2) (Fig. 16A and B, middle) for all virally infected samples. Transcription initiated and elongating RPB1, in the Elongin A knockdown cells, were comparable to control siRNA-treated cells. The infection was monitored by staining for LACV N protein, which showed comparable infections between both LACV wt and LACV ΔNSs, and between the different knockdown cells (Fig 16A). However, in growth experiments, on Elongin subunit knockdown A549 cells, both LACV wt and LACV ΔNSs displayed reduced titers, by ~1 log, in Elongin A and C knockdown cells 24 h.p.i. (Fig. 17).

Thus, the knockdown of especially Elongin C partially rescues RPB1 from degradation by LACV wt, indicating that the interaction between LACV NSs and Elongin C plays a role in RPB1 degradation.

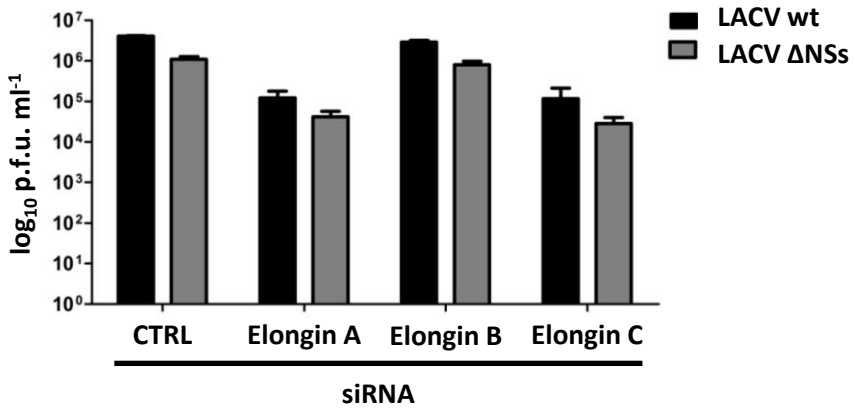

Figure 17. siRNA mediated knockdown of Elongin A and C, partially decreases LACV wt and LACV ΔNSs growth. A549 cells were either treated with control or siRNAs against the indicated subunits of the Elongin complex. The knockdown was performed twice over a 96 h time period after which the cells were infected with either LACV wt or LACV ΔNSs (MOI 0,01). 24 h.p.i. samples were taken and titrated by plaque assay. The graph depicts the mean value, with standard deviation, for three independent experiments.

5.7.2. Host cell transcription in Elongin subunit knockdown cells

Due to the partial rescue of RPB1 from degradation in Elongin C knockdown cells, it was of interest to determine the effect on the type I IFN induction in Elongin subunit knockdown cells under infection. The same knockdown procedure and infections, as performed for the Western blot experiments in Fig. 16 were repeated and the induction measured. Total cellular RNA was isolated and used as template for RT real-time PCR.

As can be seen in Fig. 18A – C, the knockdown of any one of the Elongin complex subunits, caused a partial rescue of both the type I IFN induction and general transcription in LACV wt infected cells. However, only in the Elongin C knockdown cells were the rescue of IFN-β mRNA transcription induction statistically significant. The same effect was observed also for the ISG56 mRNA transcription, but not to statistical significance. There was no difference in the induction of IFN-β and ISG56 mRNA expression in response to LACV ΔNSs infection (Fig. 18A & B). A general increase of transcription in LACV wt infected cells was also seen in the γ-actin intron assay, which measures ongoing transcription [160], however, not to statistical significant levels. In addition to this increased transcription in LACV wt infected cells, an increase in general transcription for all the samples from the Elongin C knockdown cell was observed (Fig. 18C). The same effect, but weaker, was seen also for the Elongin B knockdown samples. Both LACV wt and LACV ΔNSs displayed similar viral N RNA levels for all samples.

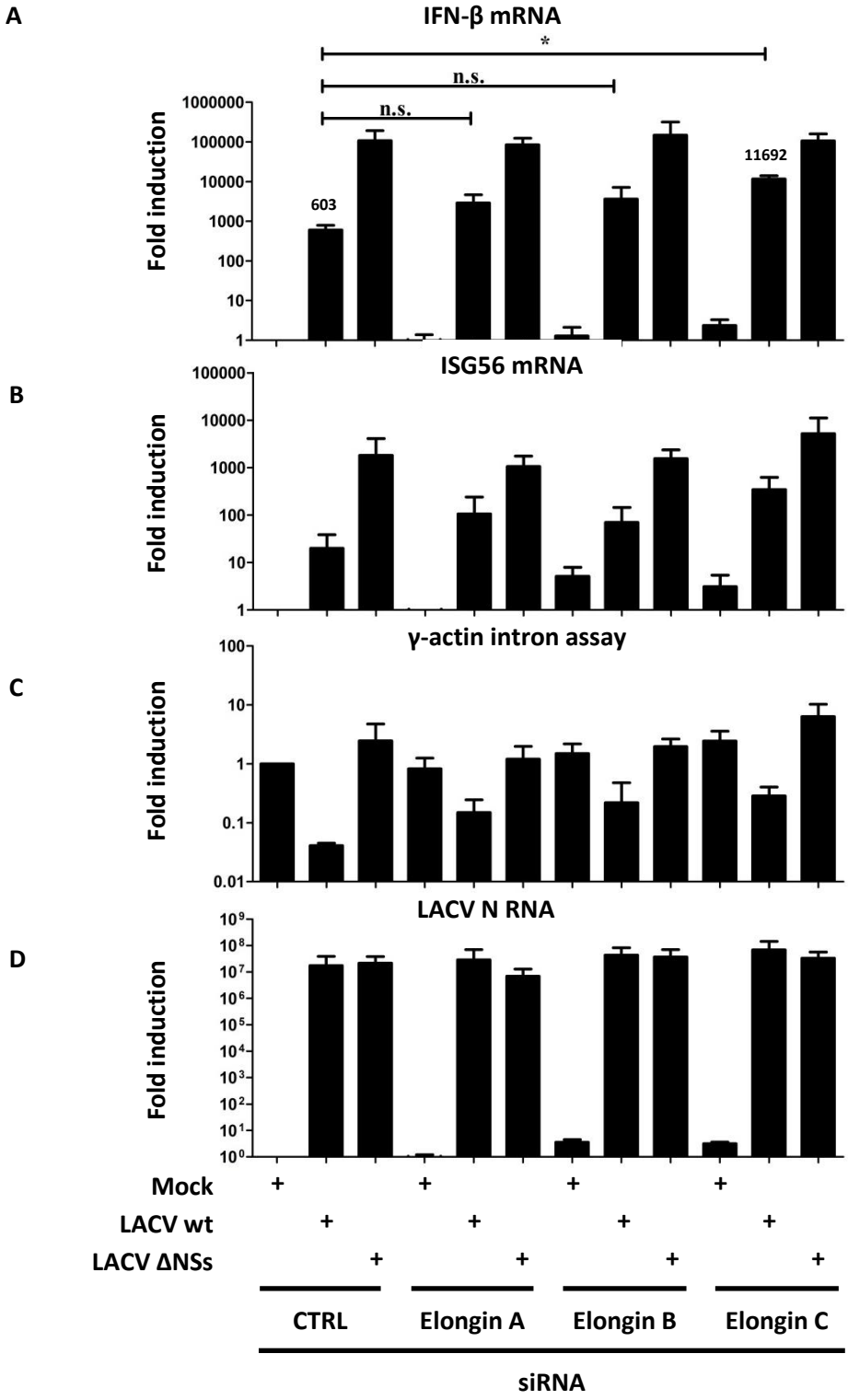

Figure 18. Partial rescue of type I IFN induction by knockdown of Elongin C in LACV wt-infected cells. The same knockdown procedure was performed as described in Fig. 16. Total cellular RNA was isolated and used for RT real time PCR. The graphs show the mean fold induction, with standard deviation, over Mock control siRNA treated cells from three independent experiments. **A)** IFN-β mRNA, **B)** ISG56 mRNA, **C)** γ-actin intron assay and **D)** LACV N RNA. (*) $P \leq 0.05$.

The partial rescue of RPB1 from degradation, in Elongin C depleted and LACV wt infected cells (Fig. 16A), correlated with an increased transcription of primarily IFN-β mRNA (Fig. 18A), but also ISG56 mRNA and general transcription. This indicates that the interaction between LACV NSs and Elongin C contributes to the inhibition of the type I IFN induction in infected cells. However, the induction levels are not comparable to those seen for LACV ΔNSs-infected cells, indicating that other mechanisms of inhibition by NSs exist.

6. Discussion

During wild type orthobunyavirus infection of mammalian cells, the main function of the NSs protein is the inhibition of type I IFN induction [20, 43, 165]. This phenotype of the NSs protein has been demonstrated for BUNV, SBV and LACV, and is due to the inhibition of transcription elongation RNAPII [13, 152, 160]. In attempts to identify host cell interactors of LACV NSs, our group identified Elongin C. Here, I have demonstrated that LACV NSs sequesters Elongin C from its nucleolar localization (Fig. 5), and re-localizes it to the cytoplasm via the nuclear export factor CRM1 (Fig. 8). While the NSs re-localized Elongin C, it had no effect on the localization of Elongin A or B (Fig. 6) and only minimal effects on the nucleolar protein Nucleolin (Fig. 7). Unlike the partial rescue of Elongin C in the nucleoli in CRM1 inhibitor treated cells, no rescue of RPB1 from degradation was seen in Western blot (Fig. 8). However, in siRNA mediated Elongin C knockdown experiments, a partial rescue of RPB1 was observed (Fig. 16). Concomitantly with the RPB1 rescue in Western blot, a partial rescue of type I IFN induction was seen in LACV wt infected cells lacking Elongin C (Fig. 18). Altogether, the results presented in this thesis give further support for the main function of the orthobunyavirus NSs in inhibiting the type I IFN induction during infection of mammalian cells, pointing towards an involvement of Elongin C.

Table 18. Summary of the results for the loss-of-function studies performed with the LACV NSs mutants.

LACV NSs		Wild typ	L11A	18to22A	33to38A	41to48A	57to59A	67to71A	78to87A
Plasmid expression	Subcellular localization	N	N	C/N	N	C	C/N	C	C/N
	Elongin C re-localization	++	++	- -	- -	- -	(-)	(-)	(-)
	Inhibition of type I IFN response	++	++	- -	-/+	- -	- -	- -	- -
	Inhibition of host cell transcription	++	+	+	++	++	+	+	+
Viral expression	RPB1 disappearance	++	-/+	+	+	+	+	n.a.	+
	Inhibition of type I IFN response	++	- -	- -	- -	- -	- -	n.a.	- -
	Inhibition of host cell transcription	++	+	+	+	+	+	n.a.	- -

N: nuclear, C: cytoplasmic, ++: retains function, +: decreased function, -: loss of function, - -: severe loss of function, in parenthesis (): not reproducibly seen, n.a.: not applicable.

In attempts to map the functional domains of LACV NSs, via loss-of-function mutants generated at domains of high sequence conservation, I was able to differentiate between inhibition of type I IFN induction and inhibition of general host cell transcription. An overview of the results for the LACV NSs mutants is presented in Table 18. By ectopic expression all mutants, except L11A, had reproducibly lost the ability to inhibit type I IFN induction (Fig. 12A) while all mutants retained the ability to inhibit general transcription (Fig. 12B). The loss of type I IFN inhibition roughly correlated with the loss of Elongin C re-localization (compare Fig. 12A with Fig. 11). However, the most C-terminal mutants: 57to59A, 67to71A and 78to87A, will require further experiments to determine their ability to re-localize Elongin C.

Similar to the results seen for the ectopically expressed LACV NSs mutants, all virally expressed mutants had lost the ability to inhibit type I IFN induction (Fig. 15A and B). In addition, most of the virally expressed LACV NSs mutants, except 78to87A, partially inhibited general host cell transcription (Fig. 15C). The inhibition of general transcription by the virally expressed LACV mutants correlated partially with the ability to induce RPB1 degradation (compare Fig. 14B top with Fig. 15C). On the other hand, the lack of type I IFN inhibition partially correlated with the lack of inhibiting transcriptionally active RPB1 (compare Fig. 15A & B with Fig. 14A and B middle). Unfortunately, attempts to determine the intracellular localization of Elongin C in cells infected with recombinant RVFV'es expressing LACV NSs mutants failed, most probably because the fixation protocol for BSL-3 samples impaired the epitope recognition by the Elongin C antibody. Additional experiments are still needed for statistical evaluations of the virally expressed LACV NSs mutants, and to try and clarify the function of the two mutants, L11A and 78to87A, that displayed differences depending on the expression system.

In summary, LACV NSs might inhibit general transcription by inducing the degradation of RPB1 while type I IFN induction is inhibited by decreasing transcriptionally elongating RNAPII (primarily CTDpSer 2), possibly via the re-localization of Elongin C. To my knowledge, this is the first time a differentiation between inhibition of type I IFN and general host cell transcription has been demonstrated for an orthobunyavirus NSs protein. Further experiments are needed to determine the different mechanisms.

6.1. LACV NSs transcription inhibition compared to other Bunyaviridae NSs proteins

The NSs proteins of the orthobunyaviruses LACV, BUNV and SBV all inhibit RNAPII-dependent transcription [13, 152, 160]. The BUNV NSs was demonstrated to interact with the Mediator subunit MED8 *in vitro* [89], while our group observed the reproducible *in vitro* pull down between bacterially expressed LACV NSs and *in vitro* transcribed/translated Elongin C, but not MED8 [159]. The Mediator complex is essential and has been determined to be involved in both assembly of the RNAPII preinitiation complex, and in transferring signals from transcription factors to RNAPII. MED8 is part of the head region and has a function in preinitiation complex assembly and as a positive regulator of RNAPII transcription [33]. MED8 can also form a ubiquitin E3 ligase consisting of Elongin B/C, Cullin 2 and Rbx1 [27], however the target(s) for this E3 ligase was never identified. The orthobunyavirus NSs proteins might converge on a small set of proteins, which can interact with each other. The BUNV NSs interaction with MED8 may prevent its function in promoting RNAPII transcription, while LACV NSs interacts with Elongin C.

The NSs of RVFV (genus: phlebovirus) indirectly inhibits RNAPII transcription, by degrading the p62 subunit, and sequestering the p44 subunit, of the general transcription factor THIIH [75, 76, 87]. The lack of a functional THIIH will cause RNAPII to stall at the promoter, eventually leading to pre-mature transcription termination. Since THIIH is a general transcription factor needed for all RNAPII transcription, the lack of it in RVFV infected cells causes a severe inhibition in transcription but has no direct effect, unlike LACV NSs, on RPB1 in RNAPII, although some most likely secondary late effects are visible (see Fig. 3, total RPB1 RVFV 4 h.p.i.). RVFV NSs promotes the proteasomal-degradation of p62 by assembling a ubiquitin E3 ligase containing the Skp1 protein [75]. Skp1 and Elongin C have been demonstrated to share both similar amino acid sequences and three-dimensional structure [172]. Both proteins, Skp1 and Elongin C, also fulfil the same function in assembly of ubiquitin E3-ligases, where both function as adaptors, recruiting Cullin 2/Rbx1 or Cullin 1/Rbx2, respectively [172].

6.2. Is LACV NSs-induced RPB1 degradation a primary or secondary effect?

The LACV wt induced proteasomal degradation of RPB1 in transcriptionally active RNAPII is very rapid, starting between 1 to 3 h.p.i. depending on the viral expression (Fig. 2 and Fig. 3) but is completely rescued in proteasome inhibitor treated cells (Fig. 9 and [160]). RPB1 is stable for 6 h in translation inhibited cells [4] while in transcription elongation inhibited cells, RPB1

degradation was detected first after 12 h of treatment [13]. The rapid induction of RPB1 degradation by the proteasome, in LACV wt infected cells, indicates that NSs has a direct effect on RPB1 stability and not a secondary effect due to transcription/translation inhibition.

6.3. Difference in RPB1 degradation kinetics between authentic and heterologous viral LACV NSs expression

As demonstrated in Fig. 2 and Fig. 3, the disappearance kinetics of the RPB1 signal in Western blot, for LACV wt and RVFV expressing LACV NSs, is slightly different. Using the same MOI and the same cell-type, LACV wt induced RPB1 degradation already 1 h.p.i. while the same degradation started 3 h.p.i. in RVFV LACV NSs infected cells. This dissimilarity might be due to the difference in receptor usage between LACV and RVFV, or the difference in coding strategy between the two S segments. LACV NSs is translated from a +1 ORF embedded in the mRNA of the N protein while the RVFV NSs is translated from its own mRNA (Fig. 13). Due to the phlebovirus S segment ambisense coding strategy, the NSs mRNA is transcribed from the viral anti-genome, which necessitates both primary transcription and one round of replication before NSs mRNA is synthesised. LACV NSs on the other hand is translated directly after primary transcription, from the N mRNA, which might give a slightly faster expression kinetics and therefore also a faster kinetic in inducing RPB1 degradation.

6.4. RPB1 phosphorylation dynamics in infected cells

A band for total RPB1 with a slightly higher mobility, just under the II_O band, can be seen early in infection for LACV wt (Fig. 2). A similar band is seen in herpes simplex virus 1 (HSV-1) infected cells, called the II_I band, that represents RPB1 primarily phosphorylated on CTD serine 5 that is needed for viral transcription [47]. In both LACV wt and HSV-1 infected cells RPB1 CTDpSer 2 (the transcriptionally elongating form) is targeted by viral proteins. In LACV wt-infected cells, the NSs rapidly induces the disappearance of the RPB1 CTDpSer 2 form while it has less effects on CTDpSer 5 RPB1 (transcriptionally initiated form), which is detected in Fig. 2 as the appearance of the "II_I" band. However, unlike HSV-1, LACV wt does not need RNAPII for its own transcription. The appearance of the "II_I" form of RPB1, early in LACV wt infection, is a phenotype of the NSs induced degradation of transcriptionally elongating RPB1, and not a form of RNAPII transcribing viral genes. In agreement with this, the staining for CTDpSer 5 in LACV wt infected cells is much stronger in Fig. 2. A slight increase can also be seen for α-amanitin or Actinomycin D treated cells. The increase in CTDpSer 5 modification in these cells might be an attempt by the cells to compensate for the RNAPII transcription

elongation block. Since the CTDpSer 5 is a prerequisite for the serine 2 modification, an increase by the cell of serine 5 phosphorylation would normally push for elongation but leads here to an increased degradation by NSs, since primarily elongating RPB1 is targeted for degradation.

6.5. Mapping the functional domains of LACV NSs

6.5.1. Functional domains in orthobunyavirus NSs

Attempts to map the functional domains, for some of the reported NSs functions, have been made throughout the work for this thesis. The LACV NSs mutants I used were based on conserved sites throughout the orthobunyavirus genus (Fig. 10). Others have reported functional domains for SBV NSs in inducing RPB1 degradation [13] or determined amino acid residues important for BUNV NSs stability [157].

I have not directly looked at the stability of the mutants, but based on immunofluorescences analysis the mutants, except L11A, are more highly expressed than LACV NSs wt (Fig. 11). It is hard to draw a conclusion on the stability of the NSs mutants based on the Western blot results in Fig. 12C, since here the plasmids containing the NSs mutants are co-transfected with other plasmids that might compete for expression. The clearest result for the NSs mutants' stability is seen in Fig. 11, since the plasmid was transfected alone in this experiment. The increased signal for all ectopically expressed LACV NSs mutants, except L11A, seemingly correlates with the lack of RPB1 degradation for these mutants. However we cannot exclude that the lack of lysine residues required for ubiquitinylation and proteasomal degradation, demonstrated for BUNV NSs [157], or a disturbed substrate recognition due to the alanine residues by the responsible E3 ligase, might play a role.

For NSs of the related SBV, the functional domains required to induce RPB1 degradation was mapped to the C terminal part of the protein by ectopic expression of point of short deletion mutants [13]. The mutants in the C terminal part of SBV NSs did not induce RPB1 degradation, correlating with a loss of general host cell transcription inhibition from a CMV-promoter [13]. Contrary to these results, all my LACV NSs mutants still inhibit general transcription from the SV40-promoter (Fig. 12B). The difference between my results and the ones seen for SBV NSs might be the different promoter strengths for the reporters, the CMV-promoter is stronger than the SV40-promoter [176]. A second difference is the expression strength and stability of the respective NSs mutants. All my plasmid expressed mutants are detectable in non-induced samples (compare Fig. 12B & C), which best correlate with experiments performed for the SBV NSs mutants. The SBV NSs mutants were all barely detectable, and could only be visualized

after proteasomal inhibition [13]. This indicates that the LACV NSs, and mutants of it, are more stable than SBV NSs and its mutants. In addition the NSs-induced RPB1 degradation appears faster in LACV wt-infected cells (1 - 3 h.p.i., see Fig. 2) then in SBV wt-infected cells (6 – 15 h.p.i. [13]).

In our effort to map the functional domains of LACV NSs, we looked at several properties of the NSs protein; 1) the inhibition of general host cell transcription, 2) the inhibition of type I IFN induction, 3) the subcellular localization of the LACV NSs mutants and 4) the ability to re-localize Elongin C. Via ectopic expression of the NSs mutants, the lack of Elongin C re-localization by the NSs mutants correlated with their inability to inhibit type I IFN induction (compare Fig. 11 with Fig. 12A). The L11A mutant re-localized Elongin C and inhibited the type I IFN induction, indicating that this amino acid residue is not needed for these functions of the LACV NSs protein. The remaining N terminal mutants: 18to22A, 33to38A and 41to48A, had lost the ability to re-localize Elongin C and inhibit the type I IFN induction indicating that these residues in the NSs are important for both functions. The C terminal mutants: 57to59A, 67to71A and 78to87A had all lost the ability to inhibit the type I IFN induction, but the ability of these mutants to re-localize Elongin C was inconclusive (Fig. 11 and Fig. 12A). The virally expressed LACV NSs mutants all retained the ability to induce the degradation of RPB1 to different degrees, but neither of them inhibited the transcriptionally active forms of RPB1 (primarily CTDpSer 2) (Fig. 14B). All virally expressed mutants had lost the ability to inhibit the type I IFN induction, but still partially inhibited general transcription (Fig. 15), except 78to87A.

The current model for orthobunyavirus NSs inhibition of transcription is that all host cell transcription is down-regulated due to the inhibition/degradation of transcriptionally elongating RPB1 (CTDpSer 2). My results from the mutants screening demonstrated that I could dissect the transcription inhibition function since most of the LACV NSs mutants had lost the inhibition of type I IFN but still retained general cellular transcription inhibition. The inability to inhibit type I IFN induction by the ectopically expressed mutants correlated partially with the lack of Elongin C re-localization (compare Fig. 12A and Fig. 11). On the other hand, the lack of inhibiting type I IFN gene transcription by the virally expressed LACV NSs mutants correlated partially with the lack of inhibition of transcriptionally active RPB1 (Fig. 14A and B middle/lower and Fig. 15A and B). The inhibition of general cellular transcription did not reach NSs wt levels, except for ectopically expressed 33to38A and 41to48A, but was markedly decreased compared to Mock-treated or CTRL plasmid transfected samples (Fig. 12B and Fig. 15C). A partial correlation between the ability to induce degradation of RPB1 and the inhibition of general host cell transcription was noted for the virally expressed mutants. However, the

observations made for the virally expressed NSs mutants need further experiments to be firmly established.

6.5.2. Ectopic versus viral expression of the L11A mutant

Two of the LACV NSs mutants, L11A and 78to87A, showed differences in loss-of-function depending on the expression system. The differences seen for the 78to87A mutant will be discussed in section 9.6. All the LACV mutants, except L11A, had lost the function of type I interferon inhibition, when both ectopically and virally expressed. However, the L11A mutant inhibited the type I IFN induction when ectopically expressed, but had lost the function when expressed by RVFV (Fig. 12A and Fig. 15A & B). This difference could not be explained by an increased sensitivity to the antiviral protein PKR, since the virus behaved similarly in PKR competent and knockdown cells (data not shown). RVFV is sensitive to the antiviral activity of PKR, which is relieved in infected cells by the proteasomal degradation of PKR induced by RVFV NSs wt [59]. A significant difference in protein levels could also not explain the difference between the ectopically and virally expressed L11A, since neither of the two can be detected in the respective experiment, but in RNA treated cells the ectopically expressed L11A inhibited type I IFN induction (Fig. 12A). A difference between the two experiments is the mode of type I IFN induction. In the transfection experiments a pulse of a fixed amount of inducer RNA was used. In the RVFV-infected cells there is a constant ongoing synthesis of new viral RNA, that amplifies the RIG-I pathway of the type I IFN induction [166]. Possibly, the L11A mutant is capable of inhibiting the induction due to a pulse of inducer RNA, while under conditions of ongoing viral replication, with a constant supply of RIG-I agonists, the LACV L11A mutant is not able to inhibit. This indicates that the NSs might be able to cope with small changes in its sequence for limited inductions of the type I interferon, but during the full-blown viral infection the NSs wt is needed for suppression. A similar requirement of the full-length RVFV NSs was reported, where short truncations throughout the NSs sequence resulted in a loss of anti-type I interferon activity [65].

6.6. LACV NSs interaction with Elongin C

Elongin C is clearly re-localized from the nucleus by LACV NSs (see LACV wt infected samples in Fig. 5 and Fig. 7). Published Elongin C interactors, such as Elongin A and VHL, all contain a BC box [(STP)Lxxx(CSA)xxxϕ)] [93] that mediates the Elongin C interaction. By sequence alignment of the BC boxes from the VHL and Elongin A proteins and LACV NSs, a partial complementarity, between the BC boxes and the C terminus of LACV NSs was distinguished (Fig. 4). Interestingly, this region of the LACV NSs is very close to the region in the BUNV NSs that was determined to interact with MED8 [89]. Importantly, the partial LACV

NSs BC box contains the conserved leucine residue that has been determined to be crucial for Elongin C interaction [145]. Even though the conserved leucine residue is present at the correct position, the two other positions in the BC box (amino acid residue 1 and 6) are not conserved in LACV NSs. However, a few of the residues have the same biochemical properties as those seen in the VHL and Elongin A BC boxes. In addition, the small size of the LACV NSs might adopt an induced fit structure upon binding to Elongin C that could compensate for the lack of the important residues. An induced fit model would also explain why most of the NSs protein, the C terminal ~70 amino acid residues, is needed for interaction (Fig. 11). All of the mutants still contain the important leucine residue, and only in the 78to87A mutant are parts of the potential BC box missing. Unfortunately, no clear phenotype for the Elongin C re-localization was obtained for this mutant when ectopically expressed (Fig. 12). However, this mutant was the only one to have lost both the inhibition of general host cell transcription and type I IFN induction, when virally expressed (Fig. 15A, B and C). It would be of interest in the future to create an alanine mutant of LACV NSs, lacking the BC box motif, and study its phenotype.

6.6.1. Significance of LACV NSs induced Elongin C re-localization

LACV NSs interaction with Elongin C is seen in immunofluorescence as the disappearance of the signal for Elongin C (Fig. 5). The interaction between NSs and Elongin C does not cause a visible re-localization of Elongin C, as can be seen for e.g. Cullin 5 in adenovirus infected cells where Cullin 5 is re-localized to the nucleus by the interaction with adenovirus E4orf6 protein [118], or during DNA damage where Elongin A and Cullin 5 co-localize at sites of DNA-damage [79, 174]. The reason for the disappearance of the Elongin C signal might be due to a dilution effect by the CRM1 dependent re-localization to the cytoplasm (Fig. 8). In the nucleus, Elongin C is concentrated to the nucleoli and easy to detect while no such effect is seen in the cytoplasm were it would be evenly distributed. A second possible reason for the disappearance of the Elongin C signal might be that LACV NSs binds Elongin C at the same position, or nearby, as the antibody. Steric hindrance of antibody binding to the Elongin C protein would then cause a lack of signal in immunofluorescence. Unfortunately the manufacturer does not state to which epitope, on the Elongin C protein, the monoclonal antibody was raised. Elongin C is only 14 kDa in size so the whole protein might have been used for immunization.

A surprising observation is that LACV NSs has no effect on Elongin B localization (lower part of Fig. 6), when most studies on Elongin B/C have reported that this sub-complex is needed for activity. Elongin B/C forms a stable complex and when one of the two is lacking the other is also destabilized (Fig. 16A). However, during infection by LACV wt, no obvious destabilization of Elongin B was noted (Fig. 5 and Fig. 6 lower). The lack of a destabilization during infection by LACV wt might be because not all Elongin C proteins are re-localized by

the NSs protein, leaving sufficient amounts of Elongin C to interact with Elongin B. For the Elongin C function, in increasing transcription elongation rates, the interaction with Elongin A was studied *in vitro,* and the subcellular localization of the Elongin complex has never been reported. Similarly, studies on the formation of E3 ubiquitin ligases, both cellular and viral, have been performed *in vitro*. Only the sub-cellular localization of Cullin 5 and/or Elongin A has been reported to change upon e.g. DNA damage [168] of infection with Adenoviruses [118]. The interaction between NSs and Elongin C might disrupt the Elongin C/Elongin B interaction. I tried, in pull down experiments, if I could out-compete Elongin B from Elongin C by adding increasing amounts of the LACV NSs wt protein. Unfortunately, the basic pull down procedure, to detect interaction between LACV NSs and Elongin C, could never be robustly established (see section 8.2 in the Results), therefore the possible disruption of Elongin B/Elongin C interaction, by LACV NSs, could not be studied.

6.6.2. Functional significance of Elongin C re-localization

Based on the published functions of Elongin C, the re-localization by LACV NSs might work via one of two different mechanisms. The first mechanism would be that Elongin C re-localization causes a decrease in RNAPII transcription elongation rates and an increased stalling frequency of RNAPII. RPB1 degradation would then be an indirect effect promoted by an as yet unknown E3 ligase. The second mechanism would be that LACV NSs induces the formation of a ubiquitin E3 ligase, containing Elongin C, which directly targets RPB1 for degradation.

The first mechanism, where LACV NSs re-localization of Elongin C leads to an increased stalling of RNAPII, would lead to an indirect degradation of RPB1. Elongin C potentiates the function of Elongin A, which interacts with RNAPII and increases the transcription elongation rates [9]. A sequestration of Elongin C by the NSs would probably cause a decrease in Elongin complex promoted transcription. Yet, published Elongin complex dependent transcription is so far restricted to neuronal developmental [175] and stress response genes [79], and has not been implicated in general or innate immune gene transcription. In the LMB experiment we could rescue the nuclear, and partially the nucleolar localization of Elongin C, but RPB1 was still degraded (Fig. 8 and Fig. 9). This demonstrates that RPB1 degradation takes place directly in the nucleus, and that sequestration of Elongin C by the LACV NSs might be the important step. The disappearance of the Elongin C signal during LACV wt infection might just be a phenotype of the interaction and not the mechanism. Even though Elongin C is retained in the nucleus in LMB treated cells, the LACV NSs interaction with Elongin C might sterically hinder Elongin A/Elongin C interaction and thereby cause a stalling of RNAPII.

The second mechanism is that LACV NSs forms a ubiquitin E3 ligase containing Elongin C, which could directly target RPB1 for proteasomal degradation. However, in an effort to determine components of the LACV NSs E3-ligase responsible for RPB1 degradation, knockdowns of Cullin 2 and/or Cullin 5 were performed. Both these Cullins have been demonstrated to be part of several E3 ligases also containing Elongin B/C [80, 93, 111]. Unfortunately, all cells tested had very low to undetectable levels of both Cullins. We were unable to detect even basic levels of either Cullin mRNA or protein via RT real-time PCR or Western blot, respectively, in control treated samples (data not shown). Furthermore, LACV wt infection of Cullin 2 and/or 5 knockdown cells did not result in a rescue of RPB1 from degradation (data not shown). The lack of an effect might be due to the low basic levels of Cullin 2/5 mRNA that is unaffected by siRNA directed degradation. It might also be that the low level of Cullin 2 or 5 mRNA still provides enough translated protein and/or that that these proteins are very stable. However, the lack of detection of basic levels of the two Cullins and the LACV NSs induced RPB1 degradation in all mammalian cell types tested indicate that ubiquitously expressed proteins are involved in the degradation. In addition, no Cullin box that is found in Cullin 2 or 5 interacting proteins [78], could be detected in LACV NSs. A protein forming an E3 ligase complex with Elongin B/C, contains a Cullin box downstream of the BC box, which mediates both the interaction and selection for which of the two Cullins, Cullin 2 or 5, that is recruited to the E3 ligase. No such sequence was found in LACV NSs making it unlikely that it forms a conventional E3 ligase. In parallel to my attempts to rescue RPB1 from degradation by knocking down Cullin 2/5, attempts to rescue p62 (a subunit of the general transcription factor THIIH) from degradation induced by RVFV NSs, the knockdown of Cullin 1 and/or 7 did not have any effect on the degradation [75]. Cullin 1/7 is recruited to E3 ligases by Skp1, which as already mentioned, share both amino acid sequence and function with Elongin C in ubiquitin E3 ligase formation.

Neither of these two models fully explains nor fits with the majority of the results. A mechanism where LACV NSs forms a ubiquitin E3 ligase that directly targets RPB1 for proteasomal degradation, would fit with the rapid induction of degradation (1 – 3 h.p.i.), the re-localization (formation of the E3-ligase) and the partial rescue of both RPB1 and type I IFN induction in Elongin C knockdown cells. However, the rescue in Elongin C knockdown cells is only partial and does not reach levels of RPB1 seen in Mock or LACV ΔNSs infected cells, indicating that other mechanism(s) of LACV NSs plays a role in RPB1 degradation induction.

Another protein that might also play a role in LACV NSs induced RPB1 degradation is NEDD4, the initial E3 ligase responsible for mono-ubiquitinylating RPB1 during the DNA damage response (Ref), see section 4.7.3. of the introduction. Work in our group has demonstrated that siRNA mediated knockdown of NEDD4 partially rescues both RPB1 from

degradation and induction of type I IFN. Furthermore, ectopic expression of ubiquitinylation-competent NEDD4 re-localized to the perinuclear region in LACV wt infected cells, while this was not seen during LACV ΔNSs infection or for ubiquitinylation-deficient NEDD4 (Spiegelberg, L. & Weber, F., unpublished). I have performed single or double knockdown of Elongin C and/or NEDD4 in HeLa cells. However, I did not observe any additional rescue of RPB1 from degradation or induction of type I IFN, when comparing the single and double knockdowns. The lack of additive effect in the double knockdown might be due to the HeLa cells used. NEDD4 showed the most pronounced knockdown efficiency in these cells while Elongin C knockdown was not as efficient as in A549 cells. Unfortunately, an efficient double knockdown could not be established for the same cell line.

6.7. Final Conclusions

The experiments performed and presented in the thesis have been aimed at clarifying the role of the LACV NSs interaction with Elongin C, and the function this interaction fulfils during infection. LACV NSs clearly re-localizes Elongin C from the nucleoli (Fig. 5 and Fig. 7), but the exact role of the re-localization, to induce RNAPII stalling and RPB1 degradation or formation of an E3 ligase that directly targets RPB1 for proteasomal degradation, could not be established.

With our loss-of-function alanine mutants of LACV NSs, we have established the previously unknown separation of inhibition of type I IFN induction and RPB1 degradation. All LACV NSs mutants had lost the ability to inhibit type I IFN, except L11A expressed from plasmid, while all LACV NSs mutants still inhibited general transcription, except LACV NSs 78to87A expressed by RVFV. The inhibition of general transcription by the RVFV expressed mutants partially correlated with the ability to induce degradation of RPB1. Furthermore, the loss of type I IFN inhibition correlated with the loss of Elongin C re-localization by the ectopically expressed LACV NSs mutants, and/or the inability to inhibit transcription elongating RPB1 for the virally expressed LACV NSs mutants. The separation of the inhibition of the type I IFN induction and RPB1 degradation indicates that LACV NSs might have two separate inhibitory functions on host cell transcription. General transcription inhibition is induced by degrading RPB1 while inhibition of type I IFN induction works via a different mechanism, possibly re-localization of Elongin C and/or decreased transcriptionally active RPB1 (mainly CTDpSer 2). The dissection of these two transcription inhibition mechanisms will further both the knowledge of the orthobunyavirus NSs function and mammalian RNAPII transcription.

The work presented here further establishes the critical role of LACV NSs as a model for all orthobunyavirus NSs proteins in inhibiting the type I IFN induction by inducing the degradation of transcriptionally elongating RPB1, to promote orthobunyavirus infection of mammalian cells.

7. References

1. (1977) Bunyaviridae: recent biochemical developments. J Gen Virol 37:1-14
2. (1999) La Crosse and other forms of California encephalitis. J Child Neurol 14:1-14
3. (2014) Orthobunyaviruses: recent genetic and structural insights. Nat Rev Microbiol, England, pp 673-685
4. Akhrymuk I, Kulemzin SV, Frolova EI (2012) Evasion of the innate immune response: the Old World alphavirus nsP2 protein induces rapid degradation of Rpb1, a catalytic subunit of RNA polymerase II. J Virol, United States, pp 7180-7191
5. Al-Hakim A, Escribano-Diaz C, Landry MC, O'Donnell L, Panier S, Szilard RK, Durocher D (2010) The ubiquitous role of ubiquitin in the DNA damage response. DNA Repair (Amst). 2010 Elsevier B.V, Netherlands, pp 1229-1240
6. Allen BL, Taatjes DJ (2015) The Mediator complex: a central integrator of transcription. Nat Rev Mol Cell Biol, England, pp 155-166
7. Anindya R, Aygun O, Svejstrup JQ (2007) Damage-induced ubiquitylation of human RNA polymerase II by the ubiquitin ligase Nedd4, but not Cockayne syndrome proteins or BRCA1. Mol Cell, United States, pp 386-397
8. Ariza A, Tanner SJ, Walter CT, Dent KC, Shepherd DA, Wu W, Matthews SV, Hiscox JA, Green TJ, Luo M, Elliott RM, Fooks AR, Ashcroft AE, Stonehouse NJ, Ranson NA, Barr JN, Edwards TA (2013) Nucleocapsid protein structures from orthobunyaviruses reveal insight into ribonucleoprotein architecture and RNA polymerization. Nucleic Acids Res, England, pp 5912-5926
9. Aso T, Lane WS, Conaway JW, Conaway RC (1995) Elongin (SIII): a multisubunit regulator of elongation by RNA polymerase II. Science 269:1439-1443
10. Aso T, Haque D, Barstead RJ, Conaway RC, Conaway JW (1996) The inducible elongin A elongation activation domain: structure, function and interaction with the elongin BC complex. EMBO J 15:5557-5566
11. Au-Yeung N, Mandhana R, Horvath CM (2013) Transcriptional regulation by STAT1 and STAT2 in the interferon JAK-STAT pathway. JAKSTAT, United States, p e23931
12. Barr JN, Wertz GW (2004) Bunyamwera bunyavirus RNA synthesis requires cooperation of 3'- and 5'-terminal sequences. J Virol 78:1129-1138
13. Barry G, Varela M, Ratinier M, Blomstrom AL, Caporale M, Seehusen F, Hahn K, Schnettler E, Baumgartner W, Kohl A, Palmarini M (2014) NSs protein of Schmallenberg virus counteracts the antiviral response of the cell by inhibiting its transcriptional machinery. J Gen Virol. 2014 The Authors., England, pp 1640-1646
14. Bellocq C, Kolakofsky D (1987) Translational requirement for La Crosse virus S-mRNA synthesis: a possible mechanism. J Virol 61:3960-3967
15. Bellocq C, Raju R, Patterson J, Kolakofsky D (1987) Translational requirement of La Crosse virus S-mRNA synthesis: in vitro studies. J Virol 61:87-95
16. Bennett RS, Cress CM, Ward JM, Firestone CY, Murphy BR, Whitehead SS (2008) La Crosse virus infectivity, pathogenesis, and immunogenicity in mice and monkeys. Virol J 5:25
17. Bird BH, Bawiec DA, Ksiazek TG, Shoemaker TR, Nichol ST (2007) Highly sensitive and broadly reactive quantitative reverse transcription-PCR assay for high-throughput detection of Rift Valley fever virus. J Clin Microbiol 45:3506-3513
18. Blakqori G, Kochs G, Haller O, Weber F (2003) Functional L polymerase of La Crosse virus allows in vivo reconstitution of recombinant nucleocapsids. J Gen Virol 84:1207-1214
19. Blakqori G, Weber F (2005) Efficient cDNA-based rescue of La Crosse bunyaviruses expressing or lacking the nonstructural protein NSs. J Virol 79:10420-10428
20. Blakqori G, Delhaye S, Habjan M, Blair CD, Sanchez-Vargas I, Olson KE, Attarzadeh-Yazdi G, Fragkoudis R, Kohl A, Kalinke U, Weiss S, Michiels T, Staeheli P, Weber F (2007) La Crosse bunyavirus nonstructural protein NSs serves to suppress the type I interferon system of mammalian hosts. J Virol, United States, pp 4991-4999

21. Borucki MK, Kempf BJ, Blitvich BJ, Blair CD, Beaty BJ (2002) La Crosse virus: replication in vertebrate and invertebrate hosts. Microbes Infect 4:341-350
22. Boulon S, Pradet-Balade B, Verheggen C, Molle D, Boireau S, Georgieva M, Azzag K, Robert MC, Ahmad Y, Neel H, Lamond AI, Bertrand E (2010) HSP90 and its R2TP/Prefoldin-like cochaperone are involved in the cytoplasmic assembly of RNA polymerase II. Mol Cell. 2010 Elsevier Inc, United States, pp 912-924
23. Bowden TA, Bitto D, McLees A, Yeromonahos C, Elliott RM, Huiskonen JT (2013) Orthobunyavirus ultrastructure and the curious tripodal glycoprotein spike. PLoS Pathog, United States, p e1003374
24. Bradsher JN, Jackson KW, Conaway RC, Conaway JW (1993) RNA polymerase II transcription factor SIII. I. Identification, purification, and properties. J Biol Chem 268:25587-25593
25. Bradsher JN, Tan S, McLaury HJ, Conaway JW, Conaway RC (1993) RNA polymerase II transcription factor SIII. II. Functional properties and role in RNA chain elongation. J Biol Chem 268:25594-25603
26. Bridgen A, Weber F, Fazakerley JK, Elliott RM (2001) Bunyamwera bunyavirus nonstructural protein NSs is a nonessential gene product that contributes to viral pathogenesis. Proc Natl Acad Sci U S A, United States, pp 664-669
27. Brower CS, Sato S, Tomomori-Sato C, Kamura T, Pause A, Stearman R, Klausner RD, Malik S, Lane WS, Sorokina I, Roeder RG, Conaway JW, Conaway RC (2002) Mammalian mediator subunit mMED8 is an Elongin BC-interacting protein that can assemble with Cul2 and Rbx1 to reconstitute a ubiquitin ligase. Proc Natl Acad Sci U S A 99:10353-10358
28. Brueckner F, Cramer P (2008) Structural basis of transcription inhibition by alpha-amanitin and implications for RNA polymerase II translocation. Nat Struct Mol Biol 15:811-818
29. Bupp K, Stillmock K, Gonzalez-Scarano F (1996) Analysis of the intracellular transport properties of recombinant La Crosse virus glycoproteins. Virology 220:485-490
30. Bushnell DA, Cramer P, Kornberg RD (2002) Structural basis of transcription: alpha-amanitin-RNA polymerase II cocrystal at 2.8 A resolution. Proc Natl Acad Sci U S A 99:1218-1222
31. Carlton-Smith C, Elliott RM (2012) Viperin, MTAP44, and protein kinase R contribute to the interferon-induced inhibition of Bunyamwera Orthobunyavirus replication. J Virol, United States, pp 11548-11557
32. Carre C, Shiekhattar R (2011) Human GTPases associate with RNA polymerase II to mediate its nuclear import. Mol Cell Biol, United States, pp 3953-3962
33. Casamassimi A, Napoli C (2007) Mediator complexes and eukaryotic transcription regulation: an overview. Biochimie, France, pp 1439-1446
34. Case KL, West RM, Smith MJ (1993) Histocompatibility antigens and La Crosse encephalitis. J Infect Dis 168:358-360
35. Cassidy LF, Patterson JL (1989) Mechanism of La Crosse virus inhibition by ribavirin. Antimicrob Agents Chemother 33:2009-2011
36. Cheng C, Sharp PA (2003) RNA polymerase II accumulation in the promoter-proximal region of the dihydrofolate reductase and gamma-actin genes. Mol Cell Biol 23:1961-1967
37. Colon-Ramos DA, Irusta PM, Gan EC, Olson MR, Song J, Morimoto RI, Elliott RM, Lombard M, Hollingsworth R, Hardwick JM, Smith GK, Kornbluth S (2003) Inhibition of translation and induction of apoptosis by Bunyaviral nonstructural proteins bearing sequence similarity to reaper. Mol Biol Cell, United States, pp 4162-4172
38. Conaway JW, Conaway RC (1999) Transcription elongation and human disease. Annu Rev Biochem 68:301-319
39. Conaway RC, Conaway JW (2013) The Mediator complex and transcription elongation. Biochim Biophys Acta 1829:69-75
40. Du Z, Wei L, Murti A, Pfeffer SR, Fan M, Yang CH, Pfeffer LM (2007) Non-conventional signal transduction by type 1 interferons: the NF-kappaB pathway. J Cell Biochem 102:1087-1094

41. Duggal NK, Emerman M (2012) Evolutionary conflicts between viruses and restriction factors shape immunity. Nat Rev Immunol, England, pp 687-695
42. Eick D, Geyer M (2013) The RNA polymerase II carboxy-terminal domain (CTD) code. Chem Rev 113:8456-8490
43. Elliott RM, Blakqori G, van Knippenberg IC, Koudriakova E, Li P, McLees A, Shi X, Szemiel AM (2013) Establishment of a reverse genetics system for Schmallenberg virus, a newly emerged orthobunyavirus in Europe. J Gen Virol, England, pp 851-859
44. Endres MJ, Jacoby DR, Janssen RS, Gonzalez-Scarano F, Nathanson N (1989) The large viral RNA segment of California serogroup bunyaviruses encodes the large viral protein. J Gen Virol 70 (Pt 1):223-228
45. Fontana J, Lopez-Montero N, Elliott RM, Fernandez JJ, Risco C (2008) The unique architecture of Bunyamwera virus factories around the Golgi complex. Cell Microbiol, England, pp 2012-2028
46. Forget D, Lacombe AA, Cloutier P, Al-Khoury R, Bouchard A, Lavallee-Adam M, Faubert D, Jeronimo C, Blanchette M, Coulombe B (2010) The protein interaction network of the human transcription machinery reveals a role for the conserved GTPase RPAP4/GPN1 and microtubule assembly in nuclear import and biogenesis of RNA polymerase II. Mol Cell Proteomics, United States, pp 2827-2839
47. Fraser KA, Rice SA (2005) Herpes simplex virus type 1 infection leads to loss of serine-2 phosphorylation on the carboxyl-terminal domain of RNA polymerase II. J Virol, United States, pp 11323-11334
48. Freaney JE, Kim R, Mandhana R, Horvath CM (2013) Extensive cooperation of immune master regulators IRF3 and NFkappaB in RNA Pol II recruitment and pause release in human innate antiviral transcription. Cell Rep 4:959-973
49. Frese M, Kochs G, Feldmann H, Hertkorn C, Haller O (1996) Inhibition of bunyaviruses, phleboviruses, and hantaviruses by human MxA protein. J Virol 70:915-923
50. Fuller F, Bishop DH (1982) Identification of virus-coded nonstructural polypeptides in bunyavirus-infected cells. J Virol 41:643-648
51. Fuller F, Bhown AS, Bishop DH (1983) Bunyavirus nucleoprotein, N, and a non-structural protein, NSS, are coded by overlapping reading frames in the S RNA. J Gen Virol 64 (Pt 8):1705-1714
52. Gaensbauer JT, Lindsey NP, Messacar K, Staples JE, Fischer M (2014) Neuroinvasive arboviral disease in the United States: 2003 to 2012. Pediatrics 134:e642-650
53. Gauld LW, Yuill TM, Hanson RP, Sinha SK (1975) Isolation of La Crosse virus (California encephalitis group) from the chipmunk (Tamias striatus), an amplifier host. Am J Trop Med Hyg 24:999-1005
54. Gerber M, Tenney K, Conaway JW, Conaway RC, Eissenberg JC, Shilatifard A (2005) Regulation of heat shock gene expression by RNA polymerase II elongation factor, Elongin A. J Biol Chem, United States, pp 4017-4020
55. Gerhardt RR, Gottfried KL, Apperson CS, Davis BS, Erwin PC, Smith AB, Panella NA, Powell EE, Nasci RS (2001) First isolation of La Crosse virus from naturally infected Aedes albopictus. Emerg Infect Dis 7:807-811
56. Goodfellow SJ, Zomerdijk JC (2013) Basic mechanisms in RNA polymerase I transcription of the ribosomal RNA genes. Subcell Biochem 61:211-236
57. Guu TS, Zheng W, Tao YJ (2012) Bunyavirus: structure and replication. Adv Exp Med Biol 726:245-266
58. Habjan M, Penski N, Spiegel M, Weber F (2008) T7 RNA polymerase-dependent and -independent systems for cDNA-based rescue of Rift Valley fever virus. J Gen Virol 89:2157-2166
59. Habjan M, Pichlmair A, Elliott RM, Overby AK, Glatter T, Gstaiger M, Superti-Furga G, Unger H, Weber F (2009) NSs protein of rift valley fever virus induces the specific degradation of the double-stranded RNA-dependent protein kinase. J Virol 83:4365-4375
60. Haddow AD, Odoi A (2009) The incidence risk, clustering, and clinical presentation of La Crosse virus infections in the eastern United States, 2003-2007. PLoS One 4:e6145

61. Haller O, Kochs G, Weber F (2006) The interferon response circuit: induction and suppression by pathogenic viruses. Virology, United States, pp 119-130
62. Haller O, Kochs G, Weber F (2007) Interferon, Mx, and viral countermeasures. Cytokine Growth Factor Rev, England, pp 425-433
63. Haller O, Staeheli P, Schwemmle M, Kochs G (2015) Mx GTPases: dynamin-like antiviral machines of innate immunity. Trends Microbiol 23:154-163
64. Hart TJ, Kohl A, Elliott RM (2009) Role of the NSs protein in the zoonotic capacity of Orthobunyaviruses. Zoonoses Public Health, Germany, pp 285-296
65. Head JA, Kalveram B, Ikegami T (2012) Functional analysis of Rift Valley fever virus NSs encoding a partial truncation. PLoS One, United States, p e45730
66. Hefti HP, Frese M, Landis H, Di Paolo C, Aguzzi A, Haller O, Pavlovic J (1999) Human MxA protein protects mice lacking a functional alpha/beta interferon system against La crosse virus and other lethal viral infections. J Virol 73:6984-6991
67. Heidemann M, Hintermair C, Voss K, Eick D (2013) Dynamic phosphorylation patterns of RNA polymerase II CTD during transcription. Biochim Biophys Acta 1829:55-62
68. Hiscott J, Grandvaux N, Sharma S, Tenoever BR, Servant MJ, Lin R (2003) Convergence of the NF-kappaB and interferon signaling pathways in the regulation of antiviral defense and apoptosis. Ann N Y Acad Sci 1010:237-248
69. Hiscott J (2007) Convergence of the NF-kappaB and IRF pathways in the regulation of the innate antiviral response. Cytokine Growth Factor Rev, England, pp 483-490
70. Hollidge BS, Nedelsky NB, Salzano MV, Fraser JW, Gonzalez-Scarano F, Soldan SS (2012) Orthobunyavirus entry into neurons and other mammalian cells occurs via clathrin-mediated endocytosis and requires trafficking into early endosomes. J Virol 86:7988-8001
71. Honda K, Taniguchi T (2006) IRFs: master regulators of signalling by Toll-like receptors and cytosolic pattern-recognition receptors. Nat Rev Immunol, England, pp 644-658
72. Ivashkiv LB, Donlin LT (2014) Regulation of type I interferon responses. Nat Rev Immunol, England, pp 36-49
73. Iwai K, Yamanaka K, Kamura T, Minato N, Conaway RC, Conaway JW, Klausner RD, Pause A (1999) Identification of the von Hippel-lindau tumor-suppressor protein as part of an active E3 ubiquitin ligase complex. Proc Natl Acad Sci U S A 96:12436-12441
74. Jensen S, Thomsen AR (2012) Sensing of RNA viruses: a review of innate immune receptors involved in recognizing RNA virus invasion. J Virol, United States, pp 2900-2910
75. Kainulainen M, Habjan M, Hubel P, Busch L, Lau S, Colinge J, Superti-Furga G, Pichlmair A, Weber F (2014) Virulence factor NSs of rift valley fever virus recruits the F-box protein FBXO3 to degrade subunit p62 of general transcription factor TFIIH. J Virol, United States, pp 3464-3473
76. Kalveram B, Lihoradova O, Ikegami T (2011) NSs protein of rift valley fever virus promotes posttranslational downregulation of the TFIIH subunit p62. J Virol, United States, pp 6234-6243
77. Kamura T, Sato S, Haque D, Liu L, Kaelin WG, Jr., Conaway RC, Conaway JW (1998) The Elongin BC complex interacts with the conserved SOCS-box motif present in members of the SOCS, ras, WD-40 repeat, and ankyrin repeat families. Genes Dev 12:3872-3881
78. Kamura T, Maenaka K, Kotoshiba S, Matsumoto M, Kohda D, Conaway RC, Conaway JW, Nakayama KI (2004) VHL-box and SOCS-box domains determine binding specificity for Cul2-Rbx1 and Cul5-Rbx2 modules of ubiquitin ligases. Genes Dev, United States, pp 3055-3065
79. Kawauchi J, Inoue M, Fukuda M, Uchida Y, Yasukawa T, Conaway RC, Conaway JW, Aso T, Kitajima S (2013) Transcriptional properties of mammalian elongin A and its role in stress response. J Biol Chem, United States, pp 24302-24315
80. Kobayashi M, Takaori-Kondo A, Miyauchi Y, Iwai K, Uchiyama T (2005) Ubiquitination of APOBEC3G by an HIV-1 Vif-Cullin5-Elongin B-Elongin C complex is essential for Vif function. J Biol Chem, United States, pp 18573-18578

81. Kochs G, Janzen C, Hohenberg H, Haller O (2002) Antivirally active MxA protein sequesters La Crosse virus nucleocapsid protein into perinuclear complexes. Proc Natl Acad Sci U S A 99:3153-3158
82. Kohl A, Clayton RF, Weber F, Bridgen A, Randall RE, Elliott RM (2003) Bunyamwera virus nonstructural protein NSs counteracts interferon regulatory factor 3-mediated induction of early cell death. J Virol 77:7999-8008
83. Kohl A, Hart TJ, Noonan C, Royall E, Roberts LO, Elliott RM (2004) A bunyamwera virus minireplicon system in mosquito cells. J Virol, United States, pp 5679-5685
84. Kraatz F, Wernike K, Hechinger S, Konig P, Granzow H, Reimann I, Beer M (2015) Deletion mutants of schmallenberg virus are avirulent and protect from virus challenge. J Virol. American Society for Microbiology. All Rights Reserved., United States, pp 1825-1837
85. Kudo N, Matsumori N, Taoka H, Fujiwara D, Schreiner EP, Wolff B, Yoshida M, Horinouchi S (1999) Leptomycin B inactivates CRM1/exportin 1 by covalent modification at a cysteine residue in the central conserved region. Proc Natl Acad Sci U S A 96:9112-9117
86. Lagerwerf S, Vrouwe MG, Overmeer RM, Fousteri MI, Mullenders LH (2011) DNA damage response and transcription. DNA Repair (Amst). 2011 Elsevier B.V, Netherlands, pp 743-750
87. Le May N, Dubaele S, Proietti De Santis L, Billecocq A, Bouloy M, Egly JM (2004) TFIIH transcription factor, a target for the Rift Valley hemorrhagic fever virus. Cell, United States, pp 541-550
88. Lees JF, Pringle CR, Elliott RM (1986) Nucleotide sequence of the Bunyamwera virus M RNA segment: conservation of structural features in the Bunyavirus glycoprotein gene product. Virology 148:1-14
89. Leonard VH, Kohl A, Hart TJ, Elliott RM (2006) Interaction of Bunyamwera Orthobunyavirus NSs protein with mediator protein MED8: a mechanism for inhibiting the interferon response. J Virol 80:9667-9675
90. Levy DE, Marie IJ, Durbin JE (2011) Induction and function of type I and III interferon in response to viral infection. Curr Opin Virol 1:476-486
91. Li B, Wang Q, Pan X, Fernandez de Castro I, Sun Y, Guo Y, Tao X, Risco C, Sui SF, Lou Z (2013) Bunyamwera virus possesses a distinct nucleocapsid protein to facilitate genome encapsidation. Proc Natl Acad Sci U S A, United States, pp 9048-9053
92. Livak KJ, Schmittgen TD (2001) Analysis of relative gene expression data using real-time quantitative PCR and the 2(-Delta Delta C(T)) Method. Methods 25:402-408
93. Mahrour N, Redwine WB, Florens L, Swanson SK, Martin-Brown S, Bradford WD, Staehling-Hampton K, Washburn MP, Conaway RC, Conaway JW (2008) Characterization of Cullin-box sequences that direct recruitment of Cul2-Rbx1 and Cul5-Rbx2 modules to Elongin BC-based ubiquitin ligases. J Biol Chem, United States, pp 8005-8013
94. Maxwell PH, Wiesener MS, Chang GW, Clifford SC, Vaux EC, Cockman ME, Wykoff CC, Pugh CW, Maher ER, Ratcliffe PJ (1999) The tumour suppressor protein VHL targets hypoxia-inducible factors for oxygen-dependent proteolysis. Nature 399:271-275
95. McJunkin JE, de los Reyes EC, Irazuzta JE, Caceres MJ, Khan RR, Minnich LL, Fu KD, Lovett GD, Tsai T, Thompson A (2001) La Crosse encephalitis in children. N Engl J Med 344:801-807
96. McJunkin JE, Nahata MC, De Los Reyes EC, Hunt WG, Caceres M, Khan RR, Chebib MG, Taravath S, Minnich LL, Carr R, Welch CA, Whitley RJ (2011) Safety and pharmacokinetics of ribavirin for the treatment of la crosse encephalitis. Pediatr Infect Dis J 30:860-865
97. Mesplede T, Navarro S, Genin P, Morin P, Island ML, Bonnefoy E, Civas A (2003) Positive and negative control of virus-induced interferon-A gene expression. Autoimmunity 36:447-455
98. Miller A, Carchman R, Long R, Denslow SA (2012) La Crosse viral infection in hospitalized pediatric patients in Western North Carolina. Hosp Pediatr 2:235-242

99. Miyata K, Yasukawa T, Fukuda M, Takeuchi T, Yamazaki K, Sakumi K, Tamamori-Adachi M, Ohnishi Y, Ohtsuki Y, Nakabeppu Y, Kitajima S, Onishi S, Aso T (2007) Induction of apoptosis and cellular senescence in mice lacking transcription elongation factor, Elongin A. Cell Death Differ, England, pp 716-726
100. Moreland RJ, Hanas JS, Conaway JW, Conaway RC (1998) Mechanism of action of RNA polymerase II elongation factor Elongin. Maximal stimulation of elongation requires conversion of the early elongation complex to an Elongin-activable form. J Biol Chem 273:26610-26617
101. Munir M, Berg M (2013) The multiple faces of proteinkinase R in antiviral defense. Virulence, United States, pp 85-89
102. Niu F, Shaw N, Wang YE, Jiao L, Ding W, Li X, Zhu P, Upur H, Ouyang S, Cheng G, Liu ZJ (2013) Structure of the Leanyer orthobunyavirus nucleoprotein-RNA complex reveals unique architecture for RNA encapsidation. Proc Natl Acad Sci U S A, United States, pp 9054-9059
103. Novoa RR, Calderita G, Cabezas P, Elliott RM, Risco C (2005) Key Golgi factors for structural and functional maturation of bunyamwera virus. J Virol, United States, pp 10852-10863
104. Obijeski JF, Bishop DH, Murphy FA, Palmer EL (1976) Structural proteins of La Crosse virus. J Virol 19:985-997
105. Obijeski JF, Bishop DH, Palmer EL, Murphy FA (1976) Segmented genome and nucleocapsid of La Crosse virus. J Virol 20:664-675
106. Osborne JC, Elliott RM (2000) RNA binding properties of bunyamwera virus nucleocapsid protein and selective binding to an element in the 5' terminus of the negative-sense S segment. J Virol 74:9946-9952
107. Patterson JL, Kolakofsky D, Holloway BP, Obijeski JF (1983) Isolation of the ends of La Crosse virus small RNA as a double-stranded structure. J Virol 45:882-884
108. Patterson JL, Holloway B, Kolakofsky D (1984) La Crosse virions contain a primer-stimulated RNA polymerase and a methylated cap-dependent endonuclease. J Virol 52:215-222
109. Patterson JL, Kolakofsky D (1984) Characterization of La Crosse virus small-genome transcripts. J Virol 49:680-685
110. Paulson M, Press C, Smith E, Tanese N, Levy DE (2002) IFN-Stimulated transcription through a TBP-free acetyltransferase complex escapes viral shutoff. Nat Cell Biol, England, pp 140-147
111. Pause A, Lee S, Worrell RA, Chen DY, Burgess WH, Linehan WM, Klausner RD (1997) The von Hippel-Lindau tumor-suppressor gene product forms a stable complex with human CUL-2, a member of the Cdc53 family of proteins. Proc Natl Acad Sci U S A 94:2156-2161
112. Pekosz A, Griot C, Nathanson N, Gonzalez-Scarano F (1995) Tropism of bunyaviruses: evidence for a G1 glycoprotein-mediated entry pathway common to the California serogroup. Virology 214:339-348
113. Pekosz A, Gonzalez-Scarano F (1996) The extracellular domain of La Crosse virus G1 forms oligomers and undergoes pH-dependent conformational changes. Virology 225:243-247
114. Pekosz A, Phillips J, Pleasure D, Merry D, Gonzalez-Scarano F (1996) Induction of apoptosis by La Crosse virus infection and role of neuronal differentiation and human bcl-2 expression in its prevention. J Virol 70:5329-5335
115. Perry RP, Kelley DE (1970) Inhibition of RNA synthesis by actinomycin D: characteristic dose-response of different RNA species. J Cell Physiol 76:127-139
116. Pickart CM, Fushman D (2004) Polyubiquitin chains: polymeric protein signals. Curr Opin Chem Biol, England, pp 610-616
117. Proenca-Modena JL, Sesti-Costa R, Pinto AK, Richner JM, Lazear HM, Lucas T, Hyde JL, Diamond MS (2015) Oropouche Virus Infection and Pathogenesis Are Restricted by MAVS, IRF-3, IRF-7, and Type I Interferon Signaling Pathways in Nonmyeloid Cells. J Virol. American Society for Microbiology. All Rights Reserved., United States, pp 4720-4737

118. Querido E, Blanchette P, Yan Q, Kamura T, Morrison M, Boivin D, Kaelin WG, Conaway RC, Conaway JW, Branton PE (2001) Degradation of p53 by adenovirus E4orf6 and E1B55K proteins occurs via a novel mechanism involving a Cullin-containing complex. Genes Dev 15:3104-3117
119. Raju R, Kolakofsky D (1986) Inhibitors of protein synthesis inhibit both La Crosse virus S-mRNA and S genome syntheses in vivo. Virus Res 5:1-9
120. Raju R, Kolakofsky D (1989) The ends of La Crosse virus genome and antigenome RNAs within nucleocapsids are base paired. J Virol 63:122-128
121. Reguera J, Weber F, Cusack S (2010) Bunyaviridae RNA polymerases (L-protein) have an N-terminal, influenza-like endonuclease domain, essential for viral cap-dependent transcription. PLoS Pathog 6:e1001101
122. Reguera J, Malet H, Weber F, Cusack S (2013) Structural basis for encapsidation of genomic RNA by La Crosse Orthobunyavirus nucleoprotein. Proc Natl Acad Sci U S A 110:7246-7251
123. Reichelt M, Stertz S, Krijnse-Locker J, Haller O, Kochs G (2004) Missorting of LaCrosse virus nucleocapsid protein by the interferon-induced MxA GTPase involves smooth ER membranes. Traffic 5:772-784
124. Ribar, B., Prakash, L., Prakash, S. (2006) Requirement of ELC1 for RNA polymerase II polyubiquitylation and degradation in response to DNA damage in Saccharomyces cerevisiae. Mol Cell Biol 26 (11): 3999-4005
125. Ribar B, Prakash L, Prakash S (2007) ELA1 and CUL3 are required along with ELC1 for RNA polymerase II polyubiquitylation and degradation in DNA-damaged yeast cells. Mol Cell Biol, United States, pp 3211-3216
126. Romieu-Mourez R, Solis M, Nardin A, Goubau D, Baron-Bodo V, Lin R, Massie B, Salcedo M, Hiscott J (2006) Distinct roles for IFN regulatory factor (IRF)-3 and IRF-7 in the activation of antitumor properties of human macrophages. Cancer Res, United States, pp 10576-10585
127. Rossier C, Patterson J, Kolakofsky D (1986) La Crosse virus small genome mRNA is made in the cytoplasm. J Virol 58:647-650
128. Salanueva IJ, Novoa RR, Cabezas P, Lopez-Iglesias C, Carrascosa JL, Elliott RM, Risco C (2003) Polymorphism and structural maturation of bunyamwera virus in Golgi and post-Golgi compartments. J Virol 77:1368-1381
129. Santos RI, Rodrigues AH, Silva ML, Mortara RA, Rossi MA, Jamur MC, Oliver C, Arruda E (2008) Oropouche virus entry into HeLa cells involves clathrin and requires endosomal acidification. Virus Res, Netherlands, pp 139-143
130. Sanz-Sanchez L, Risco C (2013) Multilamellar structures and filament bundles are found on the cell surface during bunyavirus egress. PLoS One, United States, p e65526
131. Schneider WM, Chevillotte MD, Rice CM (2014) Interferon-stimulated genes: a complex web of host defenses. Annu Rev Immunol 32:513-545
132. Schoen A, Weber F (2015) Orthobunyaviruses and innate immunity induction: alieNSs vs. PredatoRRs. Eur J Cell Biol
133. Schultz KL, Vernon PS, Griffin DE (2015) Differentiation of neurons restricts Arbovirus replication and increases expression of the alpha isoform of IRF-7. J Virol 89:48-60
134. Shi X, Lappin DF, Elliott RM (2004) Mapping the Golgi targeting and retention signal of Bunyamwera virus glycoproteins. J Virol, United States, pp 10793-10802
135. Shi X, Brauburger K, Elliott RM (2005) Role of N-linked glycans on bunyamwera virus glycoproteins in intracellular trafficking, protein folding, and virus infectivity. J Virol, United States, pp 13725-13734
136. Shi X, Kohl A, Leonard VH, Li P, McLees A, Elliott RM (2006) Requirement of the N-terminal region of orthobunyavirus nonstructural protein NSm for virus assembly and morphogenesis. J Virol, United States, pp 8089-8099
137. Shi X, Kohl A, Li P, Elliott RM (2007) Role of the cytoplasmic tail domains of Bunyamwera orthobunyavirus glycoproteins Gn and Gc in virus assembly and morphogenesis. J Virol, United States, pp 10151-10160

138. Shi X, van Mierlo JT, French A, Elliott RM (2010) Visualizing the replication cycle of bunyamwera orthobunyavirus expressing fluorescent protein-tagged Gc glycoprotein. J Virol, United States, pp 8460-8469
139. Sobell HM (1985) Actinomycin and DNA transcription. Proc Natl Acad Sci U S A 82:5328-5331
140. Soldan SS, Gonzalez-Scarano F (2005) Emerging infectious diseases: the Bunyaviridae. J Neurovirol, United States, pp 412-423
141. Soldan SS, Plassmeyer ML, Matukonis MK, Gonzalez-Scarano F (2005) La Crosse virus nonstructural protein NSs counteracts the effects of short interfering RNA. J Virol 79:234-244
142. Soldan SS, Hollidge BS, Wagner V, Weber F, Gonzalez-Scarano F (2010) La Crosse virus (LACV) Gc fusion peptide mutants have impaired growth and fusion phenotypes, but remain neurotoxic. Virology 404:139-147
143. Somesh BP, Reid J, Liu WF, Sogaard TM, Erdjument-Bromage H, Tempst P, Svejstrup JQ (2005) Multiple mechanisms confining RNA polymerase II ubiquitylation to polymerases undergoing transcriptional arrest. Cell, United States, pp 913-923
144. Somesh BP, Sigurdsson S, Saeki H, Erdjument-Bromage H, Tempst P, Svejstrup JQ (2007) Communication between distant sites in RNA polymerase II through ubiquitylation factors and the polymerase CTD. Cell, United States, pp 57-68
145. Stebbins CE, Kaelin WG, Jr., Pavletich NP (1999) Structure of the VHL-ElonginC-ElonginB complex: implications for VHL tumor suppressor function. Science 284:455-461
146. Streitenfeld H, Boyd A, Fazakerley JK, Bridgen A, Elliott RM, Weber F (2003) Activation of PKR by Bunyamwera virus is independent of the viral interferon antagonist NSs. J Virol 77:5507-5511
147. Szemiel AM, Failloux AB, Elliott RM (2012) Role of Bunyamwera Orthobunyavirus NSs protein in infection of mosquito cells. PLoS Negl Trop Dis, United States, p e1823
148. Tajrishi MM, Tuteja R, Tuteja N (2011) Nucleolin: The most abundant multifunctional phosphoprotein of nucleolus. Commun Integr Biol 4:267-275
149. Takagi Y, Conaway RC, Conaway JW (1996) Characterization of elongin C functional domains required for interaction with elongin B and activation of elongin A. J Biol Chem 271:25562-25568
150. Talmon Y, Prasad BV, Clerx JP, Wang GJ, Chiu W, Hewlett MJ (1987) Electron microscopy of vitrified-hydrated La Crosse virus. J Virol 61:2319-2321
151. Taylor KG, Woods TA, Winkler CW, Carmody AB, Peterson KE (2014) Age-dependent myeloid dendritic cell responses mediate resistance to la crosse virus-induced neurological disease. J Virol 88:11070-11079
152. Thomas D, Blakqori G, Wagner V, Banholzer M, Kessler N, Elliott RM, Haller O, Weber F (2004) Inhibition of RNA polymerase II phosphorylation by a viral interferon antagonist. J Biol Chem, United States, pp 31471-31477
153. Thomas MC, Chiang CM (2006) The general transcription machinery and general cofactors. Crit Rev Biochem Mol Biol 41:105-178
154. Thompson WH, Kalfayan B, Anslow RO (1965) ISOLATION OF CALIFORNIA ENCEPHALITIS GROUP VIRUS FROM A FATAL HUMAN ILLNESS. Am J Epidemiol 81:245-253
155. Utz JT, Apperson CS, MacCormack JN, Salyers M, Dietz EJ, McPherson JT (2003) Economic and social impacts of La Crosse encephalitis in western North Carolina. Am J Trop Med Hyg 69:509-518
156. van Knippenberg I, Carlton-Smith C, Elliott RM (2010) The N-terminus of Bunyamwera orthobunyavirus NSs protein is essential for interferon antagonism. J Gen Virol, England, pp 2002-2006
157. van Knippenberg I, Fragkoudis R, Elliott RM (2013) The transient nature of Bunyamwera orthobunyavirus NSs protein expression: effects of increased stability of NSs protein on virus replication. PLoS One, United States, p e64137
158. Varela M, Schnettler E, Caporale M, Murgia C, Barry G, McFarlane M, McGregor E, Piras IM, Shaw A, Lamm C, Janowicz A, Beer M, Glass M, Herder V, Hahn K,

Baumgartner W, Kohl A, Palmarini M (2013) Schmallenberg virus pathogenesis, tropism and interaction with the innate immune system of the host. PLoS Pathog, United States, p e1003133

159. Verbruggen P (2009) RNA polymerase II inhibition by La Crosse Virus non-structural protein NSs as a mechanism to suppress antiviral responses. Institut für Medizinische Mikrobiologie und Hygiene. Universität Freiburg, Fakultät für Biologie
160. Verbruggen P, Ruf M, Blakqori G, Overby AK, Heidemann M, Eick D, Weber F (2011) Interferon antagonist NSs of La Crosse virus triggers a DNA damage response-like degradation of transcribing RNA polymerase II. J Biol Chem 286:3681-3692
161. Vermeulen W, Fousteri M (2013) Mammalian transcription-coupled excision repair. Cold Spring Harb Perspect Biol 5:a012625
162. Walter CT, Barr JN (2011) Recent advances in the molecular and cellular biology of bunyaviruses. J Gen Virol, England, pp 2467-2484
163. Watts DM, Pantuwatana S, DeFoliart GR, Yuill TM, Thompson WH (1973) Transovarial transmission of LaCrosse virus (California encephalitis group) in the mosquito, Aedes triseriatus. Science 182:1140-1141
164. Weber F, Dunn EF, Bridgen A, Elliott RM (2001) The Bunyamwera virus nonstructural protein NSs inhibits viral RNA synthesis in a minireplicon system. Virology. 2001 Academic Press., United States, pp 67-74
165. Weber F, Bridgen A, Fazakerley JK, Streitenfeld H, Kessler N, Randall RE, Elliott RM (2002) Bunyamwera bunyavirus nonstructural protein NSs counteracts the induction of alpha/beta interferon. J Virol 76:7949-7955
166. Weber M, Gawanbacht A, Habjan M, Rang A, Borner C, Schmidt AM, Veitinger S, Jacob R, Devignot S, Kochs G, Garcia-Sastre A, Weber F (2013) Incoming RNA virus nucleocapsids containing a 5'-triphosphorylated genome activate RIG-I and antiviral signaling. Cell Host Microbe 13:336-346
167. Weber M, Weber F (2014) RIG-I-like receptors and negative-strand RNA viruses: RLRly bird catches some worms. Cytokine Growth Factor Rev 25:621-628
168. Weems JC, Slaughter BD, Unruh JR, Hall SM, McLaird MB, Gilmore JM, Washburn MP, Florens L, Yasukawa T, Aso T, Conaway JW, Conaway RC (2015) Assembly of the Elongin A Ubiquitin Ligase Is Regulated by Genotoxic and Other Stresses. J Biol Chem
169. Werner F, Grohmann D (2011) Evolution of multisubunit RNA polymerases in the three domains of life. Nat Rev Microbiol, England, pp 85-98
170. Wesoly J, Szweykowska-Kulinska Z, Bluyssen HA (2007) STAT activation and differential complex formation dictate selectivity of interferon responses. Acta Biochim Pol, Poland, pp 27-38
171. Wild T, Cramer P (2012) Biogenesis of multisubunit RNA polymerases. Trends Biochem Sci. 2011 Elsevier Ltd, England, pp 99-105
172. Yan Q, Kamura T, Cai Y, Jin J, Ivan M, Mushegian A, Conaway RC, Conaway JW (2004) Identification of Elongin C and Skp1 sequences that determine Cullin selection. J Biol Chem, United States, pp 43019-43026
173. Yao T, Ndoja A (2012) Regulation of gene expression by the ubiquitin-proteasome system. Semin Cell Dev Biol. 2012 Elsevier Ltd, England, pp 523-529
174. Yasukawa T, Kamura T, Kitajima S, Conaway RC, Conaway JW, Aso T (2008) Mammalian Elongin A complex mediates DNA-damage-induced ubiquitylation and degradation of Rpb1. EMBO J, England, pp 3256-3266
175. Yasukawa T, Bhatt S, Takeuchi T, Kawauchi J, Takahashi H, Tsutsui A, Muraoka T, Inoue M, Tsuda M, Kitajima S, Conaway RC, Conaway JW, Trainor PA, Aso T (2012) Transcriptional elongation factor elongin A regulates retinoic acid-induced gene expression during neuronal differentiation. Cell Rep 2:1129-1136
176. Zarrin AA, Malkin L, Fong I, Luk KD, Ghose A, Berinstein NL (1999) Comparison of CMV, RSV, SV40 viral and Vlambda1 cellular promoters in B and T lymphoid and non-lymphoid cell lines. Biochim Biophys Acta, Netherlands, pp 135-139
177. Zhang DW, Rodríguez-Molina JB, Tietjen JR, Nemec CM, Ansari AZ (2012) Emerging Views on the CTD Code. Genetics Research International 2012:19

8. Appendices

Appendix 1 – Full orthobunyavirus NSs alignment

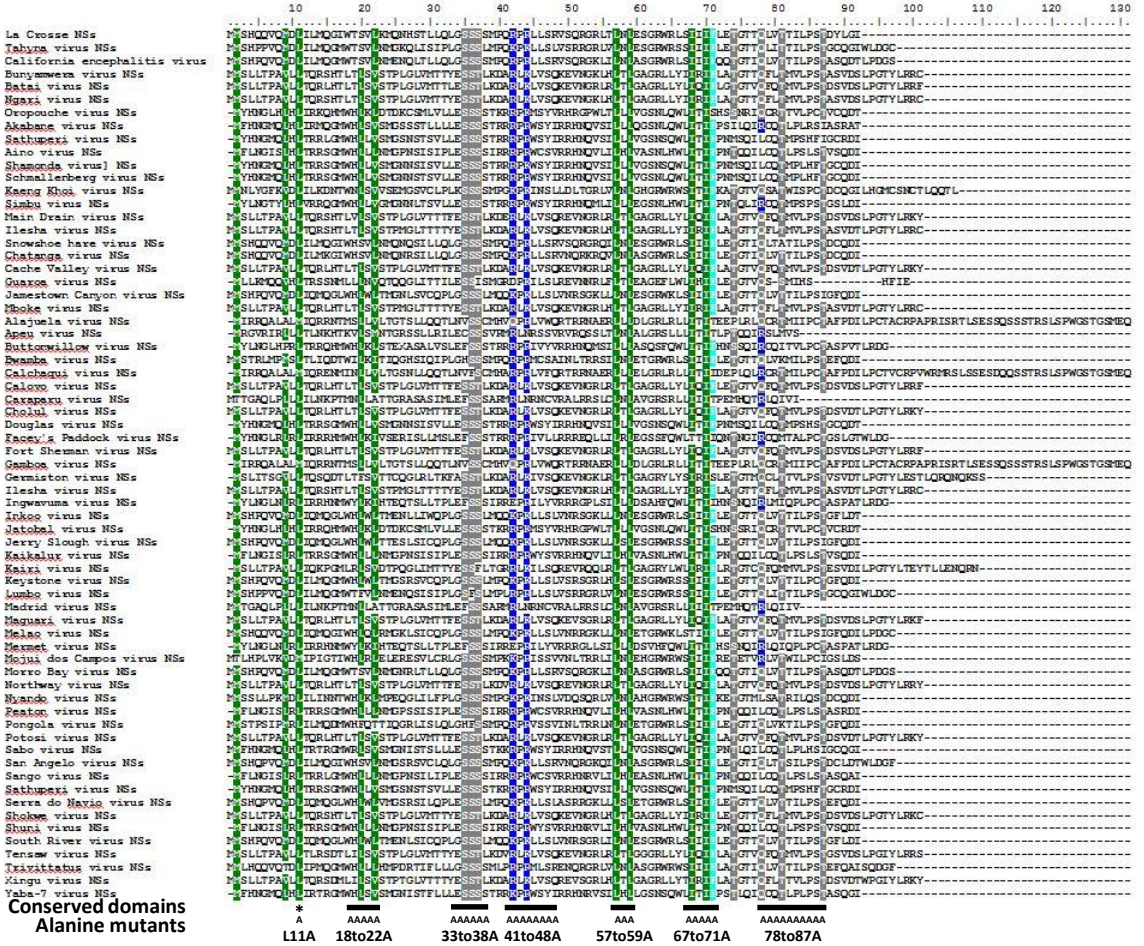

Appendix 2 – List of Figures and Tables

Figures

Tables

Appendix 3 – Academic performances

Publication

Schoen, A., Weber, F., **Orthobunyaviruses and innate immunity induction: alieNSs vs. PredatoRRs**. Eur. J. Cell Biol. (2015), http://dx.doi.org/10.1016/j.ejcb.2015.06.001.

Presentations

2012 Feb. **Functional domains of the virulence factor NSs of La Crosse virus**
Schön, A. & Weber, F., Seminar, SFB593 Retreat Kleinwalsertal

2013 Mar. **Functional domains of the virulence factor NSs of La Crosse virus**
Schön, A. & Weber, F., Progress report, SFB593, Marburg

2013 Oct. **La Crosse virus NSs sequesters Elongin C and causes a degradation of the largest subunit of RNA polymerase II**
Schön, A. & Weber, F., Seminar, SFB593 Retreat Kleinwalsertal

Posters

2012 Mar. **Mapping the functional domains of the virulence factor NSs of La Crosse virus**
Schön, A., Verbruggen, P., Weber, F. GfV-Meeting, Essen

2014 Sep. **La Crosse virus NSs sequesters Elongin C: A possible mechanism for inducing degradation of the largest subunit of RNA polymerase II**
Schön, A., Verbruggen, P., Weber, F., SFB593-Symposium, Marburg.

Appendix 4 - Verzeichnis der akademischen Lehrer

Andersson, Håkan (Assoc. Prof., PhD)

Asplund Persson, Anna (Assoc. Prof., PhD)

Blücher, Anna (Assoc. Prof., PhD)

Brodelius, Peter (Prof., PhD)

Chambers, Benedict (Assoc. Prof., PhD)

Edman, Kjell (Assoc. Prof., PhD)

Flock, Jan-Ingmar (Prof., PhD)

Gierow, Peter (Prof., PhD)

Grandér, Dan (Prof., PhD)

Hagström, Åke (Prof., PhD)

Haldosén, Lars-Arne (Prof., PhD)

Höög, Jan-Olov (Prof., PhD)

Koch-Schmidt, Ann-Christin (Assoc. Prof., PhD)

Lindberg, Michael (Prof., PhD)

Lindegård, Boel (Assoc. Prof., PhD)

Mirazimi, Ali (Assoc. Prof., PhD)

Mode, Agneta (Prof., PhD)

Moll, Markus (Assoc. Prof., PhD)

Nicholls, Ian (Prof., PhD)

Nilsson-Ekdahl, Kristina (Prof., PhD)

Paulsson-Berne, Gabrielle (Assoc. Prof., PhD)

Person, Bengt (Prof., PhD)

Ploner, Alexander (Prof., PhD)

Schultzberg, Marianne (Prof., PhD)

Selivanova, Galina (Prof., PhD)

Tågerud, Sven (Prof., PhD)

Weber, Friedemann (Prof., PhD)

Wikman, Susanne (Assoc. Prof., PhD)

Zilliacus, Johanna (Assoc. Prof., PhD)

Appendix 5 - Acknowledgements – Danksagung

I would like to start by thanking Prof. Friedemann Weber for taking me into his laboratory and allowing me to perform my PhD-study in his group. The road to this final thesis has had its ups and downs but Prof. Weber door has always been open for discussions and helpful ideas. His never ending thirst for knowledge and new things to try has been a great inspiration. I am very grateful to have been part of his group for four and a half year and I am looking forward to new challenges under his guidance.

I could not have reached the end of the thesis study without the other people in the working group of Prof. Weber. Special thanks go to Dr. Stéphanie Devignot, Dr. Markus Kainulainen and Dr. Michaela Weber (Sorry, but you will always be a Weber in my mind, so I can remember your papers in the beginning of your scientific carrier, Weber UND Weber) that always had time to discuss the experiments and help in making them better. Dr. Florian Zielecki was a great help to me with the complicated German bureaucracy when I was new in this country. The remaining long standing, current and former, members of the working group of Prof. Weber: Dr. Larissa Spiegelberg, Jennifer Würth, Simone Lau, Julia Wulle and Jörg Schmidt have been very helpfully whenever I have needed their assistance or support. To all of the above I want to say that the atmosphere in the lab have always made me want to go to work in the mornings, it has been a great time in my life and I am honoured to have been your Coffee-/Buffer- B-T-H!

The other working groups and staff at the Institute of Virology, Marburg, have always been very helpful and nice. Thank you all for organizing the different Christmas Parties and Institute Trips.

Dr. Hanna Sediri has been a great help, both scientifically and as a vent for complains. I still do not talk as much as you with my hands but you have been a *White Shadow* to me.

A special thanks goes to Dr. Annette Krause, my former supervisor for the Master Thesis. She helped and pushed me in the direction of a PhD-thesis and provided the initial contacts. Four years later we have arrived at this point and it could not have been done without your help.

Finally, I would like to thank my family and friends. They have always been there for me throughout the studies. As everyone knows, there are good days (the rare ones when an experiment works) and there are bad once (no need to explain). However, whichever day there has been they have always supported me and punched me to do better next time. Without your support, this thesis would never have been written by me!

Then it just remains to me to say:

Tack – Tanks - Danke – Merci- Kiitos – to all of you!